



# University of HUDDERSFIELD

## University of Huddersfield Repository

Boluda Navarro, Mireia

Phytoestrogen Analogues Targeting Neuroinflammation

### Original Citation

Boluda Navarro, Mireia (2017) Phytoestrogen Analogues Targeting Neuroinflammation. Other thesis, University of Huddersfield.

This version is available at <http://eprints.hud.ac.uk/id/eprint/34174/>

The University Repository is a digital collection of the research output of the University, available on Open Access. Copyright and Moral Rights for the items on this site are retained by the individual author and/or other copyright owners. Users may access full items free of charge; copies of full text items generally can be reproduced, displayed or performed and given to third parties in any format or medium for personal research or study, educational or not-for-profit purposes without prior permission or charge, provided:

- The authors, title and full bibliographic details is credited in any copy;
- A hyperlink and/or URL is included for the original metadata page; and
- The content is not changed in any way.

For more information, including our policy and submission procedure, please contact the Repository Team at: [E.mailbox@hud.ac.uk](mailto:E.mailbox@hud.ac.uk).

<http://eprints.hud.ac.uk/>



---

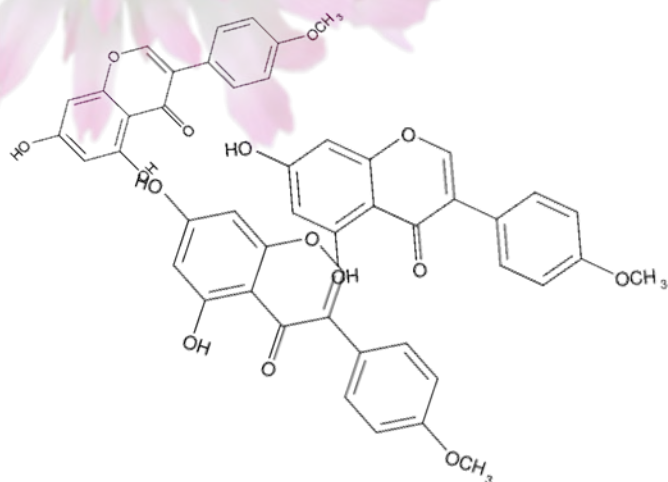
# PHYTOESTROGEN ANALOGUES TARGETING NEUROINFLAMMATION

---

MIREIA BOLUDA NAVARRO



A thesis submitted to the University of Huddersfield in partial fulfilment of the requirements for the degree of Master of Philosophy



April 2017

## **COPYRIGHT STATEMENT**

- i. The author of this thesis (including any appendices and/or schedules to this thesis) owns any copyright in it (the “Copyright”) and s/he has given The University of Huddersfield the right to use such Copyright for any administrative, promotional, educational and/or teaching purposes.
- ii. Copies of this thesis, either in full or in extracts, may be made only in accordance with the regulations of the University Library. Details of these regulations may be obtained from the Librarian. This page must form part of any such copies made.
- iii. The ownership of any patents, designs, trademarks and any and all other intellectual property rights except for the Copyright (the “Intellectual Property Rights”) and any reproductions of copyright works, for example graphs and tables (“Reproductions”), which may be described in this thesis, may not be owned by the author and may be owned by third parties. Such Intellectual Property Rights and Reproductions cannot and must not be made available for use without the prior written permission of the owner(s) of the relevant Intellectual Property Rights and/or Reproductions.

## ACKNOWLEDGEMENTS

First and foremost, I would like to thank my supervisors Dr. Olumayokun Olajide and Dr. Karl Hemming for having trusted me to conduct the present research study. Specially, I must say I am in debt with Dr. Olajide because he has not only guided me throughout this project but also he has taken into consideration my feelings and needs encouraging me to make the most out of this experience. So, for the record, I should like to be noted here that I will be waiting for his visit to the sunny Spain for a proper seafood paella.

I should not forget to offer deep thanks for the much-appreciated help from my colleagues Ravikanth Velagapudi, Abdelmeneim El-Bakoush, Anwer Abudheir, Folashade Ogunrinade for welcoming me from the very beginning and for putting up with my persistent queries.

I also thanks the University of Huddersfield for the scholarship I was awarded with in order to conduct this present project. And also to Fiona Cross, for the patience and consideration she has had with me regarding the attendance monitoring and deadlines.

I am also very grateful to Prof. Rafael Ballesteros and Prof. Rosa Giner from the “Universitat de València” for having me in their laboratories during my stays in València.

And last but not least, to my family and boyfriend, for all the skypes we have done, all the planes taken and for not giving up on me. “Moltes gràcies”.

## ABSTRACT

Hyperactivation of microglia is known to trigger the release of inflammatory mediators, which contribute to neurodegenerative disease progression and severity. Targeting of these immune mechanisms could lead to future therapeutic or preventive strategies for these diseases. Estrogens have been shown to improve the symptoms of neurodegenerative diseases by binding to estrogen receptors (ERs) and producing an anti-inflammatory effect by mainly reducing the release of pro-inflammatory cytokines like tumour necrosis factor alpha (TNF $\alpha$ ), cytokine IL-6 and IL-1 $\beta$ . Nitric oxide (NO), prostaglandin E<sub>2</sub> (PGE<sub>2</sub>) and their enzymes, the inducible nitric oxide synthase (iNOS) and cyclooxygenase-2 (COX-2), respectively, have also been shown to play a part in neuroinflammation. Isoflavones are phytoestrogens that have been known to display anti-inflammatory effects. Biochanin A (BCA) is an ER $\beta$ -selective isoflavone phytoestrogen found in red clover. Formononetin (FMN) is another phytoestrogen found in plant-derived red clover among others. In this research, two BCA and one FMN derivatives and a deoxybenzoin BCA intermediate have been synthesized. These derivatives were then evaluated for anti-inflammatory effect in lipopolysaccharide (LPS) activated BV2 cells microglia. BCA derivatives compound **1**, **2** and **3** were synthesized by producing a carbamate group, an esterification reaction and by following the synthesis route of deoxybenzoin, respectively. FMN derivative, compound **4**, was synthesized by following the same rationale as for compound **1**. Cultured BV2 cells were treated with BCA, FMN, compound **1**, **2**, **3** and **4** for 24 h after previous stimulation with LPS (100 ng/ml). Supernatants were collected and levels of NO, TNF $\alpha$ , IL-6, IL-1 $\beta$  and PGE<sub>2</sub> were measured using ELISA. Further studies were carried out on compound **1** to determine its effects on protein levels COX-2 and iNOS by western blotting. Statistical analysis was performed using one-way ANOVA with post-hoc Student Newman-Keuls test. All compounds produced a significant and concentration dependent reduction in the production of NO. However, FMN, compound **1** and **4** reduced the release of TNF $\alpha$  and IL-6, while BCA only blocked TNF $\alpha$  and compound **2** not only did not show a significant reduction on TNF $\alpha$  but increased IL-6 production. BCA, FMN and compound **4** successfully decreased IL-1 $\beta$  and PGE<sub>2</sub>. Whilst compound **1** showed no effects and **2** augmented it. On the other hand, compound **1** slightly reduced iNOS and COX-2 expression. Compound **3** proved to be cytotoxic for BV2 cells. Our results suggest that the addition of a carbamate group (compound **1** and **4**) to a natural precursor might be a better synthesis strategy than that of the attachment of an ester group (compound **2**). Therefore, there is a need

for further investigation on the mechanism(s) of action of these compounds and their structure activity relationship in the light of the observed effects on pro-inflammatory mediators.

# INDEX

<b>COPYRIGHT STATEMENT .....</b>	<b>2</b>
<b>ACKNOWLEDGEMENTS.....</b>	<b>3</b>
<b>ABSTRACT.....</b>	<b>4</b>
<b>LIST OF FIGURES.....</b>	<b>8</b>
<b>LIST OF SCHEMES.....</b>	<b>10</b>
<b>LIST OF TABLES .....</b>	<b>11</b>
<b>LIST OF ABBREVIATIONS .....</b>	<b>12</b>
<b>CHAPTER 1: GENERAL INTRODUCTION .....</b>	<b>15</b>
1.1 NEUROGLIA CELLS .....	15
1.2 ROLE OF MICROGLIA CELLS IN NEUROINFLAMMATION .....	16
1.3 TOLL-LIKE RECEPTORS IN NEURODEGENERATION.....	23
1.4 NUCLEAR RECEPTORS OF INTEREST, ESTROGEN RECEPTORS: HOW DO THEY SIGNAL AND WHAT ARE THEIR TARGETS?.....	33
1.5 PHYTOESTROGENS .....	39
1.6 SYNTHESIS STRATEGY: THE USE OF ESTERS AND CARBAMATES IN DRUG DESIGN .....	45
1.7 GAP IN KNOWLEDGE .....	47
1.8 OBJECTIVES OF THE STUDY .....	48
<b>CHAPTER 2: MATERIALS AND METHODS .....</b>	<b>49</b>
2.1 GENERAL CHEMISTRY METHODS.....	49
2.2 PHARMACOLOGICAL EXPERIMENTS.....	56
<b>CHAPTER 3: SYNTHESIS AND PHARMACOLOGICAL STUDIES ON BIOCHANIN A DERIVATIVES.....</b>	<b>70</b>
3.1 INTRODUCTION .....	70
3.2 RESULTS .....	72
3.3 DISCUSSION .....	82

<b>CHAPTER 4: SYNTHESIS AND PHARMACOLOGICAL STUDIES ON FORMONONETIN DERIVATIVES .....</b>	<b>85</b>
4.1 INTRODUCTION .....	85
4.2 RESULTS .....	87
4.3 DISCUSSION .....	92
<b>CHAPTER 5: DISCUSSION AND CONCLUSIONS .....</b>	<b>95</b>
<b>REFERENCES.....</b>	<b>100</b>
<b>ANNEX I: ADDITIONAL MATERIAL .....</b>	<b>112</b>
<b>ANNEX II: BUFFERS PREPARATION.....</b>	<b>118</b>
1. GELS COMPOSITION FOR WESTERN BLOT .....	118
2. BUFFERS PREPARATION FOR WESTERN BLOT .....	118

## LIST OF FIGURES

Figure 1. Microglia mobility.....	17
Figure 2. Time-lapse imaging of microglia cells.....	18
Figure 3. Polarization of microglia.....	20
Figure 4. Ligands and activation pathways of TLRs.....	26
Figure 5. Scheme of the MyD88-dependent pathway activated upon TLR-4 dimerization.....	28
Figure 6. Diagram of NF- $\kappa$ B protein structure.....	31
Figure 7. The NF- $\kappa$ B classical pathway .....	33
Figure 8. Molecular structure of the endogenous estrogen 17 $\beta$ -estradiol (E2) .....	34
Figure 9. Schematic representation of the structural and functional organization of nuclear receptors.....	36
Figure 10. Structure of mammalian endogenous estrogen.....	40
Figure 11. Isoflavone structures.....	43
Figure 12. Comparison between the structure of a derivative of isoflavone (genistein) and estrogen (estradiol).....	43
Figure 13. Equol structure. A metabolite from formononetin.....	45
Figure 14. Structural representation of a carbamate group.....	46
Figure 15. Chemical structure of a) rivastigmine and b) muraglitazar.....	47
Figure 16. Representation of a column chromatography.....	52
Figure 17. Chemical reactions involved in the measurement of NO <sub>2</sub> <sup>-</sup> using the Griess Reagent System .....	59
Figure 18. Oxidation reaction of TMB by HRP.....	61
Figure 19. Diagram of the immunedetection of proteins on a Western Blot membrane .....	66
Figure 20. Diagram of the developing of membrane.....	66
Figure 21. Assembly of the transference process.....	67
Figure 22. Diagram of the protocol of a protein detection by Western Blot .....	68

Figure 23. Cell viability of BV2 cells for BCA compound and its derivatives and intermediate .....	75
Figure 24. Effect of Biochanin A (BCA), compound 1, compound 2 and compound 3 on nitric oxide (NO) in BV2 cells stimulated with LPS.....	76
Figure 25. Effect of compound 1 on iNOS expression in BV2 microglia cells.....	77
Figure 26. Effect of BCA on TNF $\alpha$ , IL-6 and IL-1 $\beta$ production in LPS-activated BV2 microglia.....	78
Figure 27. Effect of compound 1 on TNF $\alpha$ , IL-6 and IL-1 $\beta$ production in LPS-activated BV2 microglia.....	79
Figure 28. Effect of compound 2 on TNF $\alpha$ and IL-6 production in LPS-activated BV2 microglia .....	80
Figure 29. Effect of BCA, compound 1 and compound 2 on PGE <sub>2</sub> production in LPS-activated BV2 microglia.....	81
Figure 30. Effect of compound 1 on COX-2 expression in BV2 microglia cells.....	82
Figure 31. Formononetin-dithiocarbamate synthesized by Fu <i>et al.</i> (2017) following a rational molecular hybridation strategy.....	86
Figure 32. Cell viability of BV2 cells for FMN and compound 4.....	89
Figure 33. Effect of Formononetin and compound 4 on nitrite production in LPS-activated BV2 microglia.....	89
Figure 34. Effect of FMN on TNF $\alpha$ , IL-6 and IL-1 $\beta$ production in LPS-activated BV2 microglia.....	90
Figure 35. Effect of compound 4 on TNF $\alpha$ , IL-6 and IL-1 $\beta$ production in LPS-activated BV2 microglia.....	91
Figure 36. Effect of FMN and compound 4 on PGE <sub>2</sub> production in LPS-activated BV2 microglia.....	92

## LIST OF SCHEMES

Scheme 1. Synthesis of the acid chloride .....	54
Scheme 2. Synthesis of BCA derivatives .....	54
Scheme 3. Synthesis of BCA intermediate (compound 3) through a Friedel-Craft reaction .....	55
Scheme 4. Synthesis of Formononetin (FMN) .....	55
Scheme 5. Synthesis of FMN derivative (compound 4) .....	56

## LIST OF TABLES

Table 1. Different subtypes for M2 microglial cells.....	23
Table 2. Toll-like receptor expression in the central nervous system.....	25
Table 3. Five members of NF- $\kappa$ B (nuclear factor kappa-light-chains-enhancer of activated B cells) family in mammals .....	31
Table 4. Recipes and comments on visualization reagents.....	50
Table 5. Representation of the compounds synthesized and used in the present work .....	52
Table 6. Percentage of acrylamide to be used on the confection of running gel depending on the size of the protein to be analyzed.....	64
Table 7. General information for primary antibodies used .....	68

## LIST OF ABBREVIATIONS

15-PGDH (15-hydroxyprostaglandin dehydrogenase)

AD (Alzheimer's disease)

ALS (Amyotrophic lateral sclerosis)

AF-1 (activation function-1 domain)

AF-2 (activation function-2 domain)

Ag (antigen)

ANOVA (analysis of variance)

BBB (blood brain barrier)

CD204 (macrophage scavenger receptor)

CD206 (mannose receptor)

CK (cytokines)

CNS (central nervous system)

Compound **1** (5-hydroxy-3-(4-methoxyphenyl)-4-oxo-4H-chromen-7-yl undecylcarbamate)

Compound **2** (5-hydroxy-3-(4-methoxyphenyl)-4-oxo-4H-chromen-7-yl dodecanoate)

Compound **3** (2-(4-methoxyphenyl)-1-(2,4,6-trihydroxyphenyl)ethan-1-one)

Compound **4** (3-(4-methoxyphenyl)-4-oxo-4H-chromen-7-yl undecylcarbamate)

COX1 (active cyclooxygenases)

COX2 (inducible cyclooxygenases)

DAMPs (damage-associated molecular patterns)

DBD (DNA-binding domain)

DPBS (Dulbecco's phosphate-buffered saline)

E2 (17  $\beta$ -estradiol)

ED (extracellular domain)

EDTA (ethylenediaminetetraacetic acid)

ENS (enteric nervous system)

ERE (estrogen response element)

ERs (estrogen receptors)  
FMN (Formononetin)  
GI (gastrointestinal)  
HAT (histone acetyltransferase)  
HDACs (histone deacetylases)  
HSP (heat-shock proteins)  
HRE (hormone response element)  
HCMEC/D3 (Human Brain Endothelial Cell Line)  
ID (intracellular domain)  
IL (interleukin)  
IL-1 $\beta$  (interleukin 1-beta)  
IL-6 (interleukin 6)  
iNOS (inducible nitric oxide synthase)  
IC<sub>50</sub> (half maximal inhibitory concentration)  
IRF3 (Interferon regulatory factor 3)  
LBP (LPS-binding protein)  
LPS (lipopolysaccharide)  
LRR (leucine-rich repeats)  
M1 (microglia classical activation)  
M2 (microglia alternative activation)  
MAPK (mitogen-activated protein kinase)  
MD-2 (myeloid differentiation factor 2)  
MHC II (major histocompatibility complex II)  
MMPs (matrix metalloproteinases)  
MS (Multiple Sclerosis)  
MyD88 (myeloid differentiation primary response gene 88)  
NO (nitric oxide)  
NOD-like (nucleotide-binding oligomerization receptors)

NR (nuclear receptor)

PAMPs (pathogen-associated molecular patterns)

PBS (phosphate-buffered saline)

PMS (N-methyl dibenzopyrazine methyl sulfate)

PD (Parkinson's disease)

PGE<sub>2</sub> (prostaglandine E<sub>2</sub>)

PGs (prostaglandins)

PNS (peripheral nervous system)

PRRs (pattern recognition receptors)

RLGs (RIG-like receptors)

ROS (reactive oxygen species)

SARM (sterile and HEAT-Armadillo motifs-containing protein)

SEM (standard error of the mean)

SERM (selective estrogen receptor modulator)

TGF- $\beta$  (transforming growth factor beta)

THF (tetrahydrofuran)

TIR (Toll-interleukin-1 receptor)

TIRAP (TIR domain-containing adaptor protein)

TLRs (Toll-like receptors)

TLR-4 (Toll-like receptor 4)

TNF- $\alpha$  (tumor necrosis factor alpha)

TRAM (TRIF-related adaptor molecule)

TRIF (TIR domain-containing adaptor inducing IFN-b)

# CHAPTER 1: GENERAL INTRODUCTION

## 1.1 NEUROGLIA CELLS

The concept of neuroglia, glial cells or merely glia, was introduced in 1858 by Rudolf Virchow who suggested the existence of a “connective substance, which forms in the brain, in the spinal cord, and in the higher sensory nerves a kind of Nervenkitz (neuroglia), in which the nervous system elements are embedded”. In other words, Virchow considered neuroglia an element that fills “space not occupied by neurones” that “also contains a certain number of cellular elements”. However, the second part of 19th century was a golden age of cellular histology, and soon after initial findings, many different forms of glial cells were described. Conversely, after all these years, the function of glial cells in the nervous system is still not well understood (Verkhatsky and Butt, 2015).

The term *glia* (from the Greek word meaning “glue”) reflects the nineteenth-century belief that these cells held the nervous system together somehow. The word still remains, despite the lack of any evidence that binding neurons together is among the many functions of glial cells. Glial roles that are actually well-established include maintaining the ionic milieu of nerve cells, modulating the rate of nerve signal propagation, modulating synaptic action by controlling the uptake of neurotransmitters, providing a scaffold for some aspects of neural development, and aiding in (or preventing, in some occasions) recovery from neural injury (Purves *et al.*, 2001).

Glia cells are a far cry from neurons. That is so, that glial do not participate directly in the synaptic process meaning they cannot send electrical signals as such but instead, they support neurons during this task (Purves *et al.*, 2001). The more recent definition is based on the systemic function of all neuroglia cells and defines neuroglia as “*nonneuronal* cells residing in the brain responsible for the homeostatic maintenance of the nervous system, represented by highly heterogeneous cellular populations of different origin, structure, and function” (Verkhatsky and Butt, 2013).

Neuroglia in the mammalian nervous system is divided into the central nervous system (CNS) glia and peripheral nervous system (PNS) glia. Microglia are glial derived from hematopoietic stem cells in mesodermal tissue within the CNS. They share many characteristics with macrophages from the periphery since they derive from monocytes

precursors. Hence, their main function is to remove cellular debris from sites of injury and to initiate an immune response (Purves *et al.*, 2001).

## **1.2 ROLE OF MICROGLIA CELLS IN NEUROINFLAMMATION**

### **1.2.1 Overview**

It is widely assumed that the CNS is an immune-privileged tissue, suggesting that any antigen or strange organism entering the brain and spinal cord do not initiate an immune response. While this idea has been hypothesized over the last 70 years, it is clear that immune privilege is not unconditional since immune responses do take place in the CNS and are vital for both modelling the brain during development and controlling infections in the brain. However, it is undeniable that the brain is much better protected than other organs given the presence of the blood brain barrier (BBB) and any type of cell or strange body cannot just enter at their will. Nonetheless, when the BBB is compromised, it is unable to control such selection, thus contributing to the tissue damage (Woodrooffe and Amor, 2013). Besides the presence of this gatekeeper, there are specific cells responsible for initiating an immune response at this level, that is microglia cells.

Microglia are one of the glia cell types known as the brain immune cells acting as specialized macrophages capable of phagocytosis that protect neurons of the central nervous system. They can either phagocyte dead neurons or assist them after brain tissue injury. To accomplish its function, microglia cell undergoes dynamic changes on its structure. Microglia also participate in the physiology of the nervous system through regulation of development and connectivity of neural networks, combining thus, a defensive role with homeostatic and neuroprotective functions (Verkhratsky and Butt, 2015).

Nevertheless, for the major part of a century, the function of microglia in the CNS was a topic of controversy. Originally identified by Franz Nissl in 1899 as ‘Stabchenzellen’ or rod-like cells and further classified by Pío del Río Hortega in 1919, these cells were described as non-neuronal and non-astrocytic population. Furthermore, Hortega’s observation suggested a capacity for phagocytosis, indicating that these cells were more than just space filler or connective cells between neurons, a breakthrough that was not accepted until 60 years later, not even by Hortega’s mentor, Ramon y Cajal, who urged Hortega not to publish. Thus, it was not until the early 1980s, when the

development of new technologies and ideas began to reveal the true nature of microglia as the brain's resident immune cells giving Hortega the credit he deserved (Cherry *et al.*, 2014).

### 1.2.2 Microglia distribution and morphology

Microglial cells are mesodermal in origin but their precursors are not simply blood macrophages, but rather derive from primitive myeloid progenitors that originate from the extraembryonic yolk sac (Verkhatsky and Butt, 2015).

Microglia are well-organised in the brain and are homogeneously distributed throughout the CNS, with more or less similar densities in different regions. The microglial cells in the healthy CNS have small cell bodies from which several main processes are extending. Every cell has its own territory, about 15-30  $\mu\text{m}$  diameter, so rare is the occasion in which microglia's processes overlap.

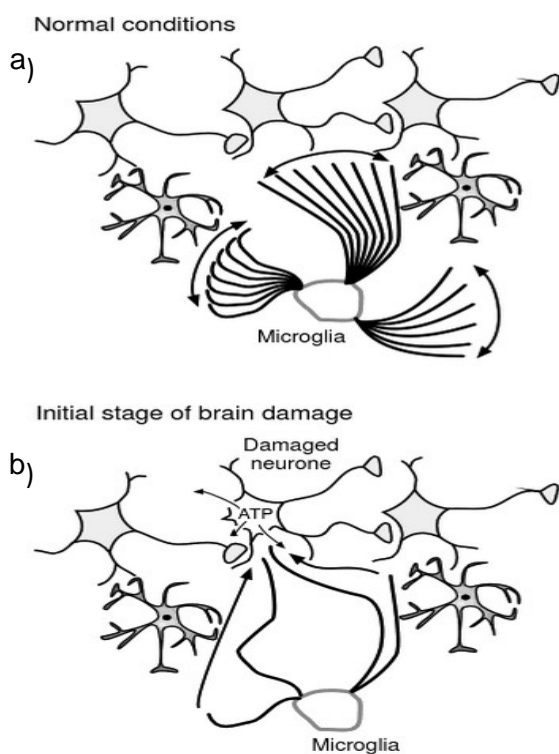


**Figure 1. Microglia mobility.** a) Microglia processes in health tissue scanning its territory. b) Microglia responding to injury by addressing its processes to the site of insult (Verkhatsky and Butt, 2013).

As *resting microglia*, these cells are the fastest moving cells in the brain. Their processes are continuously scanning their territory in search of any anomaly; this is a fairly rapid movement with a speed of nearly 1.5  $\mu\text{m}/\text{min}$  and thus microglial processes represent the fastest moving structures in the brain. At the same time, microglial processes also constantly send out and retract small protrusions, which can grow and contract by 2–3  $\mu\text{m}/\text{min}$ . Considering the velocity of these movements, the parenchyma of the brain can be completely scanned by microglial processes every several hours (Figure 1). Such sophisticated system, endows the CNS with the ability of immediately respond to CNS damage and a pathological event, in which *resting microglia* become *activated* undergoing a morphological transformation from resting cells to amoeboid-like morphology which gain more motility and act as tissue

macrophages (Figure 2). These activated cells have the capacity to migrate, proliferate and phagocytise. During this transition, resting microglia retract their processes, which become fewer and much thicker, increase the size of their cell bodies acquiring an amoeboid-like shape, change the expression of various pro-inflammatory enzymes and receptors and begin to produce immune response molecules such as cytokines (CKs) triggering a state of acute neuroinflammation (Verkhratsky and Butt, 2013).

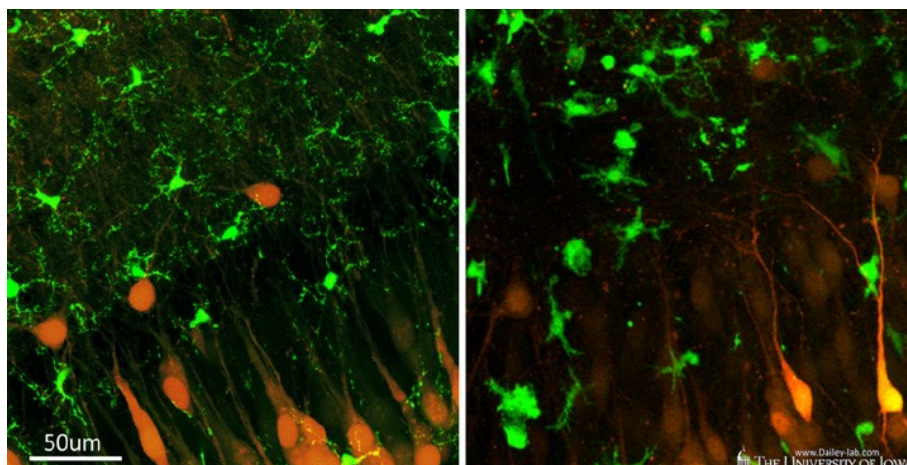


**Figure 2. Time-lapse imaging of microglia cells.** a) Inactivated microglia cells with highly ramified branches. b) Activated microglia possess an enlarged cell body with shorter branches (Dailey, n.d.).

### 1.2.3 The two faces of microglial cells in neuroinflammation

Within the CNS, inflammation and innate immunity are believed to contribute to the pathogenesis and neurodegeneration that occur in several diseases and conditions. In the context of neuroinflammation, research had been focusing on the roles of innate immune cells (macrophages, dendritic cells and granulocytes) of the periphery and which are capable of egress in the brain. However, bias has changed in order to study the roles of CNS resident cells, including astrocytes and microglia. In the subsequent sections of this chapter, we will discuss the emerging roles of CNS microglia resident cells.

#### 1.2.3.1 Defining neuroinflammation

Inflammation is a complex phenomenon within the body triggered by mechanical, chemical or biological factors. The characteristics of any of these factors along with the time of exposure to them determine the type of inflammatory response generated: acute or chronic. Acute inflammation may be beneficial as a mean to restore the

homeostasis at the place of injury. Problem arises when the source of the stimuli is permanent in a way that the immune system enters in a vicious cycle and a state of chronic inflammation is established. In the central nervous system (brain and spinal cord) that state is termed as neuroinflammation.

Unresolved neuroinflammation generally leads to chronic neurodegenerative diseases, which are commonly characterized by the decline of cognitive functions. These include Alzheimer's disease, Multiple Sclerosis, Parkinson's disease and other dementias. Due to the implication of neuroinflammation in such kind of diseases, the regulation of inflammation in the CNS is one of the relevant processes involved in the pathogenesis of neurodegenerative disorders. Immune activation in the CNS always involves the innate immunity activation as a first step and, therefore, the activation of microglia and astrocytes cells, which in normal conditions are in charge of the regulation of homeostasis of the brain tissue. Although peripheral immune cells are also important to spread the inflammatory signals within the CNS.

#### 1.2.3.2 Role of microglia cells and its parallelism with macrophages

Both *in vitro* and *in situ* studies of peripheral macrophages have demonstrated that macrophages have different phenotypes meaning that they can vary with respect to their activation state. As a result, macrophages can contribute to either pro or antiinflammatory processes (Woodroffe and Amor, 2013). The phenotype activated will depend on the "microenvironment" created by cytokines released by the immune cells, which will lead the polarization of the immune response.

In agreement with Hortege's original description, microglia have been classically described to exist in two states or phenotypes, resting and activated (Cherry *et al.*, 2014). However, due to its nature as immune cells, microglia are never truly 'resting' but constantly scanning around them for new threats in efforts to maintain homeostasis. Therefore, as the 'resting' term is not accurate neither it is considering the 'activated' state as a single state. In fact, the term 'activation' is an oversimplification of a range of different activated states.

So far, two major activated microglia states have been described. The first is *classical activation*, in which microglia cells produce a pro-inflammatory response, while the second is referred to as *alternative activation* in which microglia promotes an antiinflammatory phenotype involved in damage repair and debris clearance (Figure 3)

(Cherry *et al.*, 2014; Colton, 2009). Nonetheless, all phenotypes have in common that they work to support and protect the structural and functional integrity of the CNS (Verkhatsky and Butt, 2013).

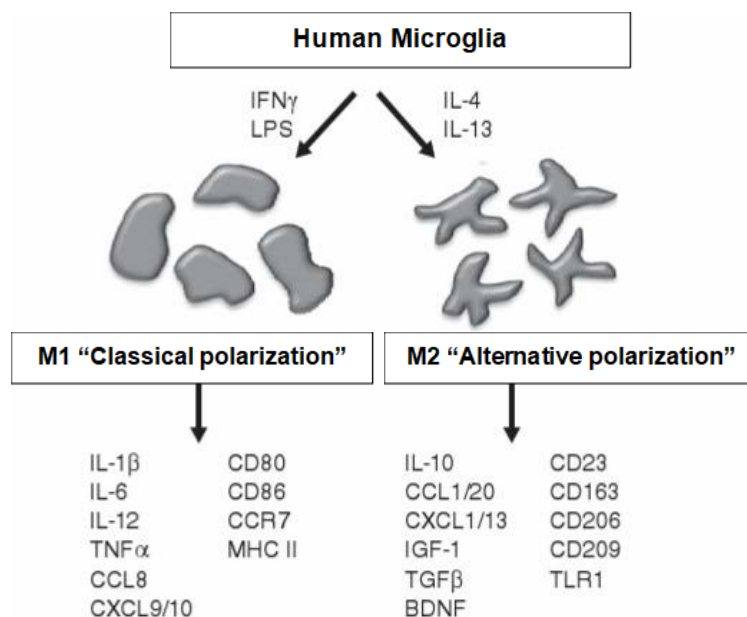


**Figure 3. Polarization of microglia.** M1 polarization (classical activation) can be accomplished in the presence of pro-inflammatory mediators whereas M2 polarization (alternative activation) is commonly achieved through the addition of IL-4 or IL-13 (adapted from Woodroffe and Amor, 2013).

### 1.2.3.3 Classical activation: M1 cells

Microglia cells, as macrophages in the periphery and other immune cells, have the ability of identifying exogenous molecules triggering the release of cytokines, among others. Cytokines function as immune messengers between cells to promote the classical activation state. The classical activation state has classically termed as M1 cells and this term is equivalent to the Th1/2 terminology used for T cells in the periphery. By these means, microglia cells manage to promote the pro-inflammatory responses required to clear the infection or to boost the adaptive immune response (Woodroffe and Amor, 2013).

The functional effects of classical activation are geared towards antigen (Ag) presentation and the killing of intracellular pathogens. Therefore, many immune receptors and enzymes are upregulated in order to serve that purpose. Once a ligand binds any of the wide range of immune receptors expressed on microglia cells, an overall upregulation of costimulatory molecules as well as the major histocompatibility

complex II (MHC II) is induced to allow for Ag-presenting activity of microglia and increased crosstalk within other immune cells (Cherry *et al.*, 2014). M1 cells also upregulate levels of some Toll-like receptors (TLRs), several cell surface and intracellular molecules (CD14, CD11b, CD45, CD68) and matrix metalloproteinases (MMPs). With respect to cytokine production, M1 cells secrete pro-inflammatory cytokines, including interleukin (IL) such as IL-1 $\beta$ , IL-6, IL-12, IL-23 and tumor necrosis factor alpha (TNF- $\alpha$ ). Especially, TNF $\alpha$  and IL-1 $\beta$  have been demonstrated to have an important role in the development of CNS inflammation through the disturbance of BBB, which further facilitates the infiltration of peripheral immune cells enhancing the inflammation process (Lei *et al.*, 2015). In addition to cytokines, several chemokines and other effector molecules are produced (Woodroffe and Amor, 2013) as well as reactive oxygen species (ROS). It is worth mentioning that one of the most important ROS is nitric oxide (NO) which is released by a key microglia enzyme, the inducible nitric oxide synthase (iNOS) (Cherry *et al.*, 2014).

Prostaglandins (PGs) are another group of molecules very present during inflammatory processes and it is a major element during chronic inflammation and cancer (Kalinski, 2012). PGE<sub>2</sub> affects microglial activation including migration, phagocytosis, and production of cytokines and nitric oxide (Nagano *et al.*, 2016). Being by-products of arachidonic acid, produced by cyclooxygenases (constitutively active COX-1 and inducible COX-2) and prostaglandin synthases, they are characterised by their lipid structure formed by 20 carbons and a pentane. PGE<sub>2</sub> is the main product of COX-2 and its presence requires a rigorous balance between COX-2 and 15hydroxyprostaglandin dehydrogenase (15-PGDH), an enzyme responsible for driving PGE<sub>2</sub> degradation process (Kalinski, 2012). Concentrations of the pro-inflammatory PGE<sub>2</sub> has proved to be elevated in patients suffering from neurodegenerative diseases having its effect on glial cells since PGE<sub>2</sub> receptors are expressed in their surface, however, they are not specific of these cells. In fact, neurons express such receptors to a higher extent than other cells in the brain (Zhu *et al.*, 2005). This situation makes harder to identify the exact role of PGE<sub>2</sub> in neuroinflammation.

All in all, the ratio of particular cytokines has been used to identify inflammatory microglia. For example, it was suggested that IL-12 high, IL-10 low production is a simple way to distinguish inflammatory cells (Mantovani *et al.*, 2004). However, due to the plastic nature of microglia cells, classifying this cells *in vivo* is not easy practice.

#### 1.2.3.4 Alternative activation: M2 cells

In contrast with pro-inflammatory M1 cells, alternatively activated microglia cells, so-called M2 cells, express cytokines and receptors that are implicated in inhibiting inflammation and restoring homeostasis once the risk of infection or damage has been dealt with. Examples of anti-inflammatory cytokines are IL-10, TGF- $\beta$  and IL-1 receptor antagonist (IL-1Ra). IL-10 exerts the opposite effects to those caused by proinflammatory cytokines, through modulation of the latest, chemokines and oxidative species in microglia (Lei *et al.*, 2015). Consequently, it appears that when there is a lack of M2 cell differentiation in the CNS, problems can arise.

As M2 macrophages, M2 microglia are characterized by their enhanced ability to phagocytise and secrete anti-inflammatory and neurotrophic factors that can promote repair. Within M2 phenotype, diverse subsets can be identified. However, their characterization by markers is not an easy matter since not many are well established. Interestingly, there are two enzymes, which despite their opposite function, can be two powerful markers. Such enzymes are the inducible nitric oxide synthase (iNOS) and the enzyme arginase 1 (Arg1). Ironically, by using arginine, which is the same substrate used by iNOS, Arg1 can effectively compete with iNOS to downregulate production of NO. Despite the benefit of having specific markers, using just one or two is limiting and ignores the overall diversity of M2 phenotypes (Cherry *et al.*, 2014; Corraliza *et al.*, 1995).

Therefore, and due to their nature, another way to classify the function and phenotype of M2 cells is based on the cytokines that induce them. In this sense, three subtypes have been identified depending on what cause their alternative activation and classify as 'M2a', 'M2b' and 'M2c' (Table 1).

An important consideration regarding M2 phenotypes is that these states were typically elucidated *in vitro* following exposure to a few stimuli. This does not represent the complex environment given in tissue. Moreover, such detailed classification has been primarily observed in the periphery. Therefore, there is a controversy whether this classification should be applied or not to the brain resident microglial cells.

**Table 1. Different subtypes for M2 microglial cells:** M2a, M2b and M2c. (IL: interleukin, TLR: toll-like receptor, NF- $\kappa$ B: nuclear factor kappa-light-chain-enhancer of activated B cells, Arg1: argenine 1, TGF- $\beta$ : Transforming growth factor beta).

M2 Subtype	Activating factor	Comments
M2a	IL-4 IL-13	Their main function appears to be suppression of inflammation. Upon activation by IL-4 and IL-13 through IL-4R $\alpha$ , a downstream process that lead to potent anti-inflammatory functions is induced (inhibition of NF- $\kappa$ B, Arg1 upregulation, production of scavenger receptors for phagocytosis) (Gadani <i>et al.</i> , 2012).
M2c	IL-10 glucocorticoids TGF- $\beta$	Appear to be involved in tissue remodelling after inflammation has been controlled (Cherry <i>et al.</i> , 2014).
M2b	TLR	No specific markers for M2 have been found for this subset. However, they do express the typical IL-10 high, IL-12 low M2 cytokine profile (Mantovani <i>et al.</i> , 2004).

### 1.3 TOLL-LIKE RECEPTORS IN NEURODEGENERATION

While the CNS was once considered an immune-privileged site, it is now recognized that both infiltrating and CNS resident cells actively participate in several aspects of innate immunity and are important for maintaining neural function (Hansson and Edfeldt, 2005). Particularly, microglia and astrocytes are the innate immune cells responsible for maintaining the homeostasis in the brain whenever a threat, either exogenous or endogenous, disturbs the biological balance. These cells do not act on their own but also recruit and activate cells that participate in the adaptive immunity. As such, they display a series of inflammatory mediators, which in turn, may also increase the expression of Toll-like receptors (TLRs) in the CNS cells. Therefore, the role of TLRs in neurodegenerative diseases has been under study, for example, in Alzheimer's disease (AD) where the absence of acute inflammation but persistent glial

activation is observed and, in Multiple Sclerosis (MS) where an adaptive immune response is provoked following glial stimulation and inflammation (Popovich *et al.*, 2008).

Taken all together, in the subsequent sections of this chapter, an overview of the innate immune system focusing on TLRs and more specifically on the Toll-like receptor 4 (TLR-4) activation and the signalling pathways for which is responsible and its role in neuroinflammation by modulating microglial cells will be given.

### **1.3.1 Overview of toll-like receptors activation and signalling**

Prior to activating the adaptive immune response, cells of the innate immune system first respond to pathogens, or danger signals, within their environment. Innate immune cells such as dendritic cells, macrophages and monocytes in the periphery and, astrocytes and microglia cells in the CNS, all possess both surface and intracellular receptors capable of recognizing pathogen-associated molecular patterns (PAMPs) and damage-associated molecular patterns (DAMPs) (Woodroffe and Amor, 2013; Suzumura and Ikenaka, 2013). Some examples of PAMPs are lipopolysaccharide (LPS), peptidoglycan, lipoteichoic acids and mannans, which are widely expressed by bacteria but are not present on host tissues. They are recognized by the pattern recognition receptors (PRRs) of the innate immune cells to distinguish pathogens from self-antigens. Amongst the large number of different PRRs are the Toll-like receptors, which are the best known group of innate immune receptors (Woodroffe and Amor, 2013; Cherry *et al.*, 2014).

The toll gene was originally identified by Christiane Nüsslein-Volhard, Eric Wieschaus and colleagues in the fruit fly *Drosophila melanogaster* in 1985 (Hansson and Edfeldt, 2005). In accordance with the *Drosophila* receptor, mammalian TLRs are expressed by cells of the innate immune system being specific for different components of microbes (Delves *et al.*, 2011; Lu *et al.*, 2008).

Different cell types express TLRs in the brain (Table 2). They are not, however, always expressed at the same extent. For instance, TLRs are barely expressed in astrocytes in normal conditions, but when the situation changes and an inflammatory process begins, higher levels of TLRs are detected on their surface (Bsibsi *et al.*, 2002). TLRs are also expressed in microglia cells, which represent the first line of innate defense against viral and bacterial infection of the CNS. These cells respond to TLR stimulation

by producing cytokines and other inflammatory mediators and by enhancing phagocytosis of microorganisms and aggregated extracellular proteins. So much so that, microglia express all TLRs expressed in humans (Table 2).

**Table 2. Toll-like receptor expression in the central nervous system.** TLR: Tolllike receptor; LPS: lipopolisacharide (Woodroofe and Amor, 2013).

TLR	LIGAND	CELL TYPE				
		Neuron	Astrocyte	Oligodendrocyte	Microglia	Brain Endothelium
<b>TLR1</b>	Tryacylated lipoproteins		✓		✓	
<b>TLR2</b>	Glycolipids, lipoproteins		✓	✓	✓	✓
<b>TLR3</b>	dsRNA	✓	✓	✓	✓	✓
<b>TLR4</b>	LPS		✓		✓	✓
<b>TLR 5</b>	Flagellin		✓		✓	✓
<b>TLR6</b>	Diacylated lipoproteins				✓	✓
<b>TLR7</b>	ssRNA	✓			✓	✓
<b>TLR8</b>	ssRNA	✓			✓	✓
<b>TLR9</b>	Unmethylate d CpG-DNA	✓	✓		✓	

Pathogen components such as LPS can readily induce the activation of microglia cell. TLR4 signalling has been well established in the pathologies of neuroinflammation. Two rather important transcription factors activated by TLR signals are NF- $\kappa$ B, which promotes the expression of various cytokines and endothelial adhesion molecules; the interferon response factor 3 (IRF3), which stimulates the production of type I interferons, cytokines that block viral replication during an antiviral response (Figure

4) (Delves *et al.*, 2011); and the p38 MAPK (mitogen-activated protein kinase) which also has essential roles in inflammation, apoptosis, cell cycle and differentiation (see review: Zarubin and Han, 2005). They also induce the activation of COX-2 and iNOS enzymes, which are essential to induce potent immune responses (Lei *et al.*, 2015). Indeed, nitric oxide (NO) production, mediated by the iNOS enzyme, has been extensively associated to neuroinflammation and neurodegenerative processes (Morales *et al.*, 2014). For instance, in patients with AD, increased production of iNOS causes post-translational modifications instigated by NO, resulting in the increment of A $\beta$  peptide aggregation in the amyloid plaques (Butterfi *et al.*, 2007; Kummer *et al.*, 2011). In addition, epidemiological studies advocate that COX inhibitors reduce the risk of AD and PD (Krause and Muller, 2010).

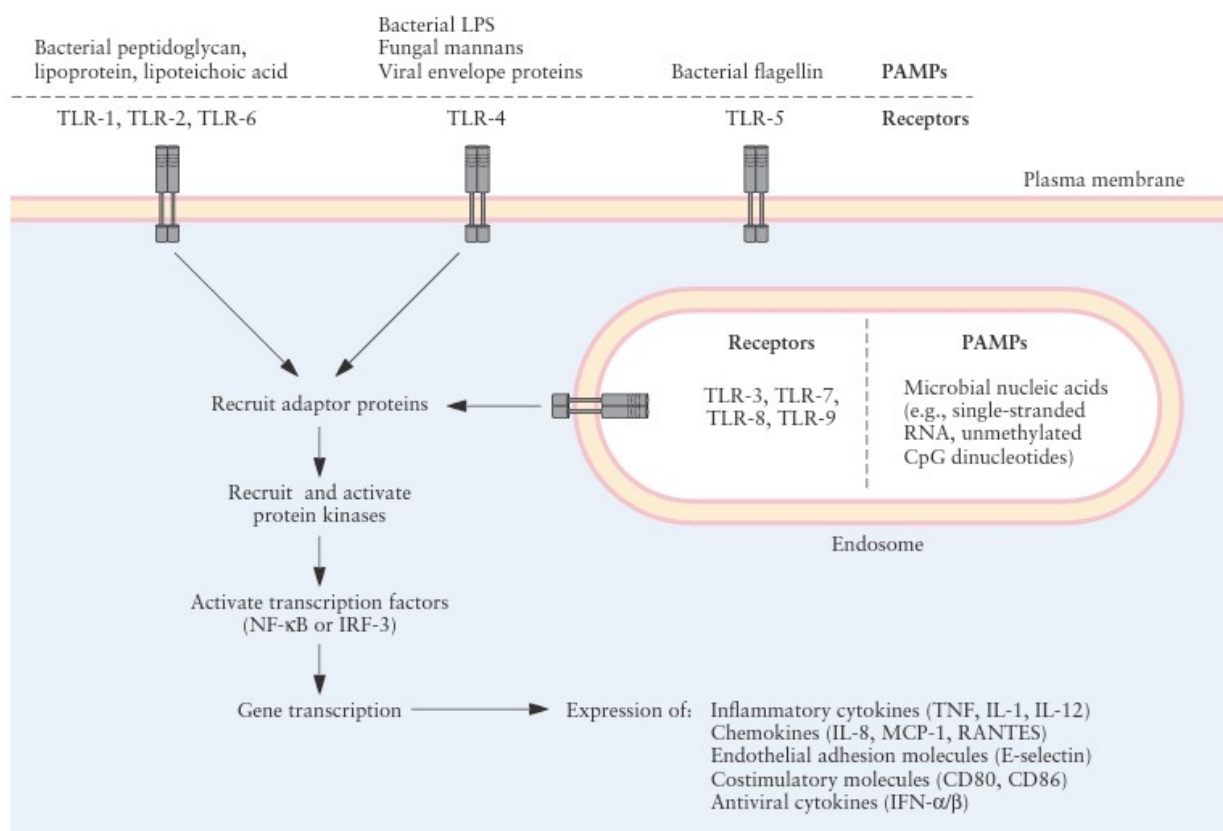


**Figure 4. Ligands and activation pathways of TLRs.** Different microbial antigens join to and stimulate different TLRs. These several TLRs, expressed either at the cell surface or in endosomes, activate similar signalling mechanisms, which provoke innate immune responses. Other receptors, such as those for viral RNA or bacterial peptides are found in the cytoplasm. (IFN, interferon; IRF-3, interferon response factor 3; LPS, lipopolysaccharide; NF- $\kappa$ B, nuclear factor  $\kappa$ B; TNF, tumor necrosis factor; MCP-1, monocyte chemoattractant protein 1) (Abbas *et al.*, 2014).

Within the wide spectrum of TLRs, in particular, TLR4 has shown to be highly expressed on microglia mediating neuroinflammatory diseases. Numerous studies have demonstrated TLR4-dependent activation of microglia in neurodegenerative diseases such as AD and PD (Yao *et al.*, 2013; Lehnardt *et al.*, 2003). LPS is one of the best studied bacteria endotoxins that could eventually cause systemic inflammation and sepsis through TLR4 if the inflammatory response is amplified and uncontrolled.

Upon LPS recognition, TLR4 undergoes dimerization and recruits its downstream adaptors. Such adaptor proteins are MyD88 (myeloid differentiation primary response gene 88), TIRAP (TIR domain-containing adaptor protein, also known as Mal, MyD88adaptor-like), TRIF (TIR domain-containing adaptor inducing IFN- $\beta$ ), TRAM (TRIF-related adaptor molecule), and SARM (sterile and HEAT-Armadillo motifs-containing protein). Different TLRs use different combinations of adaptor proteins allowing a differential downstream signalling. Interestingly, TLR4 is the only known TLR which utilizes all these adaptor proteins through the MyD88-dependent pathway.

MyD88-dependent pathway (Figure 5) was shown to be responsible for proinflammatory cytokine expression by recruiting and sequentially activating a set of adaptor proteins which in turn activate two different kinase enzymes, that is IKK (I $\kappa$ B kinase) and MAPK (mitogen-activated protein kinase). The activation of these kinases drives a rapid phosphorylation and release of two major transcription factors protein complexes: NF- $\kappa$ B and AP-1 respectively. Both transcription factors have an important role in the expression of pro-inflammatory cytokines. It should be noted that, NF- $\kappa$ B and AP-1 phosphorylation is still induced in the MyD88-deficient macrophages suggesting that they can also be activated through a MyD88-independent pathway (Lu *et al.*, 2008).

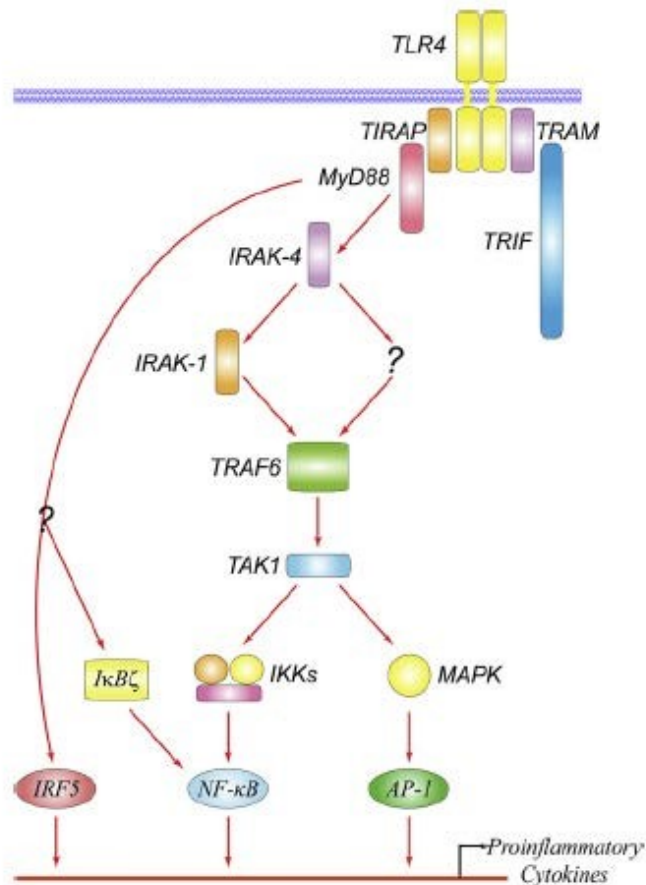


**Figure 5. Scheme of the MyD88-dependent pathway activated upon TLR-4 dimerization.** The purpose of this signal is to activate two main pro-inflammatory pathways: the IKK protein complex which allows the NF- $\kappa$ B transcription factor to enter into the nucleus, and the MAPK leading to the induction of the AP-1 transcription factor (Lu *et al.*, 2008).

### 1.3.2 Toll-like receptors and microglia in neurodegenerative diseases

As stated before, TLRs are narrowly related to pro-inflammatory mediators' release and vice versa. Therefore, their function has been associated with several neurodegenerative diseases.

Many studies have considered the way TLRs may affect, for instance, Alzheimer's disease. As the most common cause of dementia in human characterized by progressive neurodegeneration, a lot of attention has been drawn to this disease to be studied from many angles. It is widely known that AD is characterized by the extracellular accumulation of amyloid beta peptides ( $A\beta$ ) in neuritic plaques and the intercellular aggregation of hyperphosphorylated tau protein in neurofibrillary tangles. In addition to these pathological hallmarks, inflammation orchestrated by the innate

immune system is observed in the brain of AD patients (Akiyama *et al.*, 2000). That is because A $\beta$  exerts a direct action on neurons but also an indirect pro-inflammatory action through microglia cells to produce neurotoxicity promoting neurodegeneration (for reviews see: Yu and Ye, 2015; Heneka *et al.*, 2015). A $\beta$ 42 has been reported to interact with microglial cells through several reported cell surface receptors and here is where TLRs take part in the development of neuroinflammation. A $\beta$  recognition has been reported to be mediated by microglial cells TLRs through the interaction with other cell surface receptors to initiate the activation of intracellular signalling pathways.

As seen in section 1.3.1, TLRs activated by any of its ligands, in this case A $\beta$ , would lead in the production of pro-inflammatory cytokines and reactive oxygen and nitrogen radicals contributing to the inflammatory response and neuronal toxicity. However, TLRs along with CD14 have been implicated in the phagocytosis of A $\beta$  addressed by microglia (Liu *et al.*, 2012). Despite the latest beneficial role of microglia, apparently, as the disease progresses, this ability to phagocyte the accumulation of A $\beta$  decreases due to a reduction on the expression of A $\beta$ -degrading enzymes, therefore, promoting the production of pro-inflammatory modulators (for reviews see: Yu and Ye, 2015; Arroyo *et al.*, 2011).

MS is another chronic neurodegenerative disease characterized by the demyelination of neurons due to neuroinflammatory processes that involves activated lymphocytes, macrophages and resident glial cells (astrocytes and microglia) in the brain, although the etiology is not completely clear. As for AD, TLRs and microglia have also been associated to this over-inflammatory processes in MS (see Arroyo *et al.*, 2011).

### **1.3.3 The Rel/NF- $\kappa$ B signal transduction pathway**

Rel or NF- $\kappa$ B (nuclear factor kappa-light-chains-enhancer of activated B cells) complex was first discovered in B cells and described as a nuclear factor that bound to  $\kappa$ B DNA sites (Chen *et al.*, 1999). There are numerous evidences that indicate that the major signal pathway involved in the onset and amplification of the inflammatory response is that which affects to the NF- $\kappa$ B activation. These proteins comprise one of the most ubiquitous family of transcription factors that are involved in the control of several cellular processes, such as immune and inflammatory responses (since light chains kappa are immunoglobulin crucial components), cell development, cellular proliferation, and apoptosis. Hence, uncontrolled deregulation of NF- $\kappa$ B by any

pathological situation, is related to inflammatory and autoimmune diseases as well as cancer (Gilmore, 2006).

From a structural point of view, Rel/NF- $\kappa$ B is an ensemble of protein dimers that share a common N-terminal domain of 300 amino acids that controls DNA transcription. The N-terminal is a highly conserved DNA-binding/dimerization domain (DBD) so-called the Rel homology (RH) domain (Figure 6). RH domain mediates either heter- or homodimerization which is required for the transcription factor to bind to the DNA target site. Different dimers possess distinct transcriptional functions on the grounds of that they directly bind to enhancer sequences of distinct genes (Chen *et al.*, 1999). NF- $\kappa$ B dimers are originated from the combination of five different proteins: p105 or p50, p100 or p52, RelA or p65, RelB, c-Rel from which only the last three can directly activate the transcription of target genes (Table 3) (Phelps *et al.*, 2000). The p50-p65 heterodimer is the most abundant form of NF- $\kappa$ B dimers (Chen *et al.*, 1999).

Rel/NF- $\kappa$ B proteins can be divided into two classes based on the presence or absence of an activation domain (Phelps *et al.*, 2000) located in the C-terminal domain to the RH domain:

- Members of **class one** (NF- $\kappa$ B proteins p105, p100) have long C-terminal domains that contain multiple copies of ankyrin repeats, which act as transcriptional repressors. This domain is known as TRD (transrepression domain). However, p105 and p100 are not active by themselves but they need to be split into shorter sequences by either proteolysis or arrested translation to p50 and p52 respectively. As such, these first class members are usually not activators of transcription but repressors, however they can induce gene expression when forming dimers with members of the second class of Rel/NF $\kappa$ B transcription factors.
- The **second class** (the Rel proteins) includes c-Rel (and its retroviral homologue  $\nu$ -Rel), RelB, RelA (p65). This second class of Rel proteins contains a C-terminal transcriptional activation domain (TAD), which enables gene expression. Hence, Class II NF- $\kappa$ B promotes gene expression being downregulated by Class I.

The NF- $\kappa$ B active and functional is captured in the cytosol forming an inactive complex

due to its binding to NF- $\kappa$ B inhibitors (I $\kappa$ B $\alpha$ , I $\kappa$ B $\beta$ , I $\kappa$ B $\epsilon$ , I $\kappa$ BY, I $\kappa$ B $\zeta$  and Bcl-3) in resting cells (Phelps *et al.*, 2000). Therefore, NF- $\kappa$ B belongs to the category of "rapid-acting" transcription factors meaning it does not required a synthesis of *novo* (other members of this family include transcription factors such as c-Jun, STATs, and nuclear hormone receptors) (Bonizzi and Karin, 2004).

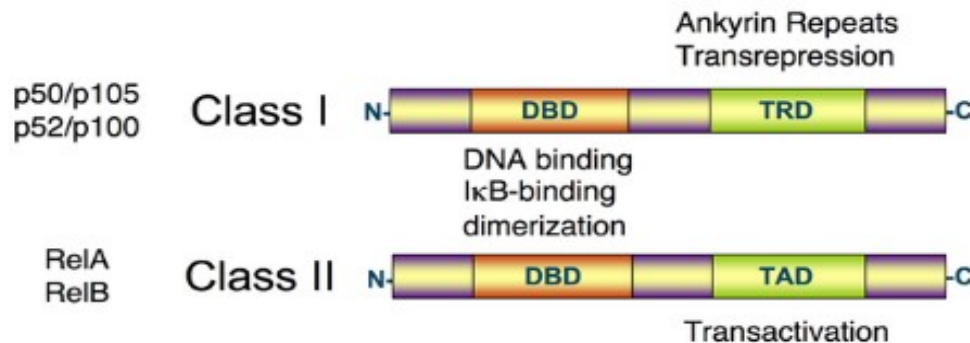


**Figure 6. Diagram of NF- $\kappa$ B protein structure.** Structurally speaking, two classes of NF- $\kappa$ B proteins can be differentiated: class I and class II. Both contain a N-terminal DNA-binding domain (DBD) and a C-terminal fragment. The latter determines the protein function. Whilst class I proteins contain ankyrin repeats endowed with transrepression activity (TRD), class II proteins are formed by a transactivation domain (TAD) which activates the transcription of target genes (Wikipedia contributors, n.d.).

**Table 3.** Five members of NF- $\kappa$ B (nuclear factor kappa-light-chains-enhancer of activated B cells) family in mammals.

CLASS	PROTEIN	ALIAS	GEN
Class I	NF- $\kappa$ B1	p105 $\rightarrow$ p50	<i>NF<math>\kappa</math>B1</i>
	NF- $\kappa$ B2	p100 $\rightarrow$ p52	<i>NF<math>\kappa</math>B2</i>
Class II	RELA	p65	<i>RELA</i>
	RELB		<i>RELB</i>
	c-REL		<i>REL</i>

Three different NF- $\kappa$ B activation pathways have been described, the *classical* or *canonical pathway* (Figure 7), the *alternative* or *non-canonical pathway* and the third *atypical pathway* which is induced by agents that damage the DNA such as reactive oxygen species or ultraviolet radiation. Nonetheless, the most frequent pathway observed is the classical, which is activated in response to various inflammatory stimuli. The TNF $\alpha$ , IL-1 $\beta$ , lymphocyte T receptor (TCR) and many bacterial products such as LPS are solely a few examples of molecules that lead to NF- $\kappa$ B activation and

rapid changes in gene expression (Bonizzi and Karin, 2004). Since the methodology followed in this work in order to induce an inflammatory response by BV2 microglia cells involves activation by LPS, only the classical pathway is deeply described below.

### Classical or canonical pathway

As recently mentioned, in unstimulated cells, the NF- $\kappa$ B dimers are sequestered in the cytoplasm by a family of inhibitors, called I $\kappa$ Bs (Inhibitor of  $\kappa$ B). Although the I $\kappa$ B family consists of I $\kappa$ B $\alpha$ , I $\kappa$ B $\beta$ , I $\kappa$ B $\epsilon$ , and Bcl-3, the best-studied and major I $\kappa$ B protein is I $\kappa$ B $\alpha$ . Because of the presence of ankyrin repeats in their C-terminal halves, p105 and p100 also function as I $\kappa$ B proteins.

In the activation of the classical pathway by LPS, firstly LPS binds to its binding protein (LBP) present in the blood. The complex LPS/LBP is combined with TLR-4 in such a way that sequentially activates various kinases, among them the NF- $\kappa$ B inducing kinase (NIK) and the I $\kappa$ B kinase (IKK). IKK is composed of a heterodimer of the catalytic IKK $\alpha$  and IKK $\beta$  subunits and a regulatory protein termed NEMO (NF- $\kappa$ B essential modulator) or IKKY, being IKK $\beta$  the predominant in this pathway. The activation of this kinase leads to the phosphorylation of I $\kappa$ B $\alpha$  in two serine residues (Ser32, Ser36) located in an I $\kappa$ B regulatory domain. When phosphorylated on these serines, the I $\kappa$ B inhibitor molecules are modified by a process called ubiquitination, followed by a subsequent degradation by the proteasome 26S (Figure 7) releasing then the NF- $\kappa$ B.

With the degradation of I $\kappa$ B, the NF- $\kappa$ B complex is then free to enter the nucleus where it can promote the expression of specific genes that have DNA-binding sites for NF $\kappa$ B nearby. NF- $\kappa$ B transcription factors bind to 9-10 base pair DNA sites (called  $\kappa$ B sites) as dimers. In general, the genes that are regulated by NF- $\kappa$ B can be classified in four groups: genes that code for inflammatory and immunomodulatory proteins, genes that regulated the cell cycle, antiapoptotic genes and those which encode negative regulators for NF- $\kappa$ B. NF- $\kappa$ B turns on expression of its own repressor, I $\kappa$ B $\alpha$ .

The newly synthesized I $\kappa$ B $\alpha$  can enter the nucleus, remove NF- $\kappa$ B from DNA, and export the complex back to the cytoplasm to restore the original latent state, thus, forming an auto feedback loop, which results in oscillating levels of NF- $\kappa$ B activity.

In light of the stated above, the activation of the NF- $\kappa$ B pathway is generally a transient process, lasting from 30-60 minutes in most cells (Gilmore, 2006; Lawrence, 2009).

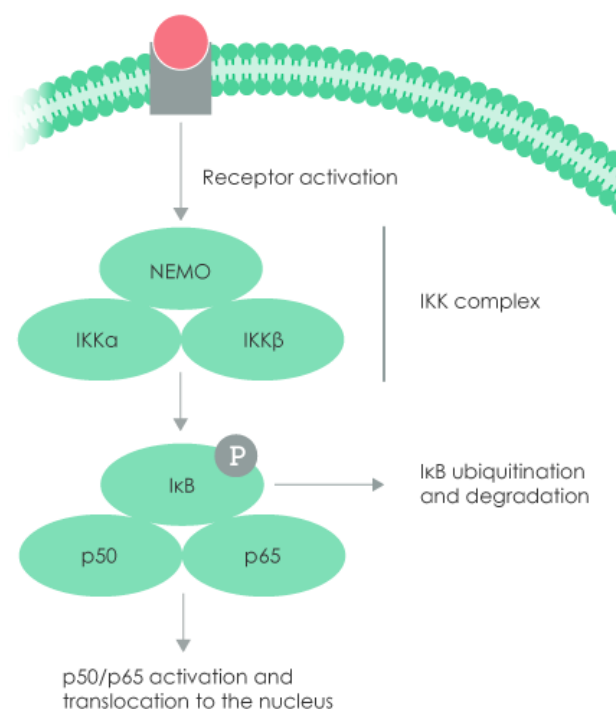


**Figure 7. The NF- $\kappa$ B classical pathway.** NF- $\kappa$ B (p50-p65 heterodimer in the figure) is placed in the cytosol forming a complex with the inhibitory protein I $\kappa$ B. A full array of extracellular signals can activate the enzyme I $\kappa$ B kinase (IKK) comprising IKK alpha and/or IKK beta catalytic subunits and two molecules of NEMO. IKK, in turn, phosphorylates the I $\kappa$ B protein, which results in dissociation of I $\kappa$ B from NF- $\kappa$ B, and eventual degradation of I $\kappa$ B by the proteasome. NF- $\kappa$ B is now activated and translocated into the nucleus where it binds to specific sequences of DNA called response elements. The DNA/NF- $\kappa$ B complex recruits other coactivators and RNA polymerase. The latter transcribes DNA into mRNA which is then subsequently translated in proteins that have an effect on cell function (Gilmore, 2006).

#### 1.4 NUCLEAR RECEPTORS OF INTEREST, ESTROGEN RECEPTORS: HOW DO THEY SIGNAL AND WHAT ARE THEIR TARGETS?

First and foremost, estrogens were considered to be essential in the development and maintenance of normal reproductive functions (Heldring *et al.*, 2007). However, estrogens are steroid hormones that have proved to regulate growth, differentiation, and function in a broad range of target tissues in the human body (Björnström and Sjöberg, 2005). Moreover, they also play very major roles in the immune system as

well as in the CNS in human body (Warner and Gustaffson, 2014). So much so that estrogens have been shown to improve the symptoms of Multiple Sclerosis and lower the risk of developing Alzheimer's disease (AD) and Parkinson's disease (PD). However, the mechanisms by which they exert these neuroprotective effects remain poorly understood (Baker *et al.*, 2004). In this chapter we will describe the structure of estrogen receptors and how they interact with a ligand in order to account for phytoestrogens, and more specifically isoflavones, acting on estrogen receptors. Besides an overview of the role of estrogen receptors in the attenuation of neuroinflammation and neurodegeneration will also be discussed.

#### 1.4.1 Structure of estrogen receptors and their affinity to their ligands

The most potent and dominant estrogen produced in the human body is 17  $\beta$ -estradiol (E2) (Figure 8) but lower levels of the estrogens estrone and estriol are also present (Björnström and Sjöberg, 2005). E2 consists of a steroid structure, being its phenolic ring and the hydroxyl group on 17C position the ones responsible for its selectivity and affinity to estrogen receptors (ERs) (Heldring *et al.*, 2007). The critical function of the phenolic A-ring for an estrogen to act on neuroprotection was determined by Green *et al.* (1997) and Behl *et al.* (1997). All modifications to the hydroxyl group at the 3-carbon resulted in total loss of neuroprotection, confirming that the phenolic nature of the A ring is critical for neuroprotection. Petron *et al.* (2014) also confirmed that three rings of the steroid nucleus are to the same extent necessary for neuroprotective activity. ERs are distributed in the cytoplasm in their free form. However, estrogen binding to the receptor triggers a series of events starting with migration of the receptor from the cytosol into the nucleus. Estrogen receptors also occur within the cell nucleus (Huang *et al.*, 2010).

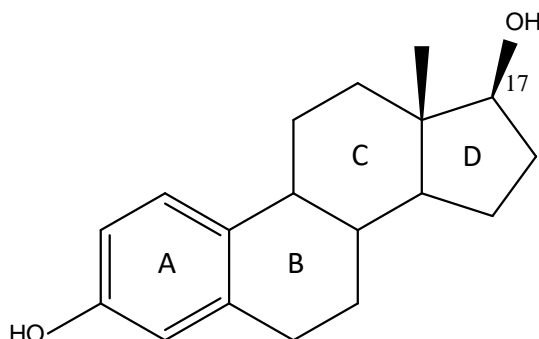


**Figure 8. Molecular structure of the endogenous estrogen 17 $\beta$ -estradiol (E2).** The rings are commonly named as A for the phenolic ring, B and C for the hexanes and D for the pentane.

In the late 1950s, Elwood Jensen discovered and started the characterization of an estrogen binding protein, today recognized as ER $\alpha$ . In 1993, nearly three decades later, the first ER $\alpha$  knockout mouse was created. Such modification did not have any type of survival effect on the mouse. Soon after the characterization of the ER $\alpha$  knockout mouse, ER $\beta$  was discovered, and this discovery raised the question of whether survival of the ER $\alpha$  knockout mouse was due to ER $\beta$  substituting for the functions of ER $\alpha$ . ER $\beta$  knockout mice were made, and this was followed by double ER $\alpha\beta$  knockouts. These different mouse models revealed that life is possible without either or both ERs but that reproductive functions are severely impaired (Heldring *et al.*, 2007). Upon such results and further investigation, it was concluded that cellular signalling of estrogens is mediated through two estrogen receptors, ER $\alpha$  and ER $\beta$  (Olajide *et al.*, 2014).

Of note is that estrogen receptor ER $\alpha$  and  $\beta$  have different tissue/cell distributions and differential affinities for ligands and non-overlapping genes that they regulate. As a result, targeting these receptors differentially can lead to selective gene activation profiles (Huang *et al.*, 2010). In the CNS, both receptors are widely expressed, in particular, in non-neuronal cells. Even though ERs are well known to have antiinflammatory effects, they may also have non-desired effects and it must be bared in mind in drug development. Evidence suggests that ER $\alpha$  also has mitogenic action, and therefore has been reported to trigger cancer; however, ER $\beta$  acts as tumour suppressor by opposing the mitogenic action of ER $\alpha$  (Fokialakis *et al.*, 2012). The ER $\alpha$  mitogenic actions are due to estrogen acting as a morphogen that is a substance that determinates the pattern of tissue development in the process of morphogenesis, and the positions of the various specialized cell types within a tissue (Liu *et al.*, 2002).

Estrogen receptors belong to the nuclear receptor (NR) family of transcription factors. NR are a type of proteins within the cells responsible for sensing steroid and thyroid hormones among others. Such receptors are characterized by directly binding to the DNA, hence being also known as transcription factors resulting in the activation of the transcription process.

A typical nuclear receptor usually contains four functional regions or domains (Figure 9):

- the **A/B region** is the N-terminal domain. A/B domain is not constant and it differs among the different subtypes and isoforms of NR.

- the **C region** with the **DNA-binding domain (DBD)** is a highly conserved region formed by two Zn fingers that binds to specific sequences of DNA called hormone response element (HRE), or in the case of estrogen receptors, estrogen response element (ERE), which are responsible for the dimerization of the NR;
- the **D region** (hinge region) connects the C and E domains;
- the **E/F region** so-called the **ligand-binding domain (LBD)** because it contains a hydrophobic ligand binding cavity it is located in the N-terminal part. It is also one of the regions more conserved in these type of receptors and alongside with DBD, LBD contributes to the dimerization of the receptor. Besides the ligand cavity it also contains binding sites for either coactivators or corepressors proteins whose shift will depend on the ligand (Heldring *et al.*, 2007).

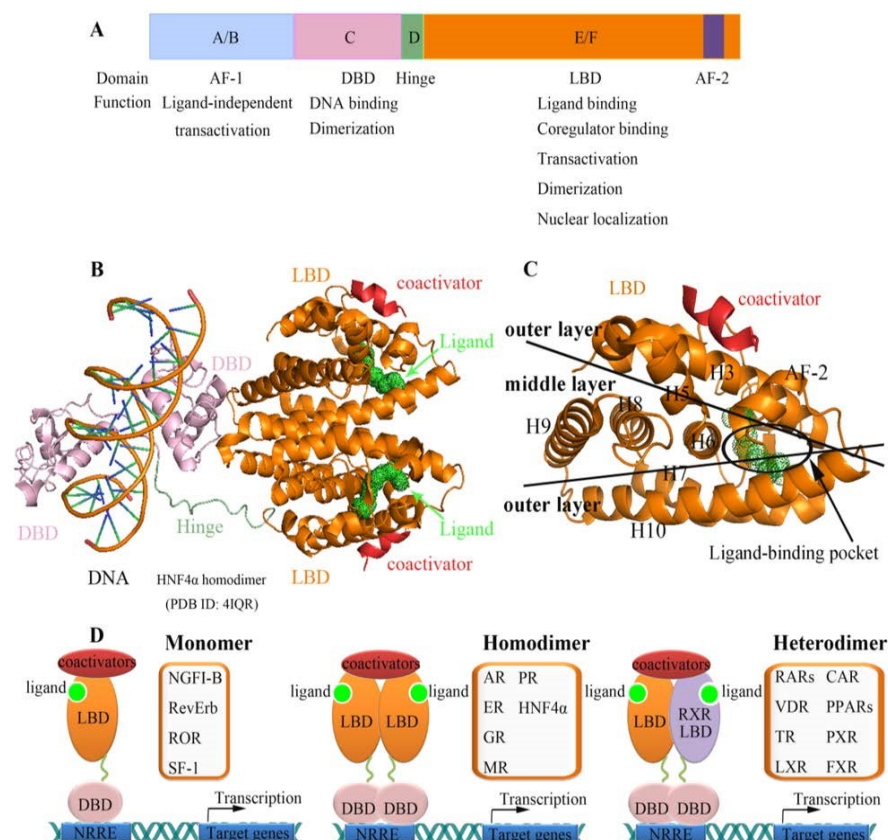


**Figure 9. Schematic representation of the structural and functional organization of nuclear receptors.** a) Simplified representation of a common domain structure of NR; b) 3D illustration of the DBD region bound to the DNA upon ligand binding to LBD; c) enlarged view of LBD showing its characteristic three-layer sandwich structure; d) metabolic regulation of NR. Ligand-activated NR complex recruit coactivator proteins that increase transcriptional activity of the gene. NRs bind DNA as monomers, homodimers or heterodimers (Yang *et al.*, 2014).

The substantial sequence homology between ERs endows them with comparable affinities for estrogen and ER agonists. It is worth mentioning that the sizes of the ligand pocket are incredibly broad as well as highly inducible both in size and in receptivity to molecules that are unrelated to endogenous ligand and for this particular reason, LBD has been the focus of structural study (Huang *et al.*, 2010; Yang *et al.*, 2014). Due to the existence of a wide range of coactivators and corepressors in different cells, a ligand for ERs can act as an agonist in one type of cell but as antagonist in another. Therefore, partial agonists are typically the most promising candidates with limited undesired side effects (Huang *et al.*, 2010).

#### **1.4.2 Mechanism of action of ERs in neuroprotection**

Both ER $\alpha$  and ER $\beta$  are present throughout the brain in humans and rodents, although their distribution throughout differs in most cases (Brann *et al.*, 2007). These receptors mediate the effects of estrogens not only in the brain but also in the rest of the tissues and cells. This mechanism is based on their role as transcription factors in the cell nucleus and in their role in mediating rapid effects by cross-talk with other membrane localized receptors and cytoplasmic signalling pathways (Nilson and Gustaffson, 2011).

The three types of immune cells in the brain: astroglia, microglia and oligodendroglia, express a substantial number of classical nuclear and non-classical membrane ERs although in different quantities. With respect to microglia, it seems clear that E2 attenuates microglial activation, phagocytic activity and nitric oxide production and that genetic elimination of ER $\alpha$  but not ER $\beta$  has the consequence of spontaneous reactive microglia in the brain (Kipp *et al.*, 2016).

Despite the controversy with the ER $\alpha$  subtype due to its association with the development of certain cancers such as breast cancer and prostate cancer, current reports strongly hint at that both ER $\alpha$  and ER $\beta$  are implicated in accomplishing substantial neuroprotection on neurological disorders through activation of various cell survival signalling pathways (see review: Chakrabarti *et al.*, 2014). For example, in one study performed with ArKO (aromatase-deficient) mice – an important enzyme in the production of E2 – using ER $\alpha$ - or ER $\beta$ -selective agonist differentially protected against dopaminergic neuronal cell death in acoustic trauma (Brann *et al.*, 2007).

## ERs subtypes in Multiple Sclerosis

The protective and possibly disease-modifying role of estrogen and the two ER subtypes has been investigated in experimental MS disease model. In this model, ER $\alpha$  revokes the disease at onset by inhibiting inflammatory responses, therefore, it appears to be the most important ER subtype in protecting against the development of MS. On the contrary, ER $\beta$  lacks the ability of abrogating this disease at onset. However, it was reported to promote recovery during the chronic phase of the disease by reducing demyelination and preserving axon numbers in white matter, as well as by decreasing neuronal abnormalities in grey matter resulting in the recovery of motor performance, which was initially severely impaired (Nilson and Gustaffson, 2011). Moreover, ER $\beta$  selective agonists reduced microglia stimulation in mice MS disease model (Wu *et al.*, 2013).

## ERs subtypes Alzheimer's Disease

AD is the leading cause of dementia with two leading hallmarks: the accumulation of extracellular  $\beta$  amyloid (A $\beta$ ) peptide and the hyperphosphorylated protein tau in the form of neurofibrillary tangles. However, in the recent years, emerging evidence support the implication of the innate immunity, and, in particular, the microglia in the pathogenesis of the AD. The aggregates of proteins deposited in the AD are recognized by microglia receptors and, consequently, they trigger an immune innate response, characterized by the release of several inflammatory mediators that contribute in the progression of the disease (Heneka, 2015). The important role of neuroinflammation is supported by findings that genes for immune receptors, including TREM (Guerreiro *et al.*, 2013) and CD33 (Bradshaw *et al.*, 2013) are associated with AD.

Regarding the estrogens role in AD, it has been described an inverse correlation between estrogen levels and the incidence of AD by directly regulating A $\beta$  levels by decreasing the production of A $\beta$  and increasing its degradation. Estrogen's neuroprotective effects may also be due to its regulation of tau phosphorylation. The decrease in tau phosphorylation is likely due to estrogen's effect on tau kinases (Petron *et al.*, 2014).

Apparently, ER $\alpha$  has also a critical role in reducing A $\beta$  accumulation in determined parts of the brain. Alike E2, the ER $\alpha$ -selective agonist PPT showed efficacy in reducing

A $\beta$  accumulation in the hippocampus, subiculum, and amygdala but less effective than E2 in the frontal cortex, resulting also in enhancement in behavioral conduct. ER $\beta$ -selective agonist DPN did not show such ability, but it did significantly reduce A $\beta$  accumulation in the hippocampus and subiculum and it was partially effective in the frontal cortex and nearly as effective as E2 in the amygdala (Carroll *et al.*, 2008).

### ERs subtypes Parkinson's Disease

PD is distinguished by progressive loss of dopaminergic neurons in the substantia nigra and by intracellular inclusions of aggregated  $\alpha$ -synuclein (Lewy bodies). Alike AD, PD is also associated with activation of the brain inflammatory response, inducing a slow but irreversible phenomenon by which destruction and loss of dopaminergic neurons is carried out.

Animal models of PD have been used to study the role of estrogens, selective estrogen modulators (SERMs), and ER subtype–selective agonists in the development of PD. A study in primates showed that 30 days of estrogen deprivation resulted in the permanent loss of more than 30% of the total number of substantia nigra dopamine cells. However, brief estrogen replacement therapy improved neuronal density. In mice, after administration of 1methyl-4-phenyl-1,2,3,6-tetrahydropyridine (MPTP), a compound that destroys dopaminergic neurons causing permanent symptoms of PD, treatment with E2 accomplished to prevent PD symptomatology. However, knockout mice for either ER $\alpha$  or ER $\beta$  were not fully protected against MPTP by E2 treatment, suggesting roles for ER $\alpha$  and ER $\beta$  in concert for dopamine neuroprotection (see review: Nilson and Gustaffson, 2011).

## **1.5 PHYTOESTROGENS**

There is a rapidly growing body of evidence, that consumption of some plants containing phytoestrogens could be an additive efficient tool to treat and prevent several dysfunctions and diseases related to aging mental processes, malignant transformation, metabolism, atherosclerosis, osteoporosis, cardiovascular diseases an reproduction, menopausal symptoms, and neurodegeneration (Sirotkin and Harrath, 2014). More than a decade has passed since the discovery that estrogens are potent neuroprotective substances and protect against cognitive decline during normal aging. These findings along with strong epidemiologic indication that described a delay in the age of commencement of Alzheimer's disease in current and former

estrogen users led rapidly to the assessment of diverse phytoestrogens in the treatment of neurodegenerative diseases (Simpkins and Singh, 2008).

Phytoestrogens (“*phyto*” = plant, “*estrus*” = sexual desire and “*gene*” = to generate) are non-steroidal plant derived natural products, related in structure to the estrogens generated within the endocrine system of mammals. The most relevant mammals’ estrogens are 17  $\beta$ -estradiol (E<sub>2</sub>), estriol and estrone being the former stronger than its counterparts (Ososki and Kennelly, 2003). These estrogens possess 18 carbon elements that shape an esteroid structure with a phenolic ring (A), which determines their selectivity and affinity for ERs, and a determinant functional group at 17 position (Figure 8 and Figure 10). Due to such similarities at a molecular level, phytoestrogens also share functional resemblance with estrogens as either agonists or antagonists. As estrogen agonists, phytoestrogens mimic endogenous estrogens causing estrogenic effects. As estrogen antagonists, they may block or modify estrogen receptors and avoid estrogenic activity, causing antiestrogenic effects (Ososki and Kennelly, 2003). Such compounds are described as endocrine disruptors, which may be related to the initiation of breast cancer and deficiency of reproductive function. On the contrary, many other studies suggest that phytoestrogen, such as genistein, can reduce the risk of some hormone-related cancers. Therefore, considering the numerous effects that estrogen exert on the human body, these naturally occurring compounds serve as a good source of leading molecules for further modifications during the drug development process (Fokialakis *et al.*, 2012; Wuttke *et al.*, 2008) that could spark improvement in the treatment or prevention of neurodegenerative diseases.

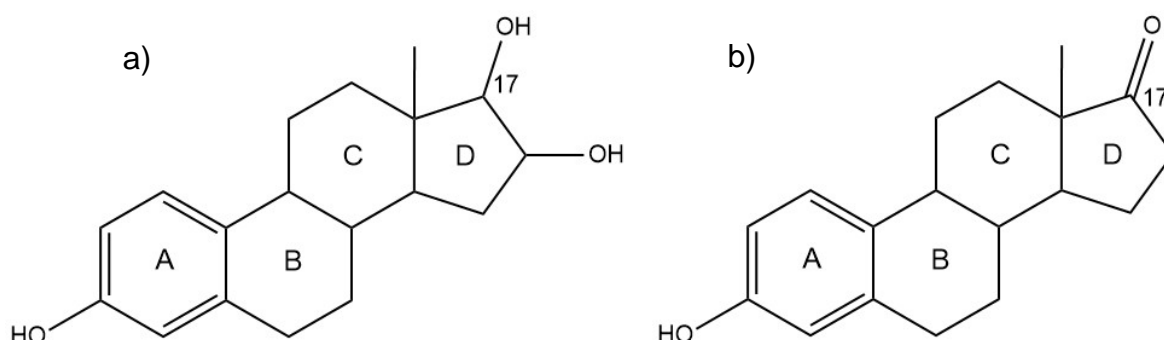


**Figure 10. Structure of mammalian endogenous estrogen.** a) Estriol and b) estrone. Five rings comprise their structure: (A) a phenolic ring that endows them with specificity and affinity for ERs, (B) and (C) are two cyclohexanes and (D) is pentane cycle with a substitute on position 17 also indispensable for their activity.

Popularly, phytoestrogens are also studied as SERMs due to a peculiar feature: a given compound can act as both agonist and antagonist depending on the tissue, ER and the amount of endogenous estrogen circulating (Ososki and Kennelly, 2003). Furthermore, phytoestrogens show a lower binding affinity than E<sub>2</sub> and some show a higher binding affinity for ER $\beta$  than for ER $\alpha$ , which may indicate different pathways for their actions and explain tissue specificity (Kuiper *et al.*, 1998).

### 1.5.1 Classification of phytoestrogens

On the basis of their chemical structure, which resembles E<sub>2</sub>, and in respect to biosynthesis patterns, phytoestrogens have been categorized in several groups:

- flavonoids (chalcones, flavones, flavonols, flavanones, isoflavonoids, catequines, pterocarpanes, rotenoids, anthocyanines, prenylflavonoids),
- lignans,
- anthraquinones and
- saponins.

Particular attention should be given to isoflavonoids, the subgroup of flavonoids that includes amongst others the chemical groups of isoflavones, isoflavanones, pterocarpanes, and coumestans (Sirotkin and Harrath, 2014).

### 1.5.2 Similarities between isoflavones and estrogens

Unlike some NRs such as the thyroid hormone receptor (TR) or the retinoic acid receptor (RAR) where the shape of the ligand binding cavity is well adapted to fit the cognate hormone, the ligand cavity for ERs appears spacious for E<sub>2</sub>. This allows ER to bind a wide range of compounds with strikingly diverse structures. In addition to estrogens, ERs also show affinity for environmental contaminants as well as phytoestrogens (Heldring *et al.*, 2007).

Epidemiological studies suggest that the consumption of plants with high phytoestrogens content are the reason why incidence of neurological disorders are lower among the Asiatic population than that in the Western world (Spencer *et al.*, 2012). *In vitro* and *in vivo* investigations have demonstrated that phytochemicals from plant sources, in particular flavonoids, exhibit anti-inflammatory activity.

Many phytoestrogens have been characterized and some of them have shown to have estrogenic activity. Isoflavones (Figure 11.a) are a major group of phytoestrogens that have been the focus of many studies and are known to display anti-inflammatory effects (Lin *et al.*, 2007). By blocking the production of pro-inflammatory cytokines and chemokines such as TNF- $\alpha$ , IL-6 and IL-1 $\beta$ , as well as the activation of proinflammatory enzymes (phospholipase A2 –PLA<sub>2</sub>, COX-2, LOX, iNOS) isoflavones serve their anti-inflammatory functions (Yu *et al.*, 2016). Moreover, epidemiological studies on isoflavones have also demonstrated that a high intake of soy lowers the incidence of cardiovascular diseases, hormone-dependent cancers, menopausal symptoms and osteoporosis (Larkin *et al.*, 2008). As such, isoflavones are characterized by eliciting either weak estrogen agonistic or antagonistic effects depending on the levels of endogenous estrogens and ERs (Yu *et al.*, 2016). Despite their structural similarity to 17  $\beta$ -estradiol, isoflavones have much higher bias for ER $\beta$  than for ER- $\alpha$  (Larkin *et al.*, 2008).

Among many others, the following isoflavones have been studied in depth: the aglycones, daidzein (4',7-dihydroxyisoflavone) and genistein (4',5,7trihydroxyisoflavone); the glycosides, daidzin and genistin; and biochanin A and formononetin, 4'-methyl ethers of daidzein and genistein (Figure 11.b). In plants, they can often be found as glycosides (Ibarreta *et al.*, 2001). In processing, isolation and analysis, these compounds are readily degraded chemically or enzymatically to the aglycone (Ososki and Kennelly, 2003).

As an example of the concordance between the isoflavones structure and human estrogens, in Figure 12 genistein is compared to estradiol. This isoflavone binds across the ligand-binding cavity very similarly to the natural ligand E2. For these types of molecules, the equivalent ring-A and the 3-hydroxyl groups occupy the same positions as the functional groups of E2. On the contrary, the antagonists often contain extended groups emerging from the center of their molecules, which directly impact on the E/F nuclear receptor region, blocking the site of coactivators and thus, affecting transcriptional activation (Figure 9) (Huang *et al.*, 2010).

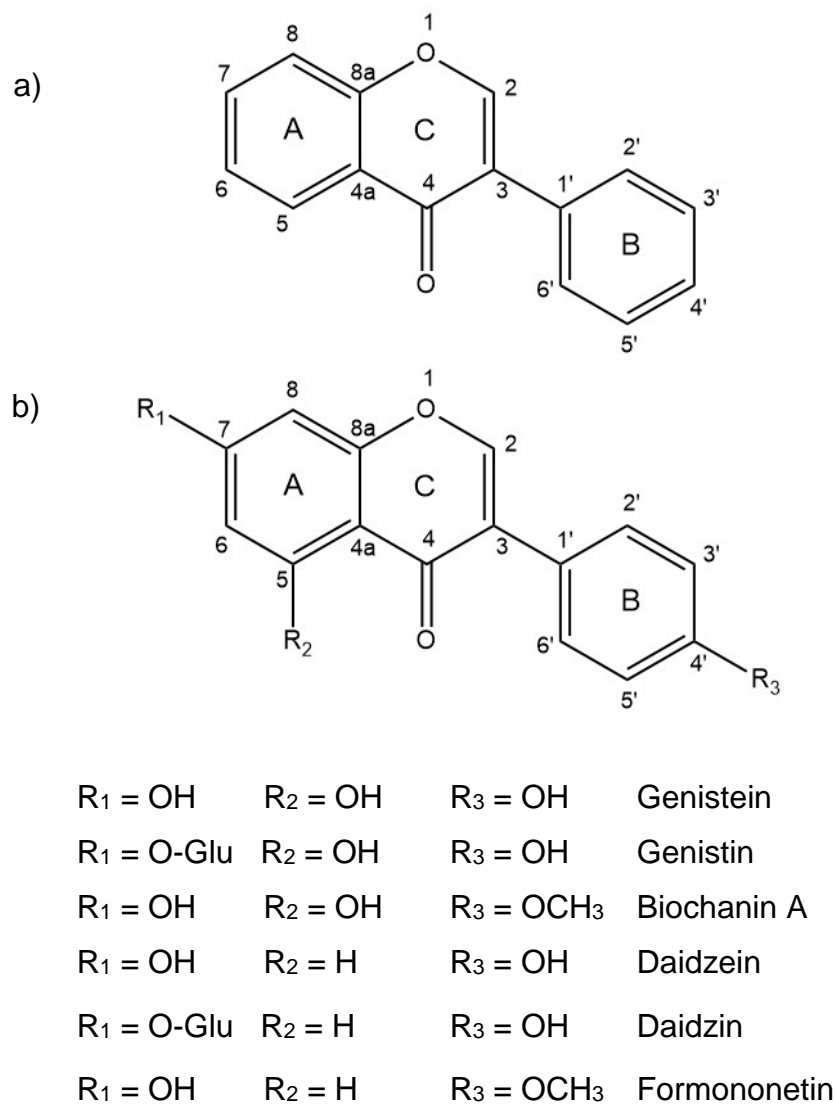


**Figure 11. Isoflavones structures.** a) General structure for isoflavones. b) Examples of isoflavones analogues.

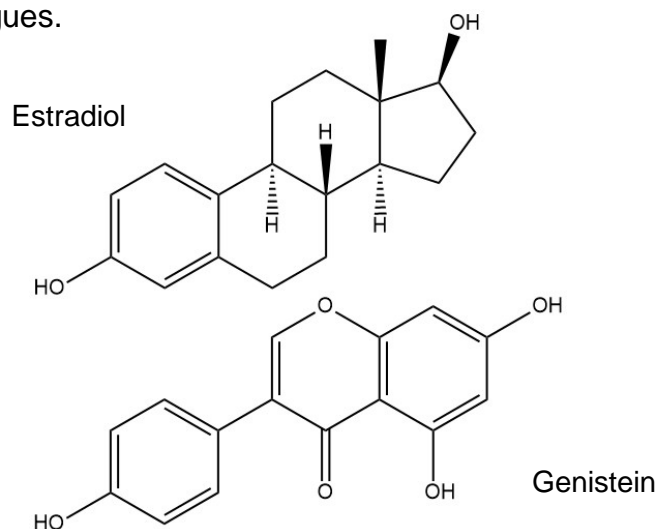


**Figure 12. Comparison between the structure of an isoflavone derivative (genistein) and estrogen (estradiol), which shows the similarities between the two molecules (adapted from Pugazhendhi *et al.*, 2008).**

### 1.5.3 Biochanin A and Formononetin: two remarkable isoflavones

Isoflavones are primarily found in the *Fabaceae* family, that is in legumes such as soy, peanut (*Arachis hypogaea L.*) and clover (*Trifolium spp.*). In particular, soy seeds and red clover contain high levels of formononetin and biochanin A (Ososki and Kennelly, 2003; Chen *et al.*, 2008).

Isoflavones are usually found in nature in their glycosides form. In humans, they are mainly hydrolyzed by the gut microflora and throughout an enterohepatic metabolism resulting into their free form. Such process allows for a better absorption and enhances the affinity of these compounds to ERs. Regarding formononetin and biochanin A they also undertake an O-demethylation to become derivatives of genistein and daidzein, respectively (Li *et al.*, 2014).

In particular, biochanin A (BCA, 5,7-dihydroxy-4'-methoxyisoflavone) (Figure 11.b), is an ER $\beta$ -selective isoflavone in red clover and many other legumes. BCA is metabolized to the soy-derived isoflavone genistein, BCA conjugates, and genistein conjugates which can be detected in plasma and bile, happening to have a high clearance and a large apparent volume of distribution resulting in a poor bioavailability for both of them (<4%) (Moon *et al.*, 2006).

Formononetin (FMN, Formononetol 7-hydroxy-4'-methoxyisoflavona 4'-O-methyl daidzein) (Figure 11.b) is another phytoestrogen extracted from plant-derived red clover among others, which also possesses potent pharmacological activities, such as improving blood microcirculation, promoting cancer cell cycle arrest (Li *et al.*, 2014), and regulating antioxidant effects. It is also one of the most important type of phytoestrogens found in legume plants such as *Trifolium pratense* and *Glycine max*, which exhibited anti-inflammatory effect on neurodegenerative diseases including Parkinson's and Alzheimer's disease by the inhibition of LPS-induced microglia activation and the generation of pro-inflammatory factors (Chen *et al.*, 2008). The metabolites of FMN are also essential in its estrogenic activity. FMN is metabolized to daidzein which is further processed into equol (Figure 13). However, equol is not metabolized equally in all humans due to differences in our intestinal bacterial composition which might account for their biological differences (Ososki and Kennelly, 2003; Tolleson *et al.*, 2002).

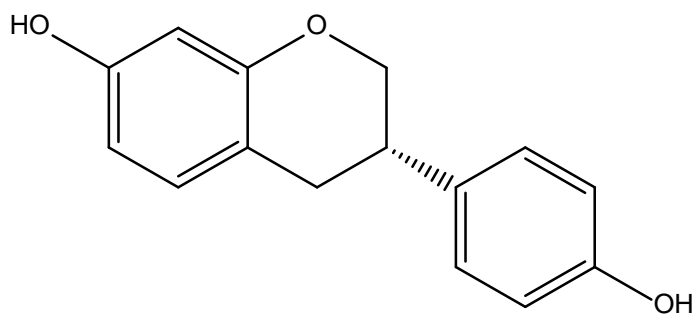


**Figure 13. Equol structure.** A metabolite from formononetin.

All in all, it must be noticed that isoflavones are known to display low bioavailability due to poor solubility, extensive metabolism and rapid clearance (Fokialakis *et al.*, 2012). Thus, enhancing its bioavailability and/or metabolic stability with esters and especially carbamate esters is of our concern. Furthermore, potential selective ER $\beta$  isoflavones such as BCA and FMN can be a good strategy to avoid the carcinogenic effect of ER $\alpha$ . Nevertheless, it must not be forgotten that isoflavones metabolites also contribute to their biological effects which may differ from the original isoflavones digested (Ososki and Kennelly, 2003).

## **1.6 SYNTHESIS STRATEGY: THE USE OF ESTERS AND CARBAMATES IN DRUG DESIGN**

Isoflavones contain a phenolic hydroxyl group, which is one of the most common functional group found in drug molecules such as estrogens and anticancer agents among others. Nevertheless, despite their functional characteristics, the presence of this group also endows the molecule with poor bioavailability and thus limited effectivity. Poor bioavailability is due to metabolic instability subjected to fast enzymatic biotransformation resulting in extensive first-pass metabolism. Moreover, the polarity of hydroxyl groups confers non-lipophilic character to the molecules, hindering the pass through the plasmatic membrane. These drawbacks of phenolic hydroxyl groups are pharmaceutically translated in the need of multiple doses of the drug to maintain a concentration-effective dose, and higher probability of accumulating toxic metabolites. In order to overcome such metabolism difficulties, a prodrug strategy would be to temporally mask polar groups resulting in an increased lipophilic molecule, which would promote membrane permeability (Férriz *et al.*, 2010).

Esterification of the hydroxyl group(s) has been one of the preferred prodrug strategies even for CNS delivery (Anderson, 1996). Many authors have described the

esterification with different mono- and poly-unsaturated fatty acids as one of the strategies followed to produce more active flavonoid derivatives. By adding an acyl group to the basic flavonoid skeleton, selectively acylated flavonoids are obtained with increase solubility and stability, resulting in potential biological activities. The nature and chain length of the acyl donor have a remarkable effect on the acylation reaction. Therefore, choosing an appropriate acyl donor significantly impacts the physicochemical and biological properties of the synthesized esters. The impact of acylation on biological activities has been copiously tested. In many modified flavonoids, their antioxidant, antiproliferative and citoprotective, anti-inflammatory, antibacterial and antifungal activities were improved by acylation. For example, the well-known flavonoid rutin improved its antioxidant activity upon acylation with unsaturated fatty acids, such as oleic and linoleic acid; isoquertin esters were shown to exhibit an antioxidant activity that depended on the acyl chain length; isoorientin esterification endowed it with higher lipophilicity; on the other hand, acylation of isoquercitrin resulted in a more effective compound at reducing inflammation via the NF-kB pathway (for review see Araújo *et al.*, 2017).

On the other hand, over the past few years, carbamate (Figure 14) derivatives have received much attention due to their application in drug design. Structurally, carbamates share similarities with esters and amides being therefore also functionally related.

Carbamates are essential motifs in many approved medicines with clinical potential. For instance, rivastigmine (Figure 15.a) is used in the central nervous system to treat Parkinson's and Alzheimer's diseases. As another example, muraglitazar (Figure 15.b) is a PPAR  $\alpha/\gamma$  agonist which regulate glucose and lipid levels (Ghosh and Brindisi, 2015). Moreover, several novel anti-cancer drugs and prodrugs derived from natural products have been obtained with the incorporation of such chemical group into the main molecule (Chaturvedi and Zaidi, 2015).

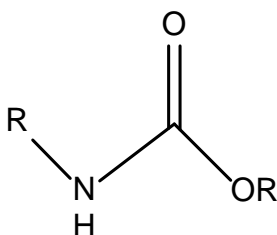


**Figure 14.** Structural representation of a carbamate group.

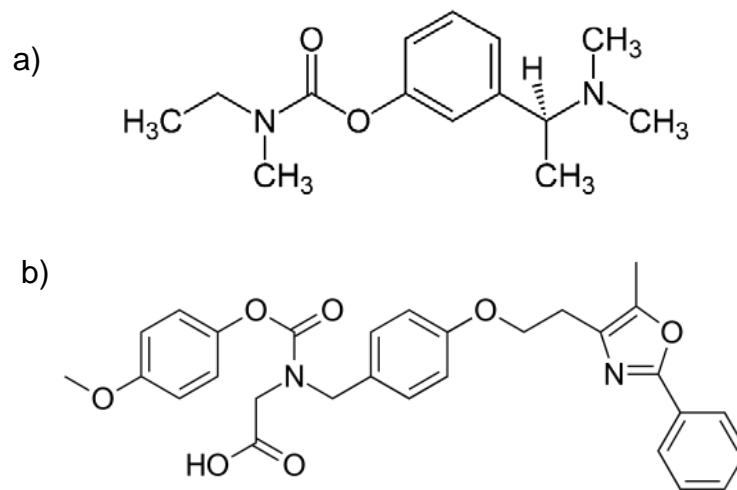


**Figure 15.** Chemical structure of a) rivastigmine and b) muraglitazar.

A carbamate group usually endows the chemical compound to which it is attached with enhanced metabolic stability – primary against amino-peptidases, which are enzymes involved in the metabolism of peptide-like drugs - and improved permeability. This group also allows for two hydrogen bonding given the carbonyl (C=O) and amine (NH) groups instead of one as it would occur with an ester (-COO-) group alone. These features make of this chemical group a very good candidate to be present in drugs or prodrugs. On the other hand, Vecondio *et al.* have observed that the rate and level of their hydrolysis is key question for the duration and intensity of their pharmacological activity. Upon hydrolysis, carbamates esters release the parent phenol or alcohol drug and carbamic acid; the latest, is further decomposed to amine and CO<sub>2</sub>.

All in all, carbamates and esters provide a good strategy to enhance isoflavones permeability through the CNS, improve their bioavailability and diminish their clearance rate. In the present project, we have compared natural compounds with and without this possible pharmacophore.

## 1.7 GAP IN KNOWLEDGE

Many studies have shown the health benefits of phytoestrogens, however, they also may exhibit side effects related to cancers depending on their affinity and specificity to ERs. ER $\alpha$  and ER $\beta$  are the main ERs found in human. Whilst ER $\alpha$  has been related to the development of carcinogenesis in breast and uterous tissues, ER $\beta$  has shown the ability to suppress ER $\alpha$ , therefore, no side effects have been attributed to ER $\beta$ . BCA and FMN are two potent isoflavones with higher affinity towards

ER $\beta$ . Bearing this in mind, new inhibitors of neuroinflammation which activate ERs in the microglia without affecting ERs in the breast or ovaries could be protective without the expected side effects.

## **1.8 OBJECTIVES OF THE STUDY**

Phytoestrogens have been shown to improve the symptoms and lower the risk of developing neurodegenerative diseases. In the light of hyperactivated microglia leading to an overproduction of inflammatory mediators, thus causing neurotoxicity and exacerbating the progress of such diseases, the present study aims to develop novel phytoestrogens that reduce neuroinflammation in the CNS.

In order to accomplish this overall aim, the following specific objectives were established:

- To synthesise bioactive derivatives phytoestrogens from the natural isoflavones Biochanin A (BCA) and Formononetin (FMN).
- To synthesise and study deoxybenzoin, which are intermediates in the synthesis of isoflavones, due to their structural similarity with isoflavones.
- To evaluate the synthesized compounds on the production of inflammatory mediators in LPS-activated microglia cells.

## CHAPTER 2: MATERIALS AND METHODS

### Overview

Upon the synthesis of the compounds, their separation and purification was performed by column chromatography unless otherwise stated. For the proper identification of the compounds obtained, nuclear magnetic resonance (NMR) and mass spectrophotometry techniques were employed. In order to test their anti-inflammatory properties, the determination of nitrite by Griess assay as well as ELISA immune assays for diverse cytokines were performed. Cell viability was assessed by XTT colorimetric assay. Lastly, primary inflammatory-involved proteins were detected by Western Blot.

### 2.1 GENERAL CHEMISTRY METHODS

All chemicals were of the highest available commercial purity. Starting materials and solvents, including the deuterated solvents used in the NMR study, were purchased from Aldrich Chemicals, stored according to the supplier's instructions and used without further purification. All anhydrous reactions were carried out either under nitrogen or argon atmosphere. In some reactions, the solvents used were first dried by distillation prior to use. Thin layer chromatography was conducted on Merck glass silica gel 60 F<sub>254</sub> and spots visualized using UV light and either vanillin-sulfuric acid reagent or permanganate (KMnO<sub>4</sub>) reagent. Liquid chromatography was performed on columns containing silica gel 60 Merck (63-200 μm). Solvent systems employed in chromatography are reported as volume to volume ratios. <sup>1</sup>H (400.13 MHz) and <sup>13</sup>C (100.62 MHz) spectra were recorded on a Bruker Ascend 400 spectrometer. Mass spectra experiments were performed on an Agilent 6210 TOF MS with a Dual ESI ionisation source (Annex I).

#### 2.1.1 Thin Layer Chromatography

In order to monitor each reaction, thin layer chromatography (TLC) was conducted and spots visualized using UV light and either vanillin-sulfuric acid reagent or permanganate (KMnO<sub>4</sub>) reagent.

TLC is a very simple technique but an exceptionally powerful analytical tool. Precoated silica chromatography plates are slightly acidic which confers the quality of being

suitable for running a wide range of compounds. This system is based both on the polarity of the compounds as well as on the polarity of the solvent. More polar compounds will be strongly retained than those with a lower polarity. Pre-coated silica gel plates need to be cut to size to fit the chromatography tank. They were marked with a pencil line to a height of around 1 cm, just above the depth of solvent poured into the tank. Samples were spotted with a suitable distance between them (0.5 cm). To do so, samples need to be dissolved in a suitable solvent prior to loading on the plates. The reaction mixture or unknown compound is spotted against starting material and a mixed spot of both. The plate was then placed vertically in the chromatography chamber. When the solvent front had travelled high enough the plate was removed and dried in air.

In order to detect the spots, the dried plates were observed under UV light and if necessary, dipped in visualization reagents (Table 4) to identify UV invisible spots.

**Table 4. Recipes and comments on visualization reagents.**

Stains	Recipe	Use/comments
<i>Vanillin</i>	Vanillin (6g) in ethanol (250ml) + conc. H <sub>2</sub> SO <sub>4</sub> (2.5 ml)	Good general reagent. Gives a range of colours.
<i>Permanganate</i>	KMnO <sub>4</sub> (3g) + K <sub>2</sub> CO <sub>3</sub> (20g) + 5% aq. NaOH (5ml) + water (300 ml)	Mainly for unsaturated compounds and alcohols. Gives yellow spots.

Retention factor (R<sub>f</sub>) is important to identify any compound formed in a given reaction since its value is constant under fixed conditions such as TLC plate, solvent system and temperature. R<sub>f</sub> has positive values from 0 to 1 representing the position of the spot on the TLC plate. TLCs are also run to help to decide on the best mobile phase to achieve a good and easy purification afterwards grounded on the R<sub>f</sub> value. If spots are running close together usually an R<sub>f</sub> of about 0.3 is optimal, however, if they are well-separated a solvent system which retains the lower spot to a R<sub>f</sub> 0.2-0.3 will usually work.

Mathematically, R<sub>f</sub> is represented as:

$$R_f = a/b$$

Where:

- 'a' is the distance from the base line to the center of the spot on the TLC plate and
- 'b' is the distance travelled by the solvent system measured from the base line.

A well standardized solvent system is that consisting of an ethyl acetate (EtOAc) – petroleum ether mixture whose polarity can be easily adjusted by changing their proportions. The best TLC solvent system for each compound and reaction mixture had to be determined by trial and error.

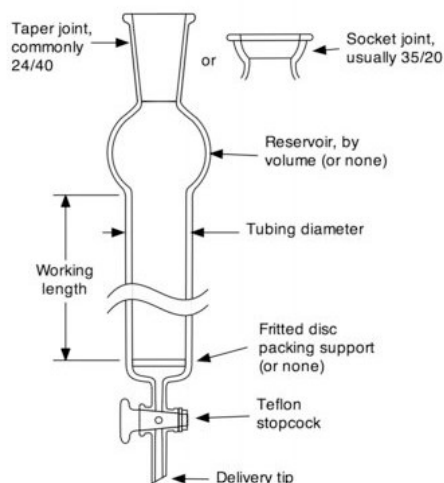
### **2.1.2 Column Chromatography**

Liquid chromatography is a standard method of purification based on the same principles than the TLC technique. When otherwise stated the purifications of the compounds synthesized were carried out by this methodology. The size in length and width of the column (Figure 16) was chosen according to the amount of sample obtained. The column was then packed with a mix of silica gel 60 Aldrich (63-200  $\mu\text{m}$ ) and the elution solvent system to give a slurry-like paste making sure to not generate any air bubbles through the process. The excess of solvent was released off the column and then a small amount of sand was poured to form a thin layer that would protect the silica gel. Subsequently, the reaction mixture dissolved in a suitable solvent (usually chloroform), was loaded carefully using a Pasteur pipette. Once the solution went through the sand to reach the silica, more eluent was immediately added to prevent the column from drying out. A reservoir was then attached to the column and gently filled up with a large volume of solvent system. The eluent was then slowly released and collected in marked test tubes. During the whole process, the solvent level was increased when necessary to ensure that the column did not dry out.

TLCs were applied to each fraction collected to find the sections containing the desired compound. These sections were combined in a round bottom flask and the solvent removed by rotary evaporation, recovering thus a purified compound.

In order to make sure that the sample was solvent-free, the dried material was once again dissolved in chloroform and taken to the rotatory vapor to be dried out. Thereafter, 30 mg were dissolved in a suitable deuterated solvent and transferred to a nuclear magnetic resonance (NMR) tube to run a complete NMR. Once the

characterization was completed, all compounds obtained were dissolved in dimethyl sulfoxide (DMSO), aliquoted and stored at -80°C.

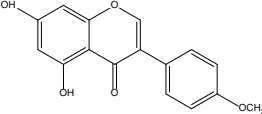
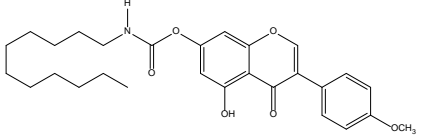
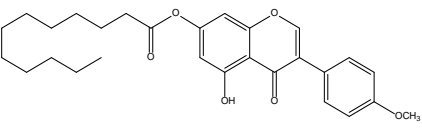
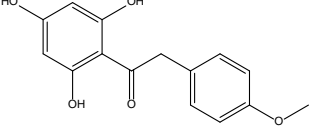
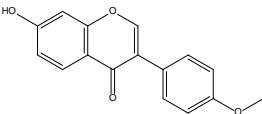
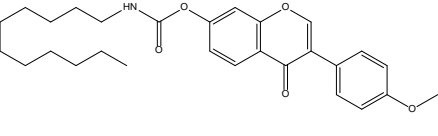


**Figure 16. Representation of a column chromatography.**

### 2.1.3 Preparation of Biochanin A and Formononetin derivatives and intermediates

Table 5 shows a summary of the compounds synthesized. The procedure used to prepare isoflavone analogs was carried out by adapting previously published methods (Fokialakis *et al.*, 2004; Fokialakis *et al.*, 2012).

**Table 5. Representation of the compounds synthesized and used in the present work.** IUPAC: International Union of Pure and Applied Chemistry.

Leading structure	Derivatives and intermediates	IUPAC denomination	Name
 <p><b>Biochanin A (BCA)</b></p>		5-hydroxy-3-(4-methoxyphenyl)-4-oxo-4H-chromen-7-yl undecylcarbamate	Compound 1
		5-hydroxy-3-(4-methoxyphenyl)-4-oxo-4H-chromen-7-yl dodecanoate	Compound 2
		2-(4-methoxyphenyl)-1-(2,4,6-trihydroxyphenyl)ethan-1-one	Compound 3
 <p><b>Formononetin (FMN)</b></p>		3-(4-methoxyphenyl)-4-oxo-4H-chromen-7-yl undecylcarbamate	Compound 4

## Biochanin A derivatives

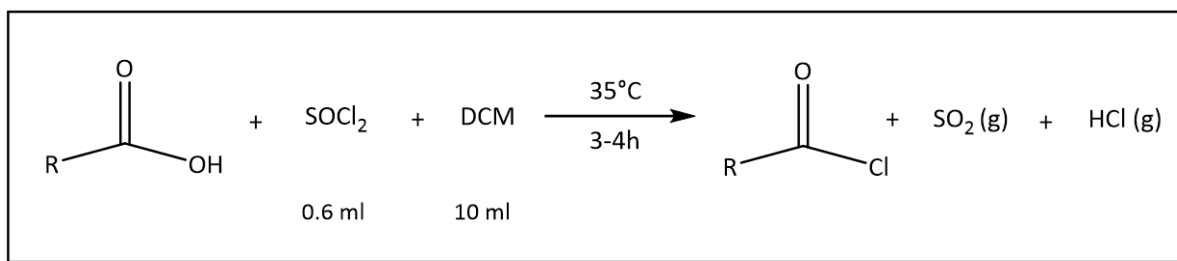
Two BCA derivatives were synthesized in this work: 5-hydroxy-3-(4-methoxyphenyl)-4-oxo-4H-chromen-7-yl undecylcarbamate and 5-hydroxy-3-(4-methoxyphenyl)-4-oxo-4H-chromen-7-yl dodecanoate referred as compound **1** and compound **2** henceforth. For the latter, a previous step was necessary (Scheme 1) and subsequently the BCA derivatives, both compound **1** and **2**, were made as shown in Scheme 2.

### **Compound 1: 5-hydroxy-3-(4-methoxyphenyl)-4-oxo-4H-chromen-7-yl undecylcarbamate**

Synthesis of compound **1** was carried out as described by Nikolas Fokialakis *et al.* (2012). 100 mg of BCA (0.35 mmol) were dissolved in 20 ml of anhydrous ether and 0.8 ml of anhydrous pyridine under stirring. The mixture was heated at 35°C on an oilbath and 0.05 ml of undecylisocyanate was added resulting in the formation of compound **1** (Scheme 2). The reaction was left overnight to assure that the maximum amount of reagents could interact. The crude material was concentrated by evaporating the remaining solvent with chloroform and dissolved one more time to run column chromatography in order to purify and separate the mixture obtained. Yield: 65%.

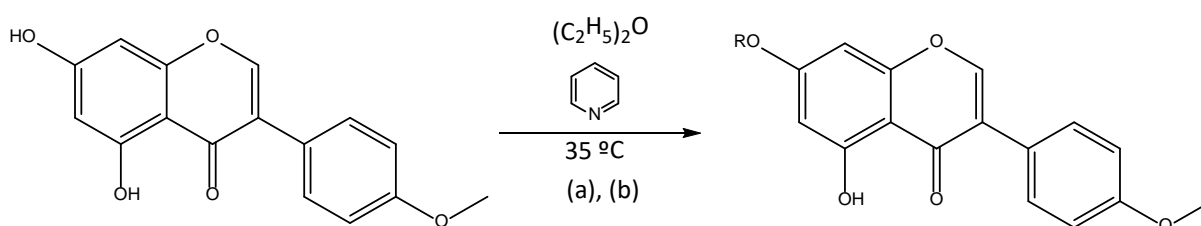
### **Compound 2: 5-hydroxy-3-(4-methoxyphenyl)-4-oxo-4H-chromen-7-yl dodecanoate**

For the preparation of compound **2**, the carboxylic acid present in dodecanoic acid was first activated by making an acyl chloride (Scheme 1). In order to do that, 0.4 g of the acid was mixed in a round flask along with thionyl chloride (0.6 ml) and dichloromethane (10 ml) and the mixture was then refluxed for 3-4h. Once the time was completed, the solvents were removed, and the residue dissolved in DCM and the solvent removed again until total dryness. 100 mg of BCA (0.35 mmol) were dissolved in 20 ml of anhydrous ether and 0.8 ml of anhydrous pyridine under stirring. The mixture was heated at 35°C on an oil-bath and 0.05 ml of the acid chloride was added resulting in compound **2** (Scheme 2). The reaction was left overnight to assure that the maximum amount of reagents could interact. A salt precipitation was observed which was cleared out by filtration. The crude material was then evaporated and was dissolved in chloroform to be purified by column chromatography. Yield: 60%.



**Scheme 1. Synthesis of the acid chloride.** SOCl<sub>2</sub> (thionyl chloride); DCM or CH<sub>2</sub>Cl<sub>2</sub> (dichloromethane).

In both cases the reactions were monitored by TLC using a hexane-ethyl acetate (1:1) solvent system resulting in a good resolution.



**Scheme 2. Synthesis of BCA derivatives.** (a) Reagents for compound 1: Py, CH<sub>3</sub>(CH<sub>2</sub>)<sub>10</sub>NCO; (b) for compound 2: Py, CH<sub>3</sub>(CH<sub>2</sub>)<sub>10</sub>COCl.

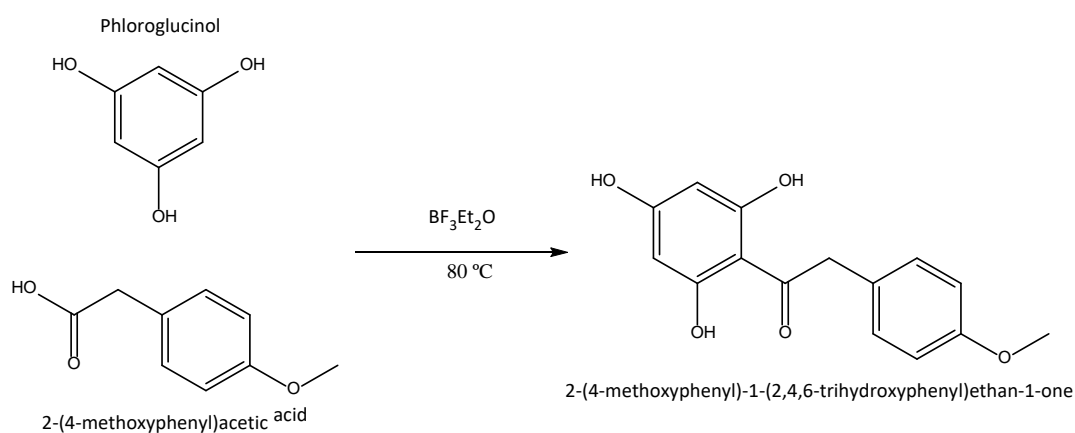
### Biochanin A intermediate

#### **Compound 3: 2-(4-methoxyphenyl)-1-(2,4,6-trihydroxyphenyl)ethan-1-one**

Deoxybenzoins are intermediates in the synthesis of isoflavones which occur in several plant and marine sources. Due to structural similarities, in the present study, a BCA intermediate named 1-(2,4,6-trihydroxyphenyl)-2-(4-methoxyphenyl)ethanone, henceforth stated as compound **3** (Scheme 3), was synthesized and assessed subsequently.

Because the synthesis of BCA consists of two consecutive reactions, the intermediate was synthesized following the method by Nikolas Fokialakis *et al.* (2012). The reaction is based on a Friedel-Craft reaction. Phloroglucinol (0.02 mol) and p-methoxy phenylacetic acid (0.02 mol) were dissolved into BF<sub>3</sub>·Et<sub>2</sub>O (5 mol equiv.) under nitrogen conditions. The mixture was stirred and heated at 80°C in an oil-bath for 90 min creating an orange solution. Thereafter, an extraction was carried out by washing off the collected material thoroughly with saturated aq. NaHCO<sub>3</sub> and ethyl acetate. When the reaction mixture was poured into the aqueous phase, an emulsion was observed and eliminated by adding brine (sodium chloride). Then, the organic phase was dried with magnesium sulphate, filtered and concentrated under vacuum. The

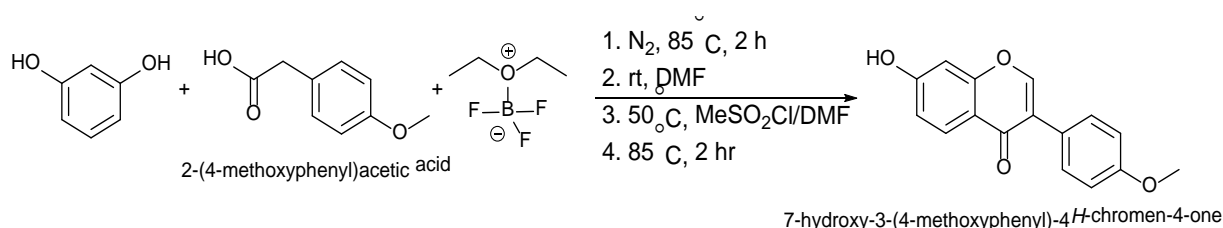
residue was purified twice by column chromatography on silica gel using firstly a mixture of dichloromethane and methanol (20: 1.2), and secondly, the same solvent system with a ratio of 22:1. The corresponding intermediate product, compound **3**, was then isolated and purified. Yield: 45%.



**Scheme 3. Synthesis of BCA intermediate (compound 3) through a Friedel-Craft reaction.**

#### Formononetin derivatives

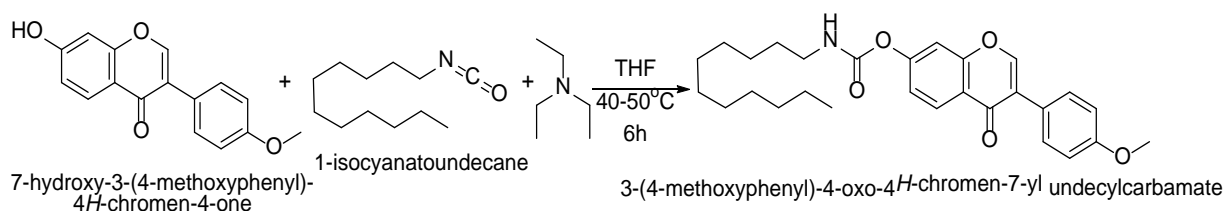
In order to synthesise a FMN derivative we first had to make FMN as detailed below. A mixture of resorcinol (3 mmol, 330 mg), 4-methoxyphenylacetic acid (3 mmol, 499 mg) were dissolved into  $\text{BF}_3\cdot\text{Et}_2\text{O}$  (15.3 mmol, 1.9 mL) under argon. The mixture was stirred at 85 °C for 2 h. For cyclization the reaction mixture was cooled down to room temperature and dry DMF (20 mol equiv., 60 mmol, 4.65 ml) was added. The mixture was heated to 50 °C and a solution of methanesulphonyl chloride (9 mmol, 0.7 ml) in dry DMF (12 mmol, 0.9 ml) was added slowly. Thereafter, the reaction was brought up to 85 °C and stopped after 2 hrs (Scheme 4). The reaction mixture was cooled to room temperature and poured, without stirring, into a solution of ice-cold aq. sodium acetate (20%, 50 mL) due to the reaction of neutralization being exothermic. The solution was left under stirring for 10-15 min to assure a good extraction afterwards. The mixture was then extracted with ethyl acetate, and the organic layer was washed with water, dried ( $\text{MgSO}_4$ ) and concentrated. Yield: 43%.



**Scheme 4. Synthesis of formononetin (FMN).**

#### Compound 4: 3-(4-methoxyphenyl)-4-oxo-4H-chromen-7-yl undecylcarbamate

In order to obtain the FMN derivative, to a solution of FMN (50 mg, 0.18 mmol) and triethylamine (0.4 ml, 0.56 mmol) in dried tetrahydrofuran (THF, 2 ml), undecyl isocyanate (0.04 ml) was added. The reaction mixture was stirred at 40-50°C for 6 hours (Scheme 5). After the reaction, the solvent was evaporated under reduced pressure and the resulting crude product was purified by crystallization. The compound was partially dissolved in methanol and boiled to fully dissolution and then cooled to room temperature to give a white powder which was then filtered under vacuum. The liquid phase was dried out under vacuum and an NMR was performed for each phase. Our desired compound, 3-(4-methoxyphenyl)-4-oxo-4H-chromen-7-yl undecylcarbamate (entitled compound **4** henceforth), was in the liquid phase, and the residual solid turned out to be excess of undecylisocyanate. Yield: 54%.



**Scheme 5. Synthesis of FMN derivative (compound 4).** THF: tetrahydrofuran.

## 2.2 PHARMACOLOGICAL EXPERIMENTS

### 2.2.1 Cell culture

BV2 microglia, which are immortalised cells were used in this study. All the experiments were conducted on BV2 mouse microglia cells (ICLCATL03001) which was purchased from Interlab Cell Line Collection (Banca Biologica e Cell Factory, Italy).

Cell cultures require an aseptic environment and a supply of nutrients to grow adequately. In terms of pH and temperature, the environment should be also stable. Therefore, upon thawing a vial of cells, these were sustained in humid atmosphere (95%), 5% of CO<sub>2</sub> and 37°C. BV2 cells were cultured in Roswell Park Memorial Institute (RPMI) medium 1640 (Sigma Aldrich) supplemented with 10% fetal bovine serum (FBS) and 5 ml of sodium pyruvate (1mM). All culture supplements were also purchased from Sigma. LPS (Innaxon®) used is derived from *Salmonella typhimurium*, S-type (smooth/wild-type).

### Subculturing semi-adherent cells

BV2 microglia are by nature semi-adherent cells. For optimal growth and maintenance, these cells were cultured in 75 cm<sup>2</sup> culture flasks. Once 80% of confluence was reached, cells were sub-cultured by washing them with Dulbecco's phosphatebuffered saline (DPBS) and using trypsin/ethylenediaminetetraacetic acid (EDTA) solution in order to detach the cells stuck on the flask wall and incubated for 1 minute at 37°C. RPMI was then added in order to inactivate the trypsin. The total volume was transferred to a 50 ml tube and centrifuged at 1,200 rpm for 5 minutes. The supernatant was removed and the pellet observed at the bottom flicked to its rupture. Cells were immediately re-suspended in fresh RPMI. Subsequently, cells were diluted 1/10 with RPMI and transferred to a new 75 cm<sup>2</sup> flask.

### Seeding out cells into plates

According to the type of experiment conducted, cells need to be seeded out into different wells with multiple volume capacities. However, in order to assure the validity of the experiments, the cell number needs to remain the same. Therefore, the cell quantification is very important. In our case, cell quantification was carried out manually by using a Neubauer's chamber. Once the cells reach the desired confluence, the medium needs to be changed to serum free medium for at least two hours before starting the stimulation.

#### **2.2.2 Determination of cell viability**

Viability of BV2 cells under-treatment was measured by 2,3-bis(2-methoxy-4-nitro-5sulfophenyl)-5-[(phenylamino)carbonyl]-hydroxide (XTT) assay (Invitrogen). XTT is a colorless compound which upon reduction becomes brightly orange. Whether this reaction takes place means that cells are enzymatically active and therefore their viability has not been compromised. The absorbance is quantified spectrophotometrically and it is directly proportional to the alive number of cells. Such determination is relevant to determine whether or not the compounds tested are cytotoxic for the cells.

In order to perform an XTT assay, BV2 cells were seeded out in a 96-well plate at a concentration of 15,000 cells per well. After 48 h incubation at 37°C, the medium was changed to serum-free medium. Thereafter, cells were treated with the compound 30 min prior to stimulation with LPS for further 24h.

After 24 hours a 10 mM PMS (N-methyl dibenzopyrazine methyl sulfate) solution in PBS (phosphate-buffered saline) was prepared (3 mg PMS into 1 ml PBS). At the same time, 4 mg of XTT was dissolved in 4 ml of RPMI at 37°C. Subsequently, 10 µl of the PMS solution was added to the 4 ml of XTT and mixed. 25 µl of the latest solution was directly added to each well containing 100 µl of cell culture. After 2 h of incubation at 37°C, absorbance was read in a microplate reader (Infinite F50, Tecan) at wavelength of 450nm.

### **2.2.3 Determination of nitrite production from BV2 microglia**

Nitric oxide (NO) is a molecular free radical produced by the nitric oxide synthases (NOSs) enzymes family which catalyze the production of NO from L-arginine. It is an important physiological messenger in the immune, nervous and cardiovascular systems. Due to its participation in these diverse systems, interest in measuring biological NO remains strong.

High concentrations of NO may produce harmful effects in our organism. During an inflammatory process, the inducible isoform of nitric oxide synthase (iNOS) is responsible for the production of NO. This NO produces a neurotoxic activity reacting with other types of pro-inflammatory substances such as reactive oxygen species (ROS). However, an uncontrolled NO production may also boost ROS levels, generating oxidative stress and damaging adjacent neurons following neuroinflammation.

The Griess assay is generally used for indirect measurement of NO. This assay relies on a diazotization reaction that was originally described by Griess in 1879. NO indeed has the feature of a short half-life, transforming almost instantly into its more stable version, nitrites ( $\text{NO}_2^-$ ) and nitrates ( $\text{NO}_3^-$ ). Nitrates are the product of a reaction between the NO and the oxihemoglobin, being commonly originated in blood and plasma. On the contrary, nitrites are the sole stable product from the NO self-oxidation in aqueous solutions. Therefore, when performing a Griess assay, what it is actually being measured are the nitrites ( $\text{NO}_2^-$ ) formed.

The Griess Reagent system is based on the chemical reaction shown in Figure 17, which uses sulphanilamide (SA) and N-1-naphthylethylenediamine dihydrochloride (NED) under acidic (phosphoric acid) conditions.  $\text{NO}_2^-$  makes, under acidic conditions,

nitrous acid (HNO<sub>2</sub>) which gets protonated and fragmented releasing water and a nitrous cation (N=O<sup>+</sup>):



Subsequently, the nitrous cation interacts with an amine generating a nitrosamine product. Bearing this in mind, when the NO<sub>2</sub><sup>-</sup> present in our sample enters into contact with SA, firstly, an aromatic diazonium salt is formed, which in turns reacts with the second reagent NED, delivering a pink colored compound giving thus, an indirect measure of the nitrite in the sample (Sun *et al.*, 2003).

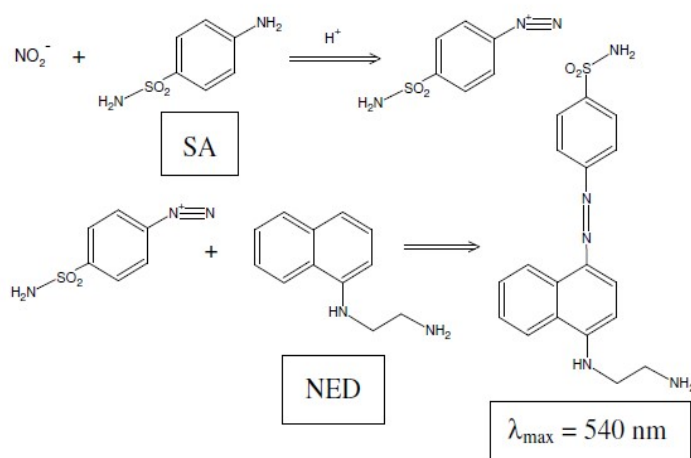


**Figure 17. Chemical reactions involved in the measurement of NO<sub>2</sub><sup>-</sup> using the Griess Reagent System (Sun *et al.*, 2003).**

For this purpose, BV2 cells were seeded at a density of  $2 \times 10^5$  cells/ml and cultured until confluent. After that, pre-treatment with different compound concentrations 30 minutes prior to stimulation with LPS (100 ng/ml) for a further 24 hours. After the incubation, culture supernatants were collected and centrifuged for 5 minutes at 2500 rpm to remove cell debris. Levels of nitrite in culture media were measured using a Griess reagent kit (Promega, Southampton). For a proper quantification, a nitrate standard curve was prepared in duplicate in a 96-well plate. Then, 50 μl of each sample was added to empty wells in the 96-well plate also in duplicate and other 50 μl of reagent 1 (SA) were added to all samples and incubated for 5-10 min protected from light. Afterwards, another 50 μl of reagent 2 (NED) were added to all wells and incubated in dark for further 5-10 min. Absorbance was read at 540 nm (Infinite F50, Tecan) and concentrations were calculated against a nitrite standard curve.

#### 2.2.4 Determination of inflammatory cytokines by immunoassays

Immune assays are widely used due to their sensitivity and specificity. They are based on the specific antigen-antibody reaction (Ag-Ab), which can be visualized through indirect mechanisms such as enzymes, fluorophores or isotopes. Such is the case of the enzyme immunoassay (EIA), which is characterized by using enzymes in order to detect the Ag-Ab reaction. Within this category, is found the Enzyme-Linked Immunosorbent Assay (ELISA). Generally, in this type of assay, the Ab is stuck on the surface of the well and the Ag is the molecule or substance we want to identify. This Ag also interacts with another Ab which is labelled with an enzyme. The substrate of the enzyme is colourless and it produces a coloured product upon enzyme activation, easily detectable by spectrophotometry.

In this study, BV2 cells were seeded in 24-well plates as specified before, cultured until 80% of confluence was reached and incubated with or without LPS (100ng/ml) in the absence or presence of the compounds desired (5, 10, 15 and 20  $\mu$ M). Supernatants were collected after 24 h and centrifuged for 5 minutes at 2500 rpm. ELISA's were performed that is plates were pre-coated with the coating antibody provided by the supplier in order to detect the Ag (in this case, cytokines) within the experimental sample. Hence, levels of TNF $\alpha$ , IL-6 and IL-1 $\beta$  in the supernatants were determined by specific ELISA kits against mouse cytokines (R&D Systems, China).

One day prior to the experiment, a 96-well plate (Corning Costar® 9018) was precoated with unlabeled capture antibody diluted in coating buffer in a proportion of 1:200. The coating buffer (5X) was firstly diluted with assay diluent to 1X. Thereafter, 100  $\mu$ l of this solution were transferred to each well of a high affinity, protein-binding ELISA plate. Plates were sealed to prevent evaporation and incubated at 4°C overnight. To detect concentrations of TNF $\alpha$  and IL-6 a standard curve was prepared by doing 6 two-fold serial dilutions (500, 250, 125, 62.5, 31.3, 15.6 and 7.8 pg/ml) starting from a stock solution of 500 pg/ml. Whilst to analyze the presence of IL-1 $\beta$  the initial stock solution was 2.000 pg/mL to give a standard curve of 1.000, 500, 250, 125, 62.5 and 31.3 pg/mL. 1X assay diluent serves as the zero standard (0 pg/mL). All antibodies and reagents were diluted with 1X assay diluent. If needed, samples were also diluted with 1X assay diluent. The plate was thoroughly washed and blotted by tapping the plate upside down on absorbent paper. Subsequently, 200  $\mu$ l of Assay diluent were added into all wells and incubated while shaking for 1h at 200 rpm. Afterwards, another washing was carried out and 100  $\mu$ l of standard dilutions or

samples were added to appropriate wells and then incubated for 2 h on a rocker at 200 rpm. The content of the plate was discarded and washed 4 more times. 100  $\mu$ l of mouse detection antibody solution were added to each well and shook for a further hour. Another washing was carried out and 100  $\mu$ l of Avidin were added for further 30 minutes while shaking. In this step, a final washing was performed and 100  $\mu$ l of Substrate Dilution were added. This substrate is tetramethylbenzidine, which is oxidated by a horseradish (HRP) enzyme giving a blue colour (Figure 18). The incubation time was carried out in the dark for either 15 min or until the desired colour intensity was achieved. The enzyme-substrate reaction was stopped by adding 100  $\mu$ l of Stop solution (sulphuric acid 2N) to each well which veered the colour towards yellow. Absorbance was measured in a plate reader (Infinite F50, Tecan) at wavelength of 450nm. The concentration of cytokines present in the samples was calculated from the absorbance compared to the relevant standard curve.

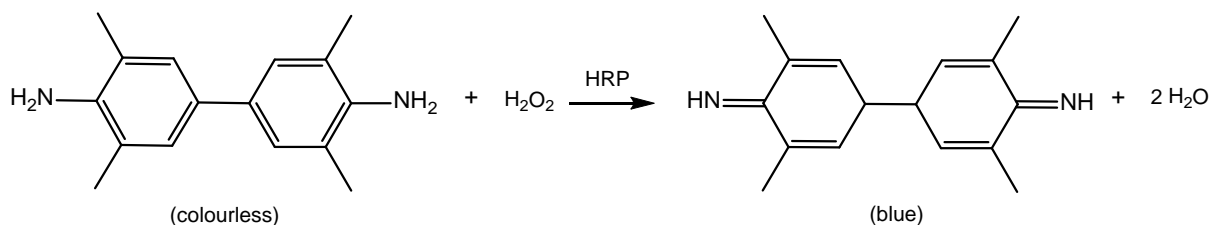


**Figure18.** Oxidation reaction of TMB by HRP.

### 2.2.5 Determination of prostaglandin E<sub>2</sub> (PGE<sub>2</sub>) by immunoassay

Prostaglandin E<sub>2</sub> (PGE<sub>2</sub>) is an arachidonic acid derivative released by activated microglia through the enzymatic action of cyclooxygenase-2 (COX-2). Several studies have shown that high levels of PGE<sub>2</sub> regulate the production of inflammatory cytokines during neuroinflammation (Kim *et al.*, 2015). This observation suggests that downregulation of PGE<sub>2</sub> in activated microglia may be beneficial in the treatment of neuroinflammation and thus, in the neurodegenerative process.

The determination of PGE<sub>2</sub> levels in culture supernatant was conducted by enzyme immune assay (EIA) with a pre-coated ELISA kit from Arbor assay (USA) using the protocol provided by the supplier. Briefly, BV2 cells were seeded in 24-well plates as specified before, cultured until 80% of confluence was reached, pre-treated with different compounds and stimulated with LPS. Supernatants were collected after 24 h and centrifuged for 5 minutes at 2500 rpm. 100  $\mu$ L of samples and standards were pipetted into wells in the plate. Thereafter, 25  $\mu$ L of PGE<sub>2</sub> conjugate (PGE<sub>2</sub>-peroxidase

conjugate in stabilising solution) and 25  $\mu$ L of the PGE<sub>2</sub> monoclonal antibody were added to each well. The plate was covered with the plate sealer to be shaken at room temperature for 2 hours. The content of the plate was discarded and washed with freshly prepared washing buffer to remove non-specifically bound proteins or antibodies. 100  $\mu$ L of 3,3',5,5'-tetramethylbenzidine (TMB) substrate were added to each well and incubated 30 minutes without shaking. Finally, 50  $\mu$ L of the stop solution (0.16M sulphuric acid) were pipetted to each well using a repeater pipette. The optical density generated was read in the plate reader at 450 nm. To the final concentration obtained, the inverse was applied in order to acquire the concentration of PGE<sub>2</sub> present in the samples.

### 2.2.6 Cytosolic protein extraction

In order to determine proteins of interest using Western Blot technique, it was necessary to separate target proteins from the tissue or cells. These are treated with a lysis buffer and subsequently are degraded mechanically to release the proteins. For that purpose and to get a sufficient amount of proteins, cells were cultured in a 6 well-plate. In our case, a nuclear extraction kit supplied by Abcam was used.

Briefly, after treating the cells, the stimulation was then stopped by placing the plate on ice. Throughout the entire process cells and their lysates were kept on ice to avoid protein degradation. Cells were washed with PBS ( $\approx$ 1 ml per well) followed by addition of 200  $\mu$ l of a protease and phosphatase inhibitor cocktail comprised of radioimmunoprecipitation assay buffer (RIPA) lysis buffer in PMSF (phenylmethylsulfonyl fluoride) and incubated on ice for 15 min. The surface of each well was scraped and cells transferred to 1.5 ml tubes to be centrifuge for 10 min at 13500 rpm at 4°C. In this case, the supernatant contains **cytosolic proteins** of interest; thus it is relocated to new labelled 1.5 ml tubes and stored at -80°C until further usage.

### 2.2.7 Protein quantification

Prior to conducting a Western Blot, protein must be quantified in order to ensure equal loading of proteins. In our case, Bradford's method was conducted. Bradford reagent contains a hydrophobic colouring substance, *Coomassie Blue*, whose stability depends on the acid/base conditions of its environment. In an acidic environment, this reddish brown coloured reagent is protonated, however, when entering into contact

with disulphide bridges (S-S) of a protein it gets deprotonated, and its colour veers toward an intense blue. The intensity of this blue colour, measured by spectrophotometry, is proportional to the protein concentration in a sample.

An aliquot of each sample is diluted, usually 1:10, and 5 µl thereof (in duplicate) is transferred into a 96 well-plate. 250 µl of Bradford reagent are added into each well and thereafter the absorbance is measured at 570 nm (Infinite F50, Tecan). In order to calculate the protein concentration of each sample, an albumin serum bovine (BSA) standard curve with known concentrations (2, 1, 0.5, 0.25, 0.125, 0.0625, 0.03125, 0 mg/ml) is also conducted. Results are then interpolated on the standard curve according to a linear equation. Once the concentration is obtained, the volume of sample of each sample that needs to be loaded must be calculated. Depending on the protein being measured, the amount needed differs.

### **2.2.8 Determination of protein expression by Western Blot**

The Western Blot technique or immunoblot of proteins, is an analytic technique employed for the detection of a specific protein from a complex mixture of proteins. Building on the physical characteristics of polypeptides, such as their size, electrical charge and shape, a complex mixture of proteins can be separated by electrophoresis in a gel matrix in the presence of electric current. In the Western Blot, the electrical charge variable is controlled by adding a reducing agent which endows all proteins with the same negative charge; as a result, the disparity on the proteins distance travelled will be only affected by their shape and size. The term “blot” refers to the process of transferring biological macromolecules from a gel to a membrane and its posterior detection on its surface by specific antibodies. Details on these processes are explained below.

#### **Electrophoresis**

Electrophoresis allows the separation of proteins according solely to their physical features. For that purpose, usually polyacrylamide gels (PAGE) are used along with a reducing agent consisting of beta-mercaptoethanol (DTT) and sodium dodecyl sulfate (SDS). Therefore, all proteins will run towards the positive electrode and the smaller proteins will travel through the gel more easily than the bigger ones, resulting in separation in bands.

The four fundamental components of a polyacrylamide gel are:

- Acrylamide;
- Bisacrylamide;
- TEMED (Tetramethylethylenediamine) and
- APS (ammonium persulfate).

The APS is the reaction initiator and in solution is found as a free radical, it is very active and acts upon acrylamide molecules to produce a linear polymer. Such reaction is catalyzed by TEMED and the bisacrylamide acts as a cross-linking reagent meaning that bisacrylamide is capable of creating cross-links between polyacrylamide chains, thus creating a network of polyacrylamide rather than unconnected linear chains of polyacrylamide.

Depending on the size of the protein to be characterized, the percentage of acrylamide used on the confection of the gel differs (Table 6). The higher the percentage of acrylamide the smaller the size of the porous of the gel.

**Table 6. Percentage of acrylamide to be used on the confection of running gel depending on the size of the protein to be analyzed.**

Size of the protein	% Acrylamide
200-130 kDa	8%
130-40 kDa	10%
40-15 kDa	15%

In a Western Blot, the gel comprises 2 different parts: on top the “*stacking gel*”, which gathers the sample, and beneath the “*running gel*”. The *stacking gel* is slightly more acidic (pH = 6.8) with a lower concentration of acrylamide, allowing all the proteins in the sample to be concentrated on the top of the running gel; in this way, all the particles are accomplished to be in the same initial conditions. The *running gel* is more basic (pH = 8.8), and it is responsible for the separation of the proteins according to their molecular weight. Both gels are set up between two glasses whose distance between them will determine the thickness of the gel (from 0.4 mm to 2 mm).

As mentioned above, the proteins are to be charged negatively so that all of them run to the same electrode. For this reason, a reducing buffer is used. This reducing buffer comprises:

- sodium dodecyl sulfate (SDS): charges the proteins negatively in a ration 1.4 g of SDS to 1 g of protein thus, the ration charge/mass of the proteins will be constant;
- beta-mercaptoethanol or dithiothreitol (DTT): reduces disulphide bridges which breaks the structure of the proteins to their primary structure allowing the SDS to cover the proteins entirely;
- glycerol: increases the density of the sample to be higher than that of the buffer;
- Tris/HCl buffer (pH 6,8) and
- Bromophenol blue: which possesses a higher electrophoretic mobility compared to the proteins, therefore it is positioned ahead being used as a marker of the front indicating when to stop the electrophoresis.

### **Electrotransfer**

Once the proteins of the sample have been separated according to the molecular weight, they are transferred onto a membrane, which can be made out of nitrocellulose or polyvinylidene fluoride (PVDF). The latest have a higher protein retention capacity, physical resistance and a wide range of chemical compatibility, consequently these are the ones used in our case.

There are different transferring systems but the most employed is the electrotransfer. This technique can be dry, semi-dry or wet. All of these are based on the same principles and only differ on the device used. The wet transfer requires a tank full of transfer buffer in which the gel obtained on the electrophoresis is soaked in contact with the PVDF membrane. Once the system is set up, the transference is produced when a constant electric current is supplied. It is an effective method but slower than that of the dry or semi-dry and it also requires more volume of transfer buffer.

After the transference is completed, the membrane is then soaked into a blocking buffer, the most common of which are those formed by inert proteins such as BSA, skimmed milk, casein or gelatin. All of them are usually dissolved in PBS-tween 20. This step is necessary to avoid cross-talk reactions between the antibodies further employed and proteins that are of no interest in our analysis.

Upon the blocking step, the membrane is incubated with a primary antibody specific to bind the protein to be detected. This antibody can be already labelled with or, on the contrary, require a secondary antibody labelled which will recognize the primary

antibody. In this case, the most common marking consists of the binding of an enzyme (such as the horseradish peroxidase [HRP] or the alkaline phosphatase [AP]) covalently to the antibody (Figure 19). This conjugated enzyme catalyzes the degradation of specific substrates generating a measurable signal that can be chromogenic, chemiluminescence or chemifluorescence (Figure 20).

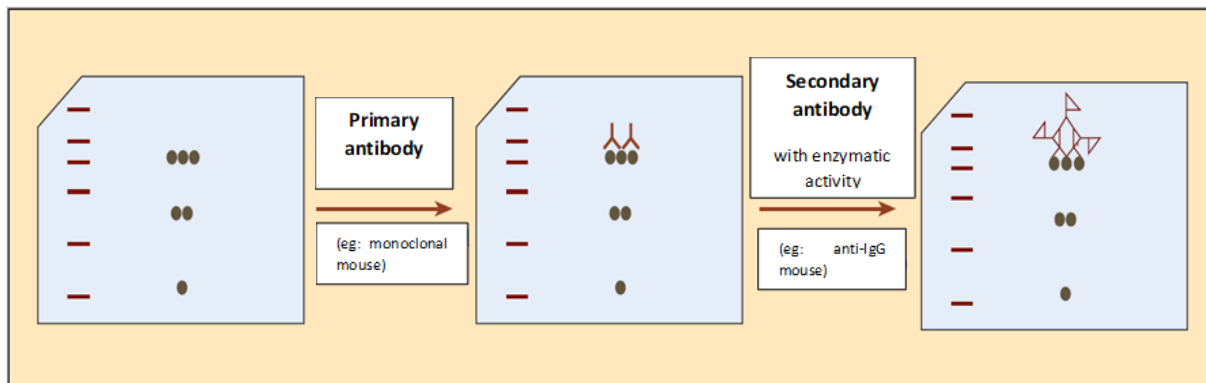


**Figure 19. Diagram of the immunodetection of proteins on a Western Blot membrane.**

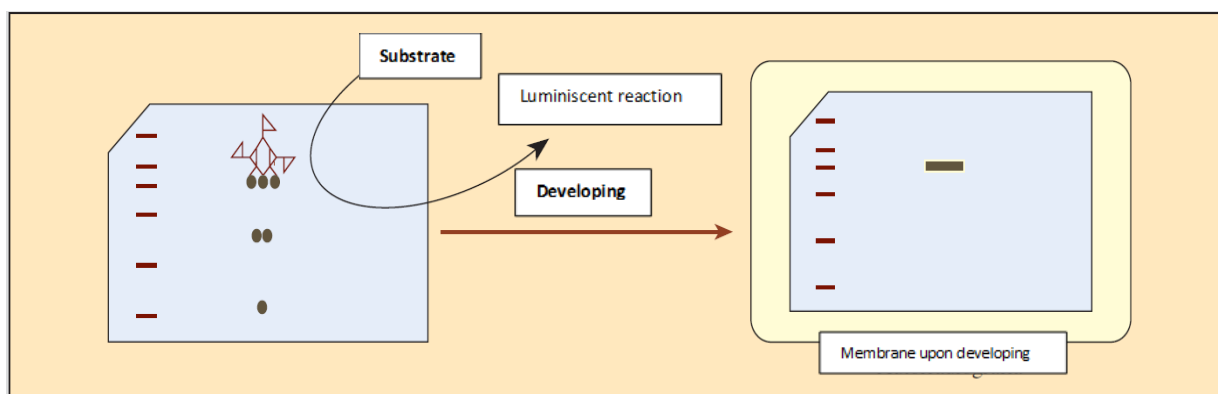


**Figure 20. Diagram of the developing of membrane.**

## PROTOCOL

- Reduction and denaturation of proteins

Upon quantification of the proteins in the samples by Bradford assay, the volumes corresponding to the same amount of protein in each sample were aliquoted in different 1.5 ml tubes. Each of them was completed with distilled water to an equal total volume, and then heated for 5 min at 99°C with a reducing buffer which contains DTT and SDS (5:1 v/v). Samples were then ready to proceed with the Western Blot.

- Western Blot

The electrophoresis device is set up with polyacrylamide gels inside and filled up with running buffer (refer to Annex I section 2 to see the composition). The same quantities of protein must be loaded in the wells of the gel, which generally has a 10% of acrylamide (see Annex II.1). The electrophoresis circuit is closed with a lid and then it is run for 50 min at 150V. Once this step was completed, the proteins on the gel were transferred to a PVDF membrane. These type of membranes have a large union capacity to proteins (100 – 300  $\mu\text{g}/\text{cm}^2$ ) but are also completely hydrophobic and they would not get wet in aqueous solutions. For this reason and to make them compatible with a wet system, they need to be “activated”. To do so, the membranes are soaked in pure methanol and then dipped in water to wash them. Right after, they are ready to be soaked in transfer buffer (Annex II.2) in order to equilibrate the pH. In all cases, the type of transference employed was the wet transference (Bio-Rad) for 90 min with a current of 300 mA. The entire process is conducted at 4 °C (due to the process being exothermic) in continued agitation. In this system, the gel is always in contact with the membrane in a system assembled as shown in Figure 21. Since the protein have a negative charge, they migrate to the anode, in other words, from the gel to the membrane where they remain attached.

Once the transference terminated, the membrane was incubated with skimmed milk to 6% (p/v) diluted in PBS-Tween (PBS buffer supplemented with Tween 20 to 0.1% (v/v)) or BSA to 3% (p/v) diluted in PBS-Tween for 1h at room temperature and gentle agitation. The aim of this step is to block the areas of the membrane where proteins have not been transferred with inert proteins, thus reducing the unspecific union of the secondary antibody.

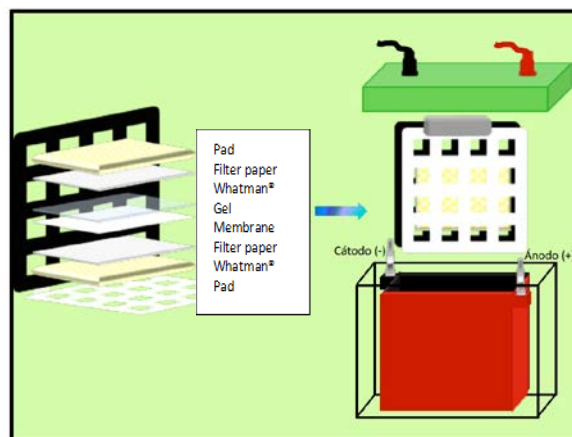


Figure 21. Assembly of the transference process.

Upon the blocking the membrane is incubated with a primary antibody diluted (Table 7) in skimmed milk (3%) or in BSA (1.5%) in PBS-Tween during 2h at room temperature. The membrane was then thoroughly washed with PBS-Tween with high speed agitation. Thereafter, the membrane was incubated with a secondary antibody (Alexa Fluor 680 goat anti-rabbit, Life technologies®) conjugated with HRP in a 1:10000 dilution in skimmed milk (5%) in PBS-Tween for 1h at room temperature at slow speed agitation.

**Table 7.** General information for primary antibodies used.

Primary antibody	Supplier	Host	Type	Dilution
<b>Anti-iNOS</b>	Abcam	Rabbit	Monoclonal	1:1000
<b>Anti-COX-2</b>	Abcam	Rabbit	Monoclonal	1:1000

Upon the incubation time, a whole set of washes was repeated to remove the excess antibody. Finally, the bands with the protein of interest where visualized by a chemiluminiscent reaction, which employs horseradish peroxidase (HRP) to catalyze a reaction whose product is UV visible. The HRP catalyzes the oxidation of luminol by using hydrogen peroxide (Immobilon™ Western HRP Substrate, Millipore). As the oxidated luminol turns into its baseline condition, it emits visible light, that was detected with a digital imaging capture system, LAS 3000 mini (Fujifilm) (Figure 22).

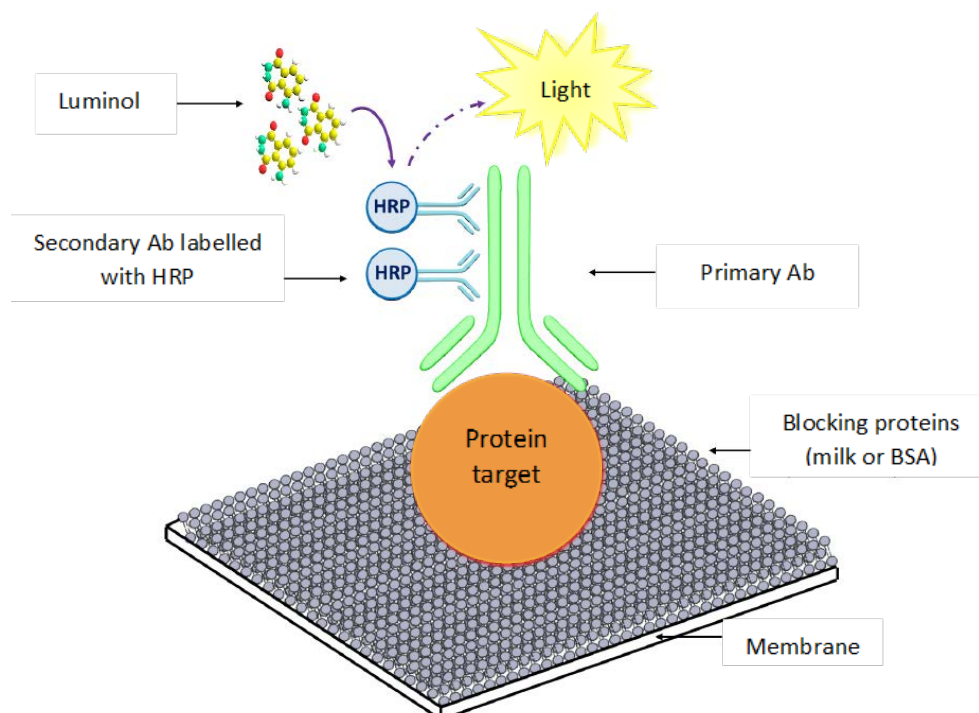


**Figure 22.** Diagram of the protocol of a protein detection by Western Blot. Ab: antibody; HRP: horseradish peroxidase.

The densitometry analysis was conducted with Image Studio Lite v5.2. This program determines the optical density emitted and calculates the area under the curve. The integrated optical density (IOD) is obtained as a number. IOD values of the proteins are normalized against the respective loading control and represented in percentage in relation to the control (100%).

### **2.2.9 Statistical analysis**

All experiments were performed at least three times and in triplicates unless otherwise stated. Data are expressed as mean  $\pm$  SEM (standard error of the mean). For individual results, statistical analysis was performed using one-way analysis of variance (ANOVA) with post-hoc Student Newman-Keuls test (multiple comparisons).

# CHAPTER 3: SYNTHESIS AND PHARMACOLOGICAL STUDIES ON BIOCHANIN A DERIVATIVES

## 3.1 INTRODUCTION

Neuroinflammation is a defense mechanism designed to protect the CNS against foreign pathogens and other type of injury. Therefore, acute neuroinflammation is a major and beneficial process that restores the homeostatic balance by eliminating the initial cause of the problem (Spencer *et al.*, 2012). In the brain, not only glial cells are responsible for this restoration but also lymphocytes, monocytes and macrophages. However, microglia play a key role by repairing the injured tissue via the secretion of chemokines, cytokines and lipid mediators and clearing the debris.

Despite its benefits, neuroinflammation and oxidative stress are also narrowly related to the pathogenesis of neurodegenerative diseases such as Parkinson's and Alzheimer's diseases. When the injury or any of the mechanisms that may activate glial cells are not resolved, cells remain permanently active and the brain enters a chronic neuroinflammation state. In this phase, microglia are termed as chronically active and fosters a chronic inflammatory state with the activation of precursors of pro-inflammatory mediators that eventually results in the release of cytokines such as IL-1 $\beta$ , IL-6, TNF- $\alpha$ , activation of the pro-inflammatory enzymes cyclooxygenase-2 (COX-2) and the inducible nitric oxide synthase (iNOS), production of reactive oxygen species (ROS) and other series of events that may induce neurodegeneration and neurotoxicity (Ong *et al.*, 2017). However, to date, the majority of drug treatments are addressed to treat the symptoms of the neurodegenerative disorders rather than preventing the underlying degeneration of neurons. Accordingly, there is a need and desire to develop novel therapies capable of preventing neuronal loss that trigger pathology in these diseases (Spencer *et al.*, 2012).

Even though isoflavones are the most absorbable and bioavailable flavonoids, phytoestrogens bioavailability, in general, has been a difficult issue to determine their physiological effects (Yu *et al.*, 2016). Bioavailability of most phytochemicals in human tissues is very low because of a rapid clearance and even poorer in brain due to the BBB. Researchers have been developing strategies to solve this problem. Leading strategies involve the synthesis of highly lipid-soluble compounds and the

development of compounds undertaking uptake transport. Production of nanolipidic particles might be another approach (Ong *et al.*, 2017).

Since the first reported synthesis of an isoflavone analogue in 1925 by Baker and Robinson, a series of synthetic procedures have been developed in order to discover new and more potent isoflavones. Three methods have been extensively used: deoxybenzoin (Wähälä and Hase, 1991) and chalcone (Pavese *et al.*, 2010) routes and the Suzuki cross-coupling reaction (Biegasiewicz *et al.*, 2014). Among our objectives, testing the intermediates deoxybenzoin to assess their pharmacological properties was one of them. Therefore, in this project, the deoxybenzoin route leading to BCA was carried out.

The deoxybenzoin route involves first the synthesis of the deoxybenzoin by a Friedel-Crafts acylation, which consists of an electrophilic substitution of a phenol with a substituted phenylacetic acid. After the acylation, the deoxybenzoin undergoes cyclisation to give an isoflavone. On the other hand, BCA derivatives were synthesized based on that carbamates and esters have been used over the years due to their properties and application in drug design.

BCA is an ER- $\beta$  selective isoflavone mostly found in *Trifolium pratense* (family *Fabeaceae*) that has been shown to effectively suppress LPS-stimulated overproduction of cytokines and certain transcriptional factors by inhibiting the activation of the MAPK pathway in BV2 cells (Wang-Yang *et al.*, 2014; Zhang *et al.*, 2015; Wang *et al.*, 2016). Moreover, BCA was also shown to possess neuroprotective effects on PC12 cells by decreasing cell viability loss and apoptosis after A $\beta$ 25-35-induced toxicity (Tan and Kim, 2016). However, a few drawbacks have been described when it comes to its potential in therapeutics. As any other isoflavone, poor water solubility, poor oral bioavailability (4.6%) due to stomach degradation, extensive hepatic first-pass metabolism and high susceptibility to hydrophilic degradation in gastrointestinal (GI) track, play a part in its characteristics (Sachdeva *et al.*, 2016). In addition to the bioavailability issue, other studies have raised concern about the possible health risk of isoflavones. Isoflavones have also shown not only to promote proliferation of cancer cells but also to be cytotoxic for noncancerous cells (Hsu *et al.*, 2010). There are two hypotheses that attempt to explain such apparently contradictory health effects. One is the fact that isoflavones act on both ERs ( $\alpha$  and  $\beta$ ) and it is the balance between both of them that determine the biological outcome. The second hypothesis put forward is the role of epigenetics in cancer (Rietjens *et al.*, 2013).

Few studies have modified the BCA pattern skeleton aiming at improving their pharmacological properties. In one study, the authors prepared a carboxy derivative of BCA (cBCA) by introducing a carboxymethyl group at position 6, based on a previous work in which carboxylation of the isoflavone genistein showed estrogenic and antiestrogenic properties similar to the SERM raloxifene (Somjen *et al.*, 2005). Fokialakis *et al.* (2012) also prepared esters and carbamate esters BCA derivatives and evaluated their estrogenic and cancer chemopreventive activity, finding that one of them particularly displayed estradiol-like stimulation of gene expression as well as inhibition of proliferation of breast and endometrial cancer cells. Besides chemical approaches, developing drug delivery systems has been another attempt to enhance their bioavailability. Sachdeva *et al.* (2016) managed to produce enteric-coated microparticles that would directly arrive at the GI avoiding stomach degradation.

Deoxybenzoins, on the other hand, are also non-steroidal molecules but hold the essential pharmacophores in order to interact with steroid receptors, therefore, acting like isoflavones in some cases. Such pharmacological properties are related to their chemical structure. Deoxybenzoins have the 4-OH and 4'-OH separated by an approximate distance of 12 Å and the presence of the aromatic rings A and B (Chandrasekharan *et al.*, 2013). Some studies have also found that the intermediates deoxybenzoins may possess SERM-like properties. For instance, Papoutsi *et al.* (2007), synthesized a deoxybenzoin with a -Br at position 4' that turned out to be antiestrogenic in breast cancer cells, and estrogenic on osteoblasts without causing stimulation of endometrial cells *in vitro*.

On the basis of the above, in this project, BCA derivatives using chemical strategies were synthesized and the anti-neuroinflammatory effects of the pattern compound and its respective derivatives were studied in LPS-induced neuroinflammation in BV2 microglia.

### **3.2 RESULTS**

In order to fulfill the objectives proposed in the present study, different natural phytoestrogen derivatives were needed to be tested. As already mentioned in the section Material and Methods, we managed to synthesize two BCA derivatives and a BCA intermediate and conduct a preliminary study on their anti-inflammatory activity. This section refers to the structure and efficacy of BCA and its derivatives regarding the effectiveness on producing the desired effect.

### 3.2.1 Synthesis of BCA derivatives and its intermediate

#### Compound 1: 5-hydroxy-3-(4-methoxyphenyl)-4-oxo-4H-chromen-7-yl undecylcarbamate

After the reaction was completed, the presence of compound **1** in the crude extract was confirmed by TLC as described in section 2.1.1. The resulting spots after the reaction took place, were compared to BCA available commercially. A good resolution was achieved running TLCs with hexane/ethyl acetate (1:1) solvent system.

TLC showed 3 spots under UV light and a fourth spot on the top was visualized with permanganate (KMnO<sub>4</sub>) reagent. By comparison with various TLCs, it was concluded that the higher spot, not being UV-active, was the remaining unreacted undecylisocyanate. The following UV-active spot was the desired compound, as was expected since the long side carbon chain provides it with less polarity than the starting material BCA, followed by the remaining BCA and a diffuse pyridine spot.

Column chromatography was performed on the crude extract following the method described in section 2.1.2 using the same solvent system as in the TLCs as the eluent. In both cases, the compounds were effectively separated from the unreacted starting materials. The compound was recovered as a yellowish solid with a 65% yield.

The <sup>1</sup>H NMR, <sup>13</sup>C NMR and mass spectra of the derivative synthesized fully agree with the expected structures.

**<sup>1</sup>H-NMR (400 MHz, δ ppm, CDCl<sub>3</sub>):** 12.8 (1H, s, OH), 7.98 (1H, s, H-2), 7.48 (2H, d, J = 8 Hz, H-2', H-6'), 7.01 (2H, d, J = 8 Hz, H-3', H-5'), 6.86 (1H, d, J=1.5 Hz, H8), 6.62 (1H, d, J = 1.5 Hz, H-6), 5.10 (1H, t, J = 5.5 Hz, CH<sub>2</sub>NH), 3.82 (3H, s, OCH<sub>3</sub>), 3.32 (2H, t, J = 7.5 Hz, CH<sub>2</sub>NH), 1.58–1.25 (18H, m, CH<sub>2</sub>), 0.91 (3H, t, J = 7.3 Hz, CH<sub>3</sub>).

**<sup>13</sup>C-NMR (100 MHz, δ ppm, CDCl<sub>3</sub>):** 181.2 (C-4), 162.2 (C-7), 159.8 (C-5), 156.9 (C-8a), 156.5 (C-4'), 153.2 (C-2), 153.0 (NHCOO), 130.1 (C-2', C-6'), 123.9 (C3), 122.6 (C-1'), 114.1 (C-3', C-5'), 109.1 (C-4a), 104.9 (C-6), 100.4 (C-8), 55.3 (OCH<sub>3</sub>), 41.3 (CH<sub>2</sub>NH), 31.9 (CH<sub>2</sub>CH<sub>2</sub>NH), 29.7-29.2 (5 CH<sub>2</sub>), 22.7 (CH<sub>3</sub>CH<sub>2</sub>), 26.7 (CH<sub>3</sub>CH<sub>2</sub>CH<sub>2</sub>), 14.1 (CH<sub>3</sub>CH<sub>2</sub>).

**HRMS (Dual ESI):** calculated m/z for C<sub>28</sub>H<sub>35</sub>NO<sub>6</sub> 482.2450, found 482.2537 [M+H]<sup>+</sup>. Known compound (Fokialakis N *et al.*, 2012).

Compound 2: 5-hydroxy-3-(4-methoxyphenyl)-4-oxo-4H-chromen-7-yl dodecanoate

Upon the reaction to obtain compound **2**, its proper characterization was conducted as for compound **1** above. The compound was recovered as a yellowish solid with 60% yield. The <sup>1</sup>H NMR, <sup>13</sup>C NMR and mass spectra of the derivatives synthesized fully agree with the expected structures.

**<sup>1</sup>H NMR (400 MHz, δ ppm, CDCl<sub>3</sub>):** 12.75 (1H, s, OH), 7.87 (1H, s, H-2), 7.41 (2H, d, J = 8 Hz, H-2', H-6'), 6.9 (2H, d, J = 8 Hz, H-3', H-5'), 6.67 (1H, d, J = 1.5 Hz, H-8), 6.5 (1H, d, J = 1.5 Hz, H-6), 3.78 (3H, s, OCH<sub>3</sub>), 2.5 (2H, t, J = 7.5 Hz, CH<sub>2</sub>), 1.59–1.07 (20H, m, CH<sub>2</sub>), 0.87 (3H, t, J = 7.5 Hz, CH<sub>3</sub>).

**<sup>13</sup>C-NMR (100 MHz, δ ppm, CDCl<sub>3</sub>):** 181.2 (C-4), 171.2 (COO), 162.37 (C-5), 159.9 (C-7), 156.8 (C-8a), 153.2 (C-2), 130.0 (C-2', C-6'), 124 – 122.5 (C-3, C-1'), 114.1 (C-3', C-5'), 109.4 (C-4a), 105.4 (C-6), 100.8 (C-8), 55.3 (OCH<sub>3</sub>), 34.4 – 22.6 (CH<sub>2</sub>), 14.1 (CH<sub>3</sub>).

**HRMS (Dual ESI):** calculated m/z for C<sub>28</sub>H<sub>34</sub>O<sub>6</sub> 467.2342, found 467.2428 [M+H]<sup>+</sup>. Unknown compound.

Compound 3: 2-(4-methoxyphenyl)-1-(2,4,6-trihydroxyphenyl)ethan-1-one

The synthesis of BCA consists of two consecutive reactions. Firstly, an intermediate product is obtained by a Friedel-Craft reaction. Once this is separated and purified, a cyclization reaction takes place producing BCA. Given this two steps reaction, the intermediate (compound **3**) was isolated. The reaction and work up of the crude material was performed as explained in section material and methods. The residue was purified twice by column chromatography on silica gel using firstly a mixture of dichloromethane and methanol (20: 1.2), and secondly, the same solvent system with a ratio of 22:1. The corresponding intermediate product 1-(2,4,6trihydroxyphenyl)-2-(4-methoxyphenyl)ethanone was isolated as a brownish solid material with a yield of 45%. The compound was identified by <sup>1</sup>H-NMR.

**<sup>1</sup> H NMR (400 MHz, δ ppm, DMSO):** 12.21 (s, 1H), 10.36 (s, 1H), 8.91(1H), 7.12 (d, J = 8.1 Hz, 2H), 6.83 (d, J = 7.5 Hz, 2H), 5.79 (s, 2H), 4.24 (s, 2H), 3.72 (s, 3H).

Known compound (Fokialakis N *et al.*, 2004).

### 3.2.2 BV2 cell viability

In order to determine whether the anti-inflammatory effect of the synthesized compounds was not due to impaired viability of BV2 cells, an XTT viability assay was carried out after incubating the cells with the corresponding compounds for 24 h. Results (Figure 23) showed that there was no significant difference in the viability of cells treated with BCA, compound **1** and compound **2** at concentrations 5, 10, 15 and 20  $\mu\text{M}$  when compared with control (untreated) cells. However, the BCA intermediate, compound **3**, produced statistically significant differences at the highest concentration.

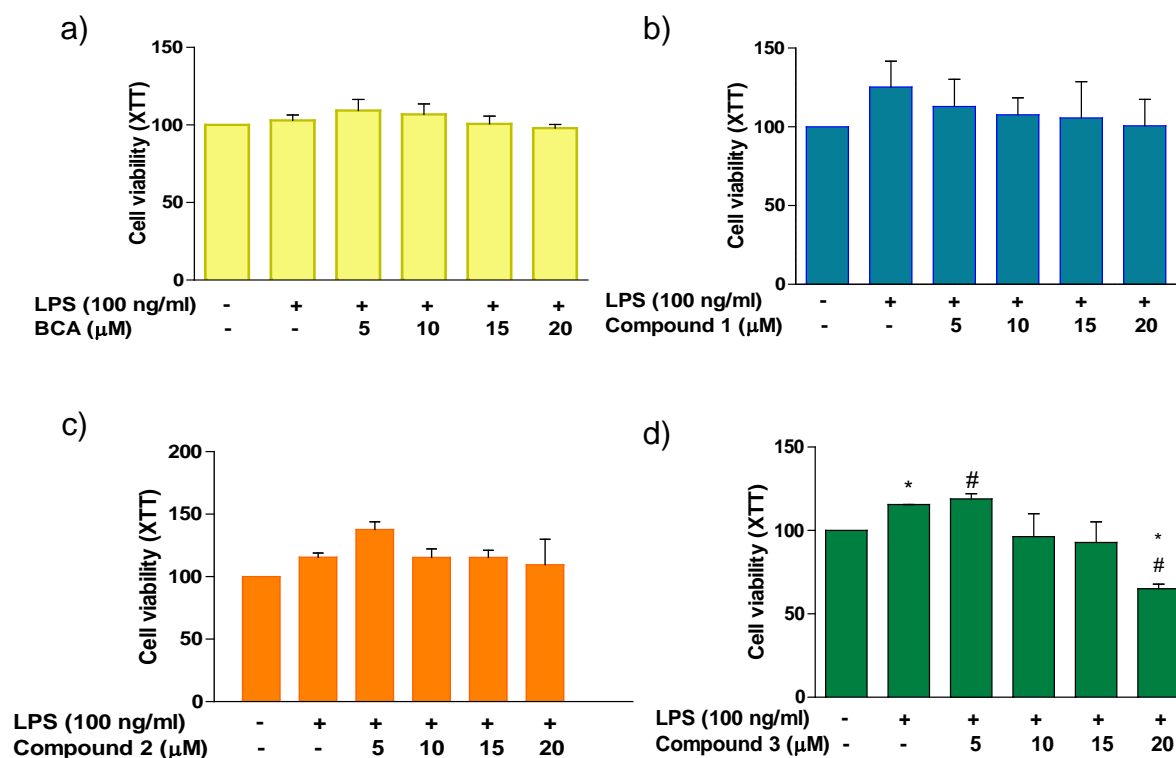


**Figure 23. Cell viability of BV2 cells for BCA compound and its derivatives and intermediate.** Following treatment with various concentrations (5, 10, 15 and 20  $\mu\text{M}$ ) of the compounds and LPS (100 ng/ml) stimulation for 24h, cytotoxicity of BCA (a), compound **1** (b), compound **2** (c) and compound **3** (d) in BV2 cells was assessed by XTT assay. Values correspond to means of 3 independent experiments and are shown as the percentage of viable cells compared with the viability of negative controls (untreated cells). \* $p < 0.05$ , \*\* $p < 0.01$ , \*\*\* $p < 0.001$  in comparison with LPS control. # $p < 0.05$ , ## $p < 0.01$ , ### $p < 0.001$  in comparison with untreated cells.

### 3.2.3 Effects on nitrite production and iNOS protein expression

Nitric oxide (NO) is an important mediator for the regulation of chronic neuroinflammation. Moreover, high concentrations of NO have been shown to be neurotoxic to adjacent neurons (Spencer *et al.*, 2012). Therefore, the effects of the compounds a 5, 10, 15 and 20  $\mu\text{M}$  were investigated for nitrite production in BV2 microglia cells using Griess assay. Figure 24 shows that there was a marked increase in nitrite production ( $p < 0.001$ ) when cells were stimulated with LPS (100 ng/ml) alone, compared with unstimulated cells. However, pre-treatment with BCA and its derivatives effectively inhibited ( $p < 0.001$ ) NO release in a dose-dependent manner.

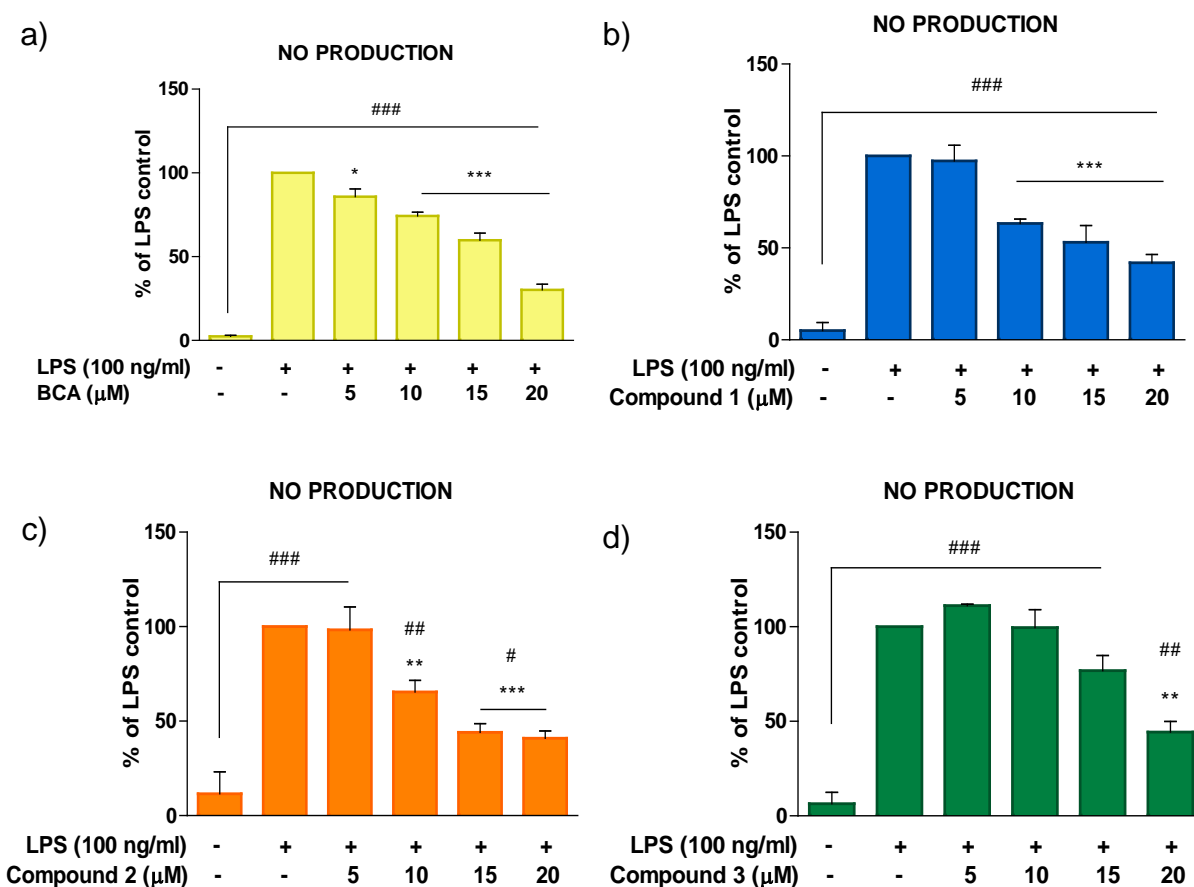


**Figure 24. Effect of BCA, compound 1, compound 2 and compound 3 on nitric oxide (NO) in BV2 cells stimulated with LPS.** This figure shows inhibition of NO release in LPS-activated BV2 cells by BCA (a), compounds 1 (b), 2 (c) and 3 (d). Data is expressed as mean  $\pm$ SEM for 3 independent experiments. Statistical analysis was performed using one-way ANOVA with post-hoc Student Newman-Keuls test (multiple comparison). \* $p < 0.05$ , \*\* $p < 0.01$ , \*\*\* $p < 0.001$  in comparison with LPS control. # $p < 0.05$ , ## $p < 0.01$ , ### $p < 0.001$  in comparison with untreated cells.

Nitric oxide is released by the inducible nitric oxide synthase (iNOS) and levels of both of them should be interrelated. Encouraged by the nitrite results, further studies were conducted with compound **1** in order to observe the correlation between NO and iNOS production. BV2 cells were pre-incubated with compound **1** for 30 minutes, followed by stimulation with LPS for further 24 hours. Upon the incubation time, cytoplasmic lysates were collected to analyse iNOS protein expression by western blotting. Overall, these results illustrate that compound **1** slightly reduces iNOS expression, in particular at a concentration of 15  $\mu\text{M}$  (Figure 25).

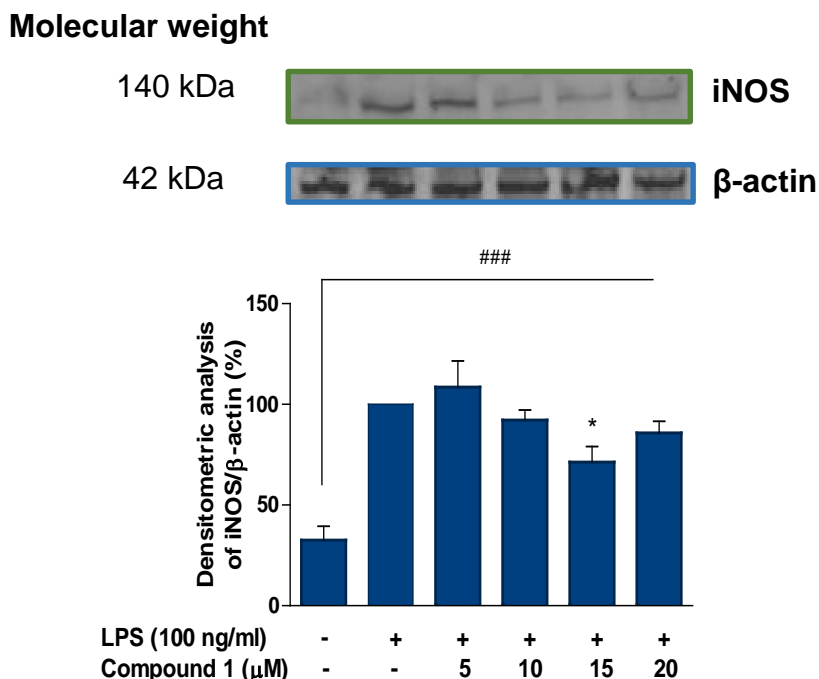


**Figure 25. Effect of compound **1** on iNOS expression in BV2 microglia cells.** Each bar represents a mean of the densitometry analysis by Western Blot of three independent experiments. Results are normalized with the housekeeping protein  $\beta$ -actin and cells treated only with LPS are considered to undertake 100% of the expression of the enzyme. Significantly different to LPS: \* $p < 0.05$ , \*\* $p < 0.01$ , \*\*\* $p < 0.001$ . Significantly different to untreated cells: # $p < 0.05$ , ## $p < 0.01$ , ### $p < 0.001$ .

### 3.2.4 Effects on release of pro-inflammatory cytokines

The primary cytokines which mediate chronic neuroinflammation are  $\text{TNF}\alpha$ , IL-6 and IL-1 $\beta$ . The three of them were investigated in order to assess whether novel compounds were able to prevent the production of these important cytokines from LPS-activated BV2 microglia. Note that due to the fact that compound **3** was affecting the viability of the cells, there are no results for this compound.

The following graphs provide an overview of the drugs effect on cytokines. Single analysis for each of the chemical compounds revealed that BCA effectively decreased TNF $\alpha$  ( $p < 0.001$ ) and IL-1 $\beta$  ( $p < 0.05$ ) but increased IL-6 ( $p < 0.01$ ) (Figure 26).

Compound **1** at various concentrations (5, 10, 15 and 20  $\mu\text{M}$ ) blocked TNF $\alpha$  ( $p < 0.001$ ), IL-6 ( $p < 0.001$ ) production gradually after stimulation with LPS for 24hr although no statistical differences were obtained for IL-1 $\beta$  (Figure 27). In contrast, compound **2** activity was characterized by causing the opposite effects by increasing such cytokines as the concentration used was increased, in particular IL-6 production ( $p < 0.001$ ) (Figure 28).

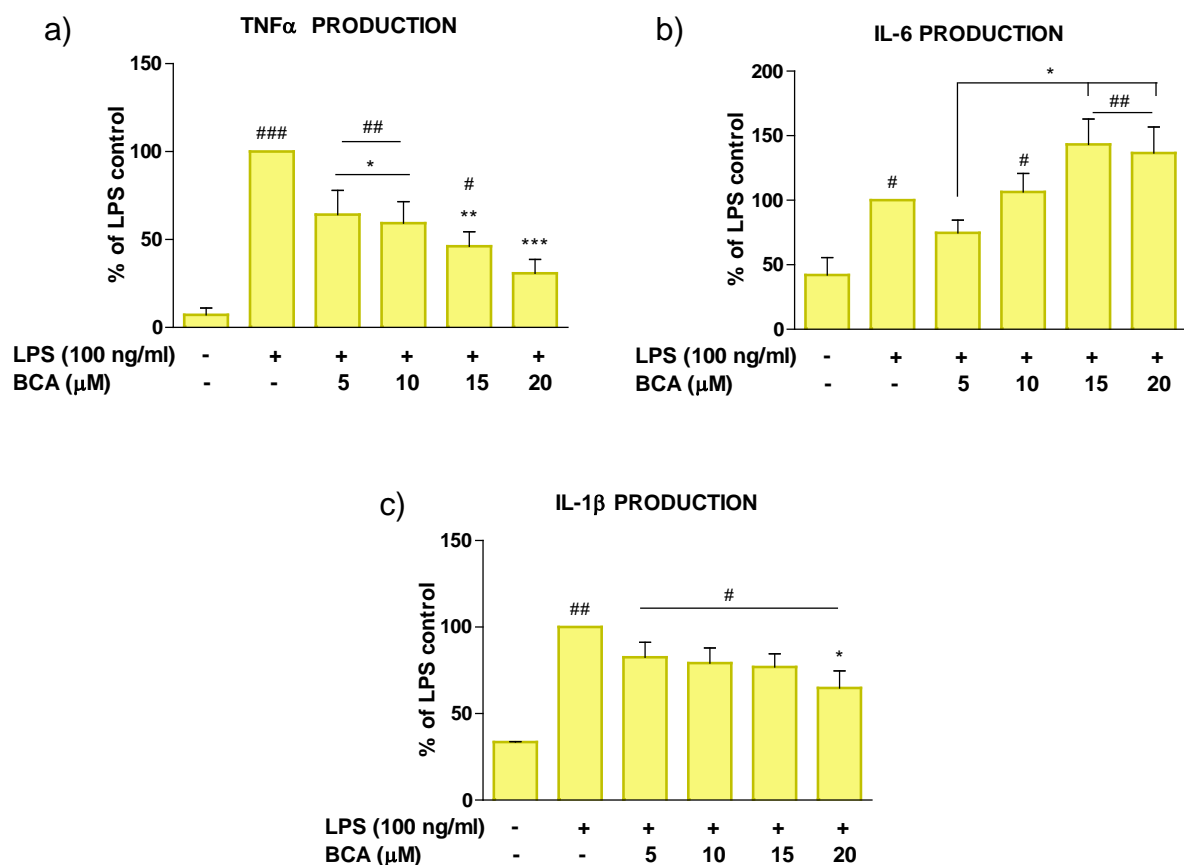


**Figure 26. Effect of BCA on TNF $\alpha$ , IL-6 and IL-1 $\beta$  production in LPS-activated BV2 microglia.** Cells were stimulated with LPS in the presence or absence of BCA (5-20  $\mu\text{M}$ ) for 24 hours. Stimulation was terminated, and supernatants were collected and levels of (a) TNF- $\alpha$ , (b) IL-6 and (c) IL-1 $\beta$  were measured using ELISA. Data is expressed as mean  $\pm$ SEM for 3 independent experiments. Statistical analysis was performed using one-way ANOVA with post-hoc Student Newman-Keuls test (multiple comparison). \* $p < 0.05$ , \*\* $p < 0.01$ , \*\*\* $p < 0.001$  in comparison with LPS control. # $p < 0.05$ , ## $p < 0.01$ , ### $p < 0.001$  in comparison with untreated cells.

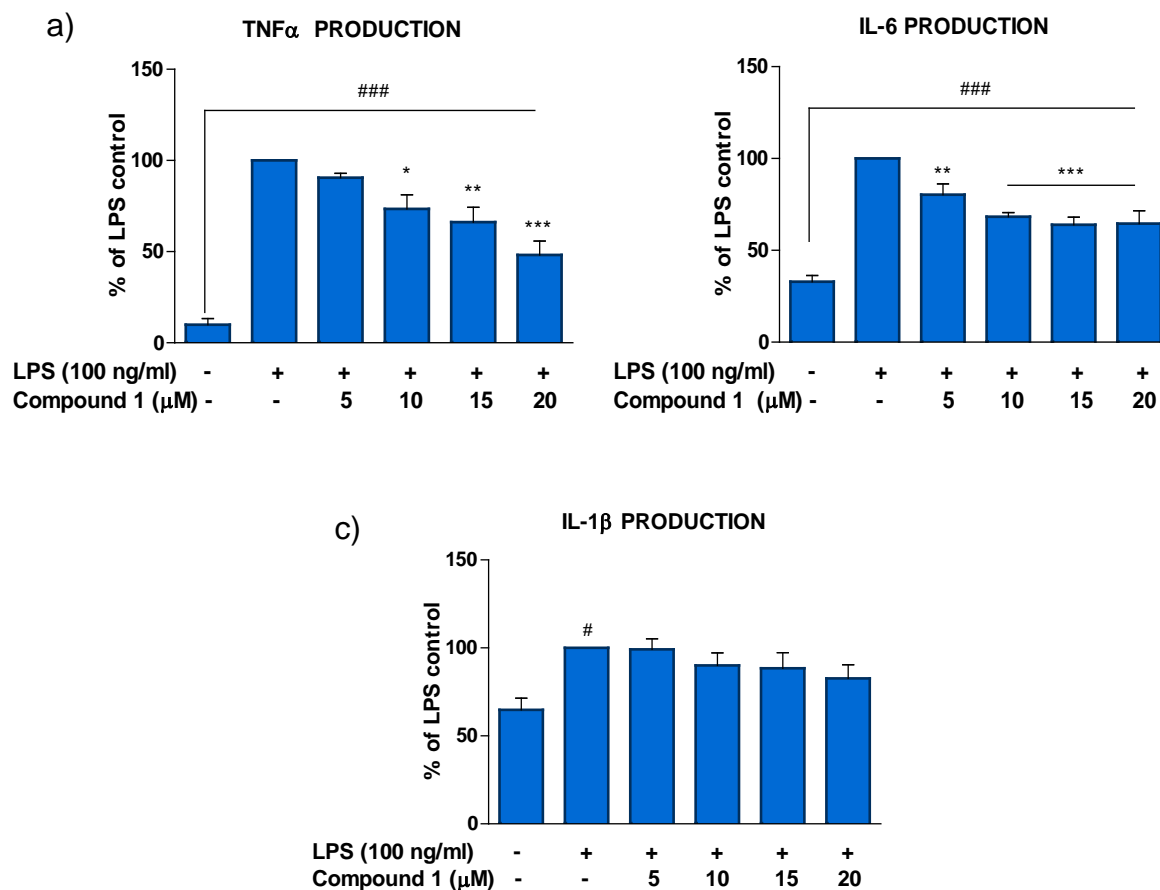


**Figure 27. Effect of compound 1 on TNF $\alpha$ , IL-6 and IL-1 $\beta$  production in LPS-activated BV2 microglia.** Cells were stimulated with LPS in the presence or absence of compound 1 (5-20  $\mu$ M) for 24 hours. Stimulation was terminated, and supernatants were collected and levels of (a) TNF- $\alpha$ , (b) IL-6 and (c) IL-1 $\beta$  were measured using ELISA. Data is expressed as mean  $\pm$ SEM for 3 independent experiments. Statistical analysis was performed using one-way ANOVA with post-hoc Student Newman-Keuls test (multiple comparison). \* $p$ <0.05, \*\* $p$ <0.01, \*\*\* $p$ <0.001 in comparison with LPS control. # $p$ <0.05, ## $p$ <0.01, ### $p$ <0.001 in comparison with untreated cells.

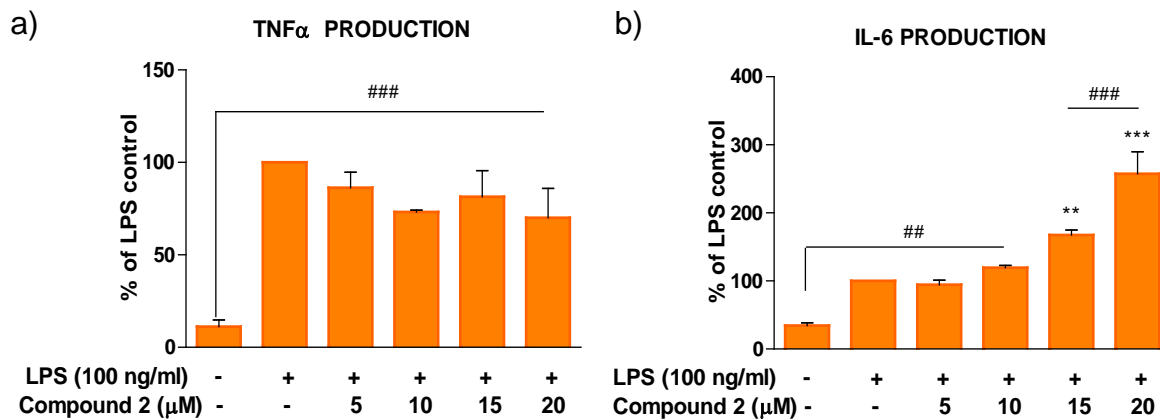


**Figure 28. Effect of compound 2 on TNF $\alpha$  and IL-6 production in LPS-activated BV2 microglia.** Cells were stimulated with LPS in the presence or absence of compound 2 (5-20  $\mu$ M) for 24 hours. Stimulation was terminated, and supernatants were collected and levels of (a) TNF- $\alpha$  and (b) IL-6 were measured using ELISA. Data is expressed as mean  $\pm$ SEM for 3 independent experiments. Statistical analysis was performed using one-way ANOVA with post-hoc Student Newman-Keuls test (multiple comparison). \* $p$ <0.05, \*\* $p$ <0.01, \*\*\* $p$ <0.001 in comparison with LPS control. # $p$ <0.05, ## $p$ <0.01, ### $p$ <0.001 in comparison with untreated cells.

### 3.2.5 Effects on Prostaglandin E<sub>2</sub> production and COX-2 protein expression

Prostaglandin E<sub>2</sub> (PGE<sub>2</sub>) is an arachidonic acid derivative released by activated microglia through the enzymatic action of cyclooxygenase-2 (COX-2). The effects of the compounds (5, 10, 15 and 20  $\mu$ M) on PGE<sub>2</sub> were evaluated after 24 h of stimulation on LPS-activated BV2 microglia. On the graphs below (Figure 29) PGE<sub>2</sub> results are plotted for BCA and its derivatives. LPS-treated BV2 cells produced detectable levels of PGE<sub>2</sub> compared to untreated microglial cells. BCA specially produced a significant ( $p$ <0.001) reduction of PGE<sub>2</sub> production at all concentrations. However, for compound 1 the inhibition was not significant and treatment with compound 2 resulted in an increase in PGE<sub>2</sub> production ( $p$ <0.01).

Due to the direct relationship between PGE<sub>2</sub> and COX-2, the expression of the latter for compound 1 was also evaluated by western blotting. Overall, these results illustrate that compound 1 slightly reduces COX-2 expression, in particular at a concentration of 15  $\mu$ M ( $p$ <0.01) (Figure 30).

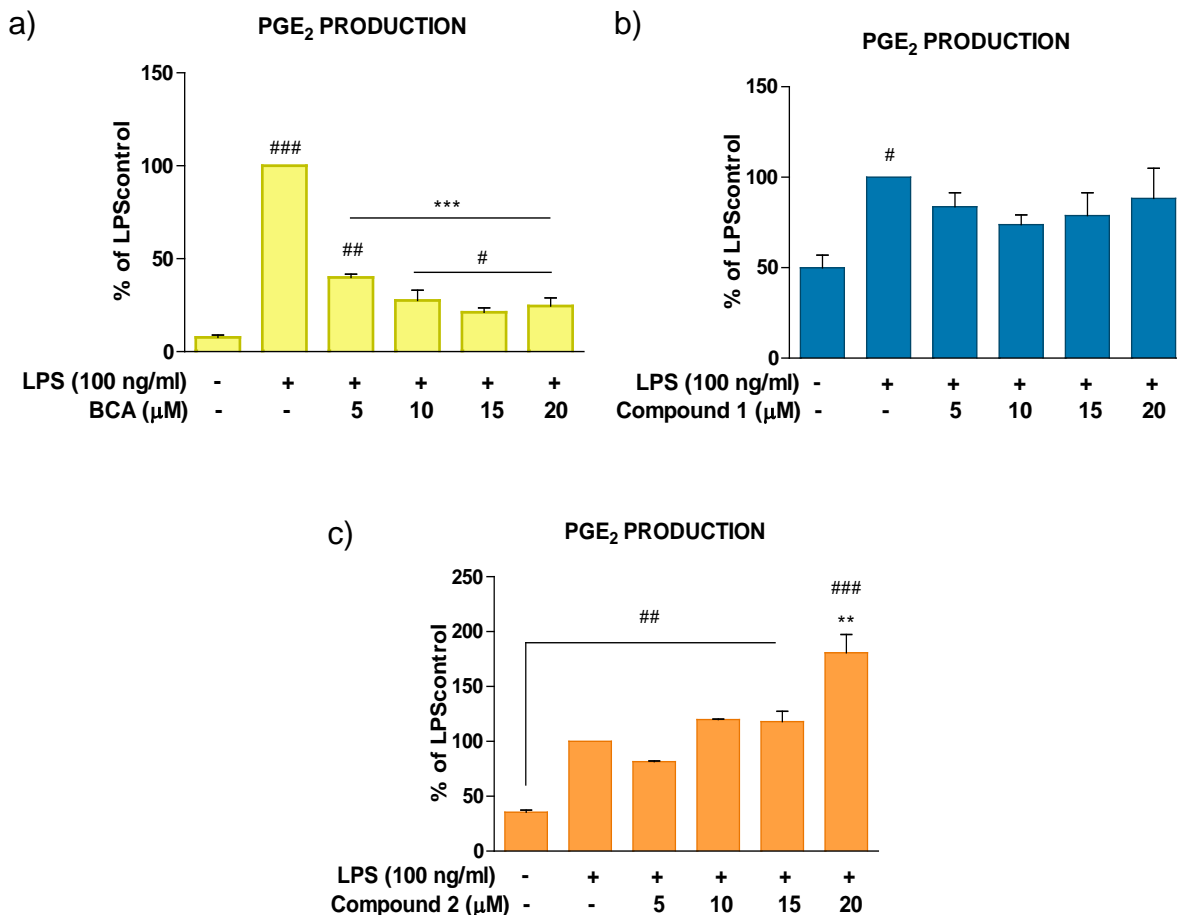


**Figure 29. Effect of BCA, compound 1 and compound 2 on PGE<sub>2</sub> production in LPS-activated BV2 microglia.** Upon treatment with compounds and BV2 cells stimulation with LPS (100 ng/ml), supernatants were collected and PGE<sub>2</sub> measured by ELISA. BCA (a) significantly reduced PGE<sub>2</sub> formation while compound 1 (b) its reduction is almost undetectable and compound 2 (c) produces an increase on PGE<sub>2</sub>. Data is expressed as mean  $\pm$ SEM for 3 independent experiments. Statistical analysis was performed using one-way ANOVA with post-hoc Student Newman-Keuls test (multiple comparison). \* $p < 0.05$ , \*\* $p < 0.01$ , \*\*\* $p < 0.001$  in comparison with LPS control. # $p < 0.05$ , ## $p < 0.01$ , ### $p < 0.001$  in comparison with untreated cells.

## Molecular weight

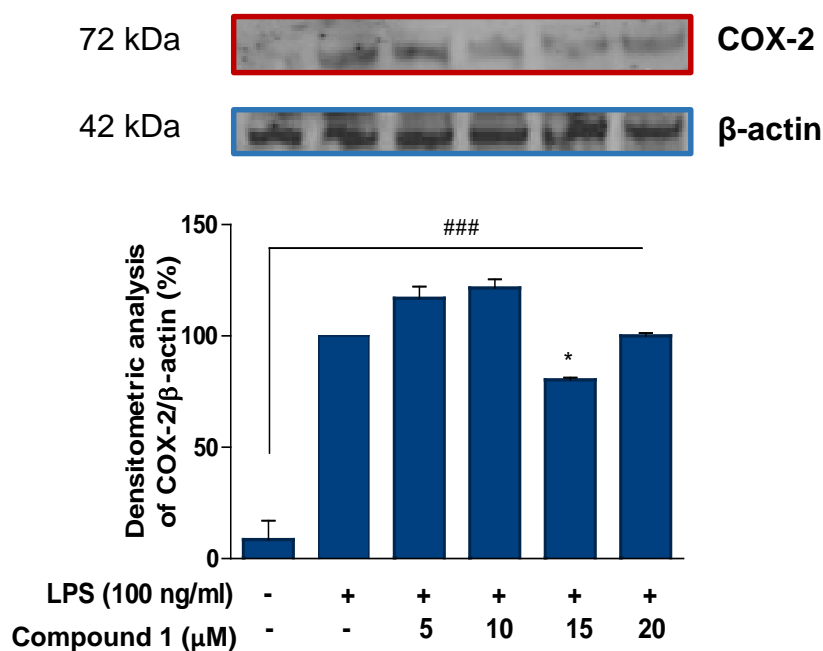


**Figure 30. Effect of compound 1 on COX-2 expression in BV2 microglia cells.**

Each bar represents a mean of the densitometry analysis by Western Blot of three independent experiments. Results are normalized with  $\beta$ -actin and cells treated only with LPS are considered to undertake 100% of the expression of both enzymes. Significantly different to LPS: \* $p$ <0.05, \*\* $p$ <0.01, \*\*\* $p$ <0.001. Significantly different to untreated cells: # $p$ <0.05, ## $p$ <0.01, ### $p$ <0.001.

### 3.3 DISCUSSION

Neuroinflammation is a critical component of a broad array of neurodegenerative diseases. Moreover, increasing evidence suggests that chronically hyperactivated microglia cells are mainly responsible for the exacerbation and maintenance of this condition. In this project, neuroinflammation inhibitory actions of the dietary isoflavonoid BCA, highly present in red clover; compound **1**, a carbamate ester BCA derivative; compound **2**, an ester BCA derivative and compound **3**, the deoxybenzoin BCA intermediate were investigated in LPS-activated BV2 microglia.

Microglia stimulation with bacterial lipopolysaccharide (LPS) derived from *Salmonella typhimurium* resulted in an increase in the production of pro-inflammatory cytokines like TNF $\alpha$ , IL-1 $\beta$  and IL-6 and other inflammatory modulators such as nitric oxide. Because disproportionate nitric oxide levels have proved to be detrimental to neurons in the brain, as it is capable of inducing protein misfolding during post-translational

modifications in the microglia, therefore, boosting transcription factors activation like NF- $\kappa$ B and further overstimulating the inflammatory process in the brain (Vauzour *et al.*, 2015), NO levels were also evaluated. Nitric oxide is released by the inducible nitric oxide synthase and levels of both of them should be interrelated. Activated microglia are also known to produce prostaglandins whose production is controlled by COX-2 enzyme (Morales *et al.*, 2014). LPS stimulated BV2 cells also generated PGE<sub>2</sub>, which is a major eicosanoid found in many CNS related inflammatory diseases and is a primary target for non-steroidal anti-inflammatory drugs (Wang *et al.*, 2015).

The present study confirms BCA's suppressive capability on BV2 cells inflammatory response. BCA effectively reduces the production of TNF- $\alpha$  and IL-1 $\beta$  in LPS-activated BV2 microglia, suggesting that the compound is capable of inhibiting neuroinflammation. However, it did not significantly suppress IL-6 release. Such results contrast other previous studies in which IL-6 had been evaluated after treatment with BCA in primary microglial cells. In this latest study, BCA effectively decreases IL-6 along with the other CKs (Wang *et al.*, 2016). Such differences may be due to the nature of the cells, since primary microglia cells slightly differ from the two commercially available cell lines BV2 and N9 (Stansley *et al.*, 2012). It is worth mentioning that IL-6 not only has been associated with pro-inflammatory processes but can also play a protective role by various means like promoting microglia cells differentiation into their phagocytic phenotype, or by inhibiting others CKs production (e.g.: TNF $\alpha$ ) (Erta *et al.*, 2012). After stimulation with LPS, BV2 cells were shown to increase the production of nitric oxide and PGE<sub>2</sub>. Upon treatment with BCA, both inflammatory modulators, NO and PGE<sub>2</sub> decreased.

Compound **1** was made from BCA by the addition of a carbon long chain through the formation of a carbamate ester. Preliminary results for NO and CKs illustrated a good response of BV2 towards the treatment with compound **1** by reducing all these inflammatory modulators. Encouraged by such results, PGE<sub>2</sub>, iNOS and COX-2 were furthered studied. Nevertheless, PGE<sub>2</sub> experiments did not show statistical significances which correlates with the studies performed on COX-2 by western blotting. On the other hand, reduction on iNOS levels were not as pronounced as for the nitric oxide ones. Such differences might be due to the accuracy differences among both techniques. All in all, it must be noticed that significant differences ( $p < 0.05$ ) when using 15  $\mu$ M of compound **1** were observed for both iNOS and COX-2.

As for compound **2**, even though it showed effectiveness on NO reduction, it was not effective at blocking TNF $\alpha$ , IL-6 and PGE<sub>2</sub> release. In fact, it significantly boosted the discharge of these pro-inflammatory modulators. Such differences must be due to the compound structures. To the natural pattern BCA, a saturated long chain was added to the –OH in position 7 by esterification. The lack of a free hydrogen in that position must have been the cause of such unfavourable results since it is widely known that the OH in the fourth carbon (4'-OH) and in the seventh (7-OH) are essential to mimic those of the estradiol in position 3 and 17 (Fokialakis *et al.*, 2012).

Compound **3** was synthesized to test the effect of deoxybenzoin, which are intermediates in the synthesis of isoflavones, due to their structural similarity with isoflavones. However, cytotoxic assays confirmed that the reduction of NO observed by compound **3** were due to the compound being cytotoxic for the cells. For this reason, this compound was excluded from the rest of the analysis conducted. In relative binding affinities for ER $\alpha$  and ER $\beta$  experiments, Fokialakis *et al.* (2004) suggested that compound **3** exhibited a moderate affinity towards ER $\alpha$ . Hu *et al.* (2013) also isolated 11 deoxybenzoin from *Arundina graminifolia* to assess their cytotoxicity towards five cancer cell lines, indicating that certain deoxybenzoin can also serve to target malignant cells.

Taken together, results on BCA experiments suggest that it may inhibit neuroinflammation in BV2 microglia; however, its deoxybenzoin intermediate (compound **3**) did not have the same properties and instead showed to be cytotoxic for these cells. On the other hand, the addition of a long carbon chain in order to augment lipophilicity using the formation of an ester and a carbamate ester resulted in completely different outcomes. While compound **1**, that of the carbamate ester, exhibited an anti-inflammatory effect on BV2 cells, compound **2** increased the production of pro-inflammatory modulators. Further investigation on molecular studies, ligand binding assays, half maximal inhibitory concentration (IC<sub>50</sub>) evaluation and transactivation assays would shed some light in determining the mechanism by which these compounds displayed such differences.

# CHAPTER 4: SYNTHESIS AND PHARMACOLOGICAL STUDIES ON FORMONONETIN DERIVATIVES

## 4.1 INTRODUCTION

Due to the evidences of that inflammation plays an important role in neurodegenerative diseases, several non-steroidal anti-inflammatory drugs (NSAID) have been the focused of many epidemiological and clinical trials reducing the risk of developing neuroinflammation (Chattopadhyay *et al.*, 2010; Vernieri *et al.*, 2013). Nevertheless, following a therapy on NSAIDs has not been as promising with AD patients. This is not very surprising if one bears in mind that neurodegenerative diseases are very context-dependent and stage-dependent (see review: Heneka *et al.*, 2015). In addition, these NSAIDs usually have adverse effects when used in long-term treatments, having a detrimental impact at a gastrointestinal, cardiovascular and renal level as well as increased ability to acquire resistance to these drugs (Minghetti *et al.*, 2004).

Therefore, other types of strategies are gaining ground, that is promoting the use of medicinal plants as preventive strategies to delay the onset of the diseases. As reviewed in Chapter 1.6, many authors have taken advantage of the presence of hydroxyl groups in isoflavones to enhance the bioavailability characteristics of phenolic hydroxyl compounds by esterification and the addition of carbamate ester groups. In fact, one of the best and most reliable strategies for delivering active drugs with low BBB crossing ability is to design an effective prodrug that can potentially cross the BBB to release the parent drug after hydrolysis (Dholkawala *et al.*, 2016). Following this strategy, a FMN carbamate ester derivative was synthesized in this project.

FMN (Formononetol 7-hydroxy-4'-methoxyisoflavona 4'-O-methyl-daidzein) is an isoflavone found in red clover plant and widespread in the *Leguminosae* family (Larkin *et al.*, 2008) that has been reported to possess many potent pharmacological activities including antitumor, antihypertensive, antibacterial, antiviral, antioxidant and antiangiogenic effects (Mu *et al.*, 2009; Li *et al.*, 2014; Sun *et al.*, 2011; Wu *et al.*, 2015). Its anti-inflammatory effects have also been widely proven, for instance, in pancreas cells (Wang *et al.*, 2012) by inhibiting NF- $\kappa$ B, and also in lung injury in mice (Ma *et al.*, 2013). Moreover, FMN also seems to induce neuroprotection by up-regulating NRF2 in TBI (traumatic brain injuries) models (Li *et al.*, 2014), and prompt dopaminergic neurons protection in a dose-dependent manner in rat mesencephalic

neuron-glia cultures (Chen *et al.*, 2008). Unpublished research conducted in our group has proven FMN efficacy at reducing the release of pro-inflammatory modulators by BV2 microglia cells via ERs.

Daidzein is the metabolite of FMN. The estrogenic effect of daidzein is largely achieved by its biotransformation to equol via a gut microflora-dependent metabolism (Tolleson *et al.*, 2002). However, by the O-methoxy substitutions of the free phenolic hydroxyl group at 4' results in FMN, whose lipophilicity is shown to be enhanced. Moreover, a study carried out by Srivastava *et al.* (2013) that identified an isomer of FMN (Isoformo) demonstrated that Isoformo reverses established osteopenia in adult rats likely via its pro-survival effect on osteoblasts.

In addition, several studies have modified the FMN pattern skeleton aiming at improving their pharmacological properties. For example, Li *et al.*, (2016) synthesized a 7-phosphoramidate derivative capable of inducing apoptosis in cancer cells and Ren *et al.*, (2012) created a mononetin nitrogen mustard derivative that was able of promoting both cell cycle arrest and initiate apoptosis. Fu *et al.* (2017) have recently design and synthesized a battery of antitumor FMN derivatives by the formation of a formononetin-dithiocarbamate (Figure 31) hybrid with antitumor related properties with IC<sub>50</sub> values of even 1.97  $\mu$ M. By following a molecular hybridation strategy, they have endowed the new molecules with several drug essential properties: i) the dithiocarbamate group possess drug-like porperties, ii) the FMN serves as the pharmacophore fragment, and iii) an alkoxy chain for lipophilicity.

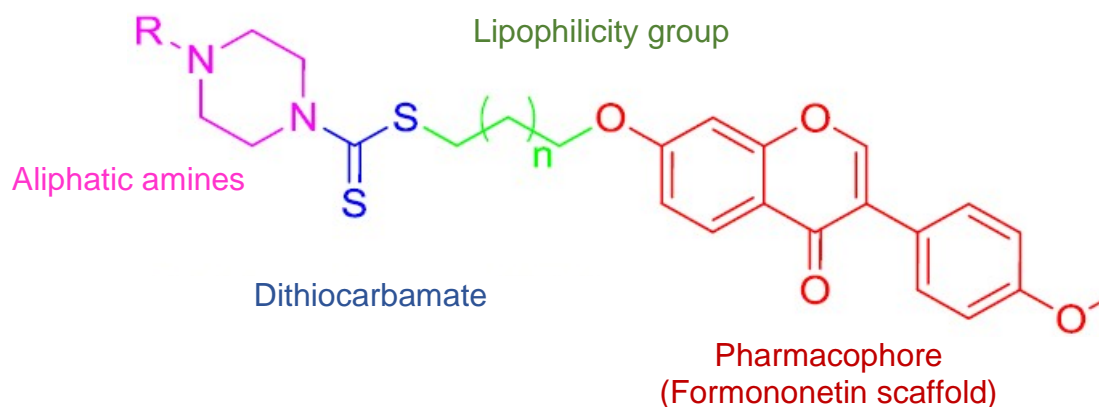


**Figure 31. Formononetin-dithiocarbamate synthesized by Fu *et al.* (2017) following a rational molecular hybridation strategy.**

On the basis of the above, in this project, a carbamate ester FMN derivative was synthesized and the anti-neuroinflammatory effects of the pattern compound and the derivative were studied in LPS-induced neuroinflammation in BV2 microglia.

## 4.2 RESULTS

In order to fulfill the objectives proposed in the present study, different natural phytoestrogen derivatives were needed to be tested. As already mentioned in the section Material and Methods, we managed to synthesize FMN and one derivative and make a preliminary study on their anti-inflammatory activity. This section refers to the structure and efficacy of FMN and its derivative regarding the effectiveness on producing the desired effect.

### 4.2.1 Synthesis of Formononetin and its derivative

Formononetin: 7-Hydroxy-3-(4-methoxyphenyl)-4H-1-benzopyran-4-one, 7-Hydroxy-3-(4-methoxyphenyl)chromen-4-one or 7-Hydroxy-4'-methoxyisoflavone)

In order to synthesize a FMN derivative we first had to make FMN as described in section materials and methods. After the reaction was completed and the crude material was extracted with ethyl acetate, the resulting product was again dissolved in ethyl acetate, brought to simmer and left to cold down. Two phases were observed, the one on the top was brownish and that on the bottom white. These were separated by decantation. This process was repeated as many times as needed to purify the white powder which was the compound of interest. This reaction gave a yield of 45%.

The  $^1\text{H}$  NMR and  $^{13}\text{C}$  NMR of the FMN fully agree with the expected structures.

**$^1\text{H}$ -NMR (400 MHz,  $\delta$  ppm, DMSO):** 10.82 (1H, s, OH-7), 8.35 (1H, s, H-2), 7.97 (1H, d,  $J = 8.8$  Hz, H-5), 7.51 (2H, d,  $J = 8.8$  Hz, H-2', H-6'), 6.99 (2H, d,  $J = 8.8$  Hz, H-3', H-5'), 6.94 (1H, dd,  $J = 2.2, 8.8$  Hz, H-6), 6.87 (1H, d,  $J = 2.2$  Hz, H-8), 3.79 (3H, s,  $\text{OCH}_3$ ).

**$^{13}\text{C}$ -NMR (100 MHz, DMSO):** 175.1 (C=O), 163.0 (qC), 159.4 (qC), 157.9 (qC), 153.6 (CH), 130.5 (2 CH), 127.8 (CH), 124.7 (C), 123.6 (C), 117.1 (C), 115.6 (CH), 114.1 (2 CH), 102.6 (CH), 55.6 ( $\text{CH}_3$ ).

**HRMS (Dual ESI):** calculated  $m/z$  for  $\text{C}_{16}\text{H}_{12}\text{O}_4$  269.0736, found 269.0808  $[\text{M}+\text{H}]^+$ . Known compound.

#### Compound 4: 3-(4-methoxyphenyl)-4-oxo-4H-chromen-7-yl undecylcarbamate

The synthesis of compound **4** was undertaken as described in the section Materials and Methods. The corresponding compound was isolated as a yellow solid material with a yield of 55%.

**<sup>1</sup>H NMR (400 MHz, δ ppm, DMSO):** 7.9 (1H, s, H-2), 7.6 (1H, d, J = 8 Hz, H5), 7.5 (2H, d, J = 8 Hz, H-2', H-6'), 7.4 (1H, t, J = 5.5 Hz, CH<sub>2</sub>NH), 6.9 (2H, d, J = 8 Hz, H-3', H-5'), 6.3 (1H, d, J = 2.2 Hz, 8 Hz, H-6), 5.9 (1H, dd, J = 2.2 Hz, H-8), 3.8 (3H, s, OCH<sub>3</sub>), 3.6 (2H, t, J = 7.5 Hz, CH<sub>2</sub>NH), 1.7 (2H, m, CH<sub>2</sub>), 1.3-1.1 (16H, m, CH<sub>2</sub>), 0.8 (3H, t, J = 7.5 Hz, CH<sub>3</sub>).

**<sup>13</sup>C-NMR (100 MHz, δ ppm, DMSO):** 175.3 (C-4), 159.8 (C-4'), 157.8 (C-7), 154.7 (C-8a), 153.2 – 153.4 (C-2, COO), 130.1 (C-2', C6'), 127.2 (C-5), 124.8 (C-1'), 123.5 (C-3), 122.4 (C-4a), 116.3 (C-6), 114.2 (C-3'), 111.1 (C-8), 55.8 (OCH<sub>3</sub>), 40.3 (NHCH<sub>2</sub>), 26.4-31.9 (CH<sub>2</sub>), 22.7 (CH<sub>2</sub>), 14.1 (CH<sub>3</sub>).

**HRMS (Dual ESI):** calculated m/z for C<sub>28</sub>H<sub>35</sub>N<sub>1</sub>O<sub>5</sub> 466.5654, found 466.5741 [M+H]<sup>+</sup>. Unknown compound.

#### **4.2.2 BV2 cells viability**

In order to determine whether the anti-inflammatory effect of the synthesized compounds was not due to impaired viability of BV2 cells, an XTT viability assay was carried out after incubating the cells with the corresponding compounds for 24 h. Results (Figure 32) showed that there was no significant difference in the viability of cells treated with either FMN nor compound **4** at concentrations 5, 10, 15 and 20 μM when compared with control (untreated) cells.

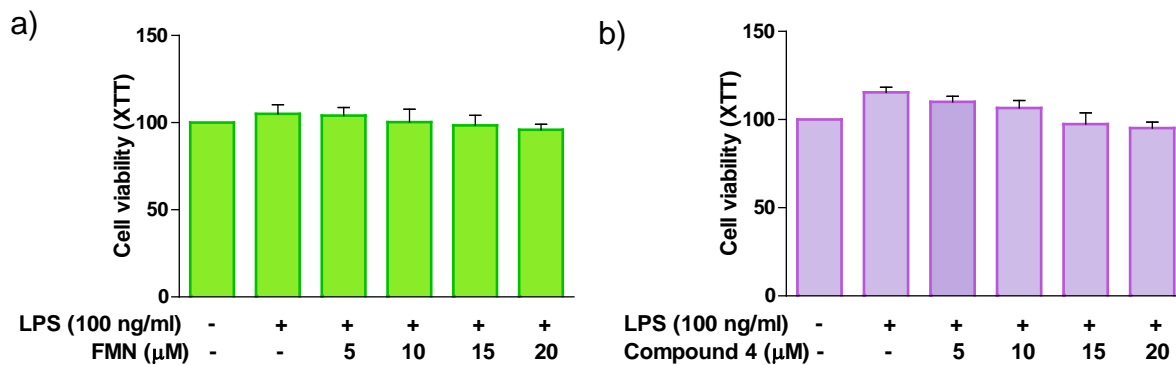


**Figure 32. Cell viability of BV2 cells for FMN and compound 4.** Following treatment with various concentrations (5, 10, 15 and 20 μM) of the compounds and LPS (100 ng/ml) stimulation for 24h, cytotoxicity of FMN (a) and compound 4 (b) in BV2 cells was assessed by XTT assay. Values correspond to means of 3 independent experiments and are shown as the percentage of viable cells compared with the viability of negative controls (untreated cells). \*p<0.05, \*\*p<0.01, \*\*\*p<0.001 in comparison with LPS control. #p<0.05, ##p<0.01, ###p<0.001 in comparison with untreated cells.

#### 4.2.3 Effects on nitrite production

Nitric oxide is an important mediator for the regulation of chronic neuroinflammation. Moreover, high concentrations of NO have been shown to be neurotoxic to adjacent neurons (Spencer *et al.*, 2012). Therefore, the effects of the compounds at 5, 10, 15 and 20 μM were investigated for nitrite production in BV2 microglia cells using Griess assay. Figure 33 shows that FMN and compound 4, effectively inhibited NO release in a dose-dependent manner (p<0.001).

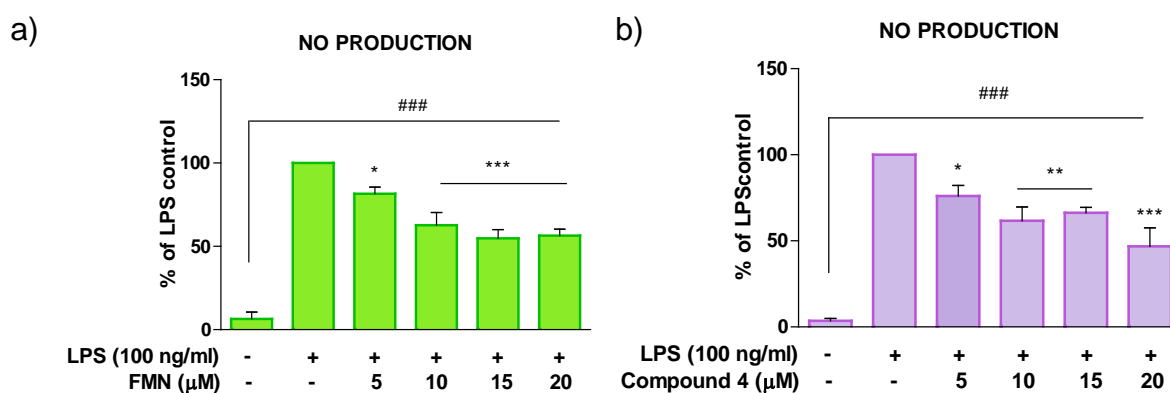


**Figure 33. Effect of FMN and compound 4 on nitrite production in LPS-activated BV2 microglia.** This figure illustrates a reduction in nitric oxide (NO) release in LPS-

activated BV2 cells after treatment with FMN (a) and compound 4 (b). Data is expressed as mean  $\pm$ SEM for 3 independent experiments. Statistical analysis was performed using one-way ANOVA with post-hoc Student Newman-Keuls test (multiple comparison). \* $p$ <0.05, \*\* $p$ <0.01, \*\*\* $p$ <0.001 in comparison with LPS control. # $p$ <0.05, ## $p$ <0.01, ### $p$ <0.001 in comparison with untreated cells.

#### 4.2.4 Effects of release of pro-inflammatory cytokines

Hyperactive microglia are known to release pro-inflammatory cytokines such as IL-1 $\beta$ , TNF  $\alpha$  and IL-6, which are considered major significant neurotoxic factors that contributes to neuroinflammation. Therefore, cytokines production in the activated microglia remains an important target in reducing neuroinflammation. The levels of IL1 $\beta$ , TNF  $\alpha$  and IL-6 in the supernatants were analyzed using ELISA in order to assess whether novel compounds were able to prevent the production of these important cytokines from LPS-activated BV2 microglia. The following graphs (Figure 34 and 35), provide an overview of the drugs effect on cytokines.

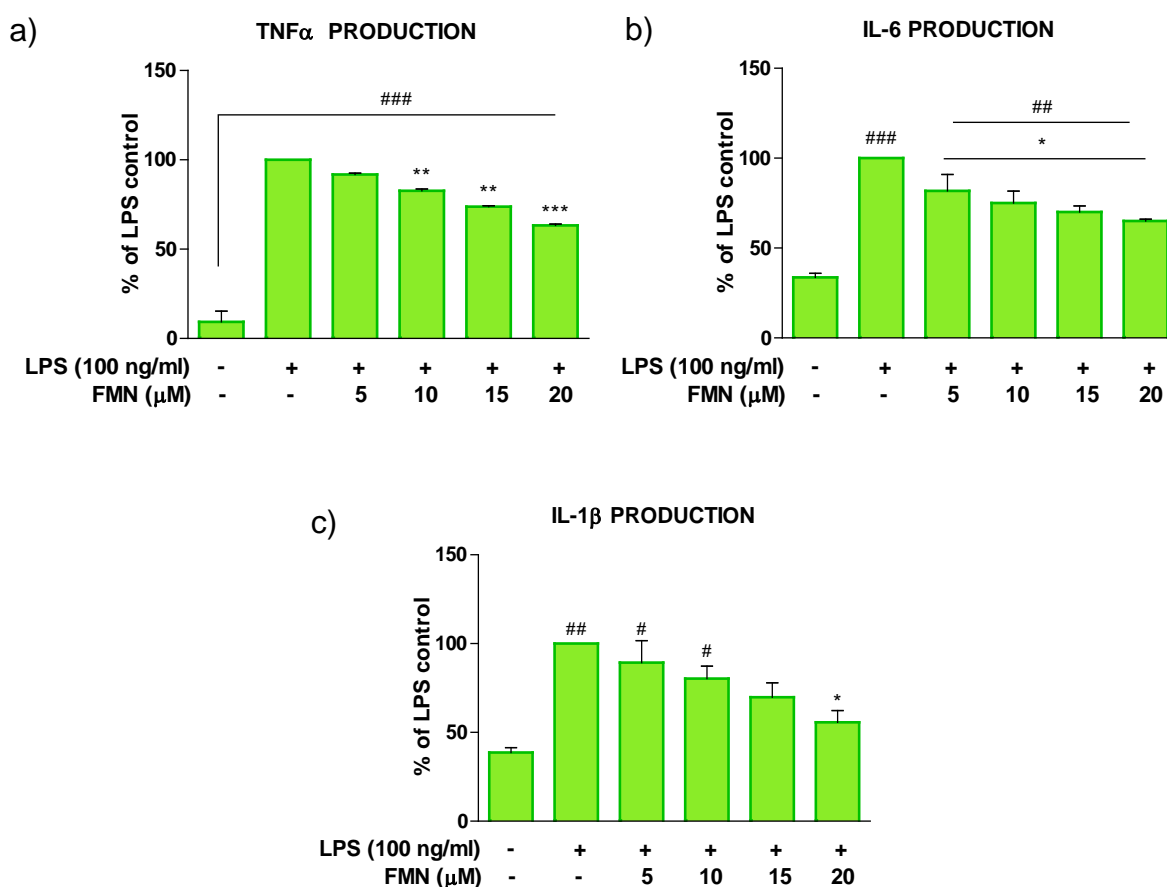


**Figure 34. Effect of FMN on TNF $\alpha$ , IL-6 and IL-1 $\beta$  production in LPS-activated BV2 microglia.** Cells were stimulated with LPS in the presence or absence of FMN

(5-20  $\mu$ M) for 24 hours. Stimulation was terminated, and supernatants were collected and levels of (a) TNF- $\alpha$ , (b) IL-6 and (c) IL-1 $\beta$  were measured using ELISA. Data is expressed as mean  $\pm$ SEM for 3 independent experiments. Statistical analysis was performed using one-way ANOVA with post-hoc Student Newman-Keuls test (multiple comparison). \* $p$ <0.05, \*\* $p$ <0.01, \*\*\* $p$ <0.001 in comparison with LPS control. # $p$ <0.05, ## $p$ <0.01, ### $p$ <0.001 in comparison with untreated cells.

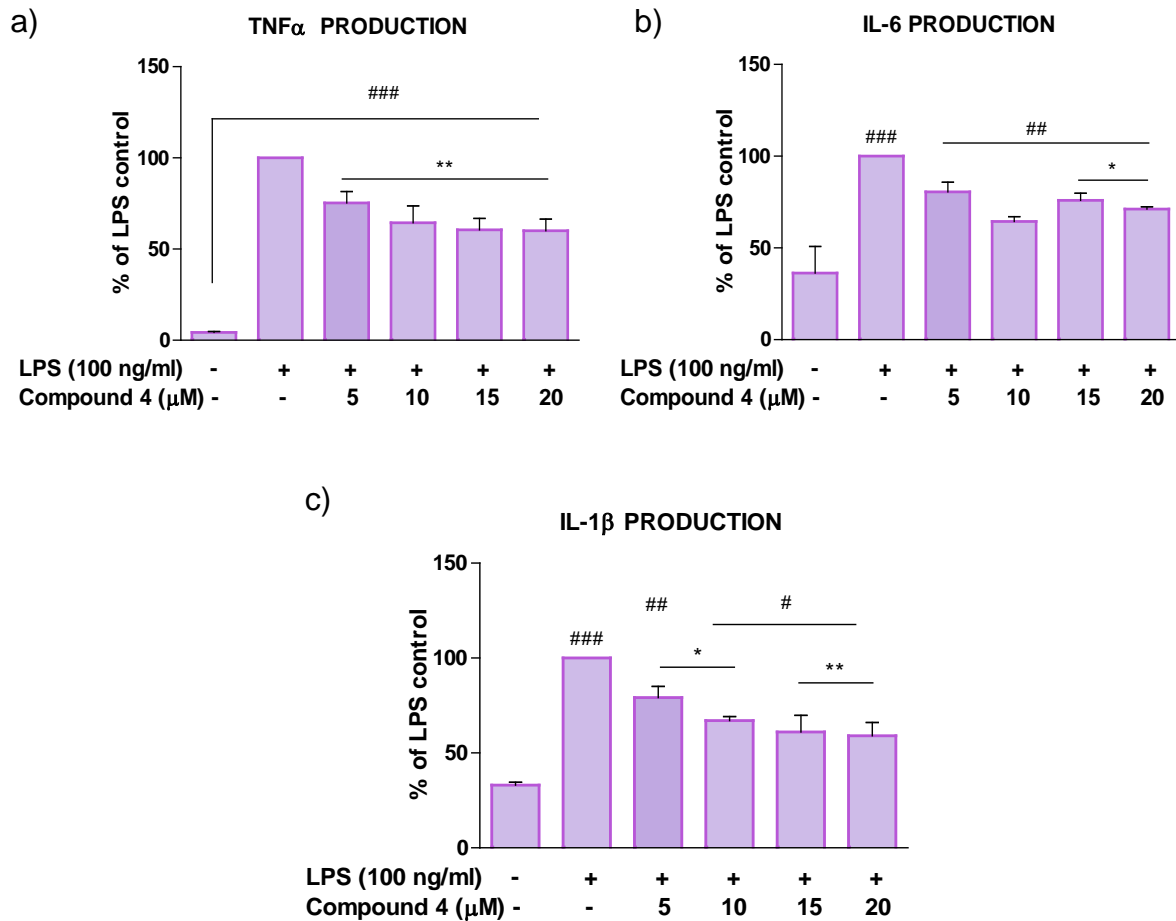


**Figure 35. Effect of compound 4 on TNF $\alpha$ , IL-6 and IL-1 $\beta$  production in LPS-activated BV2 microglia.** Cells were stimulated with LPS in the presence or absence of compound 4 (5-20  $\mu$ M) for 24 hours. Stimulation was terminated, and supernatants were collected and levels of (a) TNF- $\alpha$ , (b) IL-6 and (c) IL-1 $\beta$  were measured using ELISA. Data is expressed as mean  $\pm$ SEM for 3 independent experiments. Statistical analysis was performed using one-way ANOVA with post-hoc Student Newman-Keuls test (multiple comparison). \* $p$ <0.05, \*\* $p$ <0.01, \*\*\* $p$ <0.001 in comparison with LPS control. # $p$ <0.05, ## $p$ <0.01, ### $p$ <0.001 in comparison with untreated cells.

Single analysis for FMN and compound 4 revealed that both compounds were successful producing a relevant reduction of the cytokines studied. FMN effectively

decreased TNF $\alpha$  ( $p < 0.001$ ), IL-6 ( $p < 0.05$ ) and IL-1 $\beta$  ( $p < 0.05$ ) (Figure 34). Compound 4 blocked TNF $\alpha$  ( $p < 0.01$ ), IL-6 ( $p < 0.05$ ) and IL-1 $\beta$  ( $p < 0.01$ ) production gradually after stimulation (Figure 35).

#### 4.2.5 Effects of Prostaglandin E<sub>2</sub> production

Prostaglandin E<sub>2</sub> is an arachidonic acid derivative released by activated microglia through the enzymatic action of COX-2. The effects of the compounds at 5, 10, 15 and 20  $\mu$ M on PGE<sub>2</sub> were evaluated after 24 h of stimulation on LPS-activated BV2 microglia. On the graphs below (Figure 36) PGE<sub>2</sub> results are plotted for FMN and compound 4. Compound 4 specially produced a significant ( $p < 0.001$ ) reduction of PGE<sub>2</sub> production at 10, 15 and 20  $\mu$ M although no reduction was observed at 5  $\mu$ M. However, FMN dropped PGE<sub>2</sub> release at all concentrations ( $p < 0.01$ ).

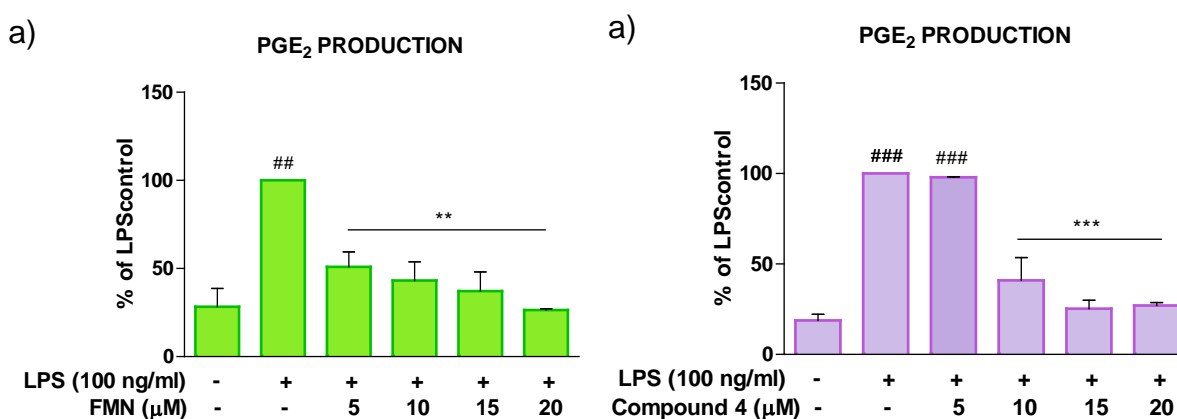


**Figure 36. Effect of FMN and compound 4 on PGE<sub>2</sub> production in LPS-activated BV2 microglia.** Upon treatment with compounds and BV2 cells stimulation with LPS (100 ng/ml), supernatants were collected and PGE<sub>2</sub> measured by ELISA. FMN (a) and compound 4 (b) significantly reduced PGE<sub>2</sub> formation. Data is expressed as mean  $\pm$ SEM for 3 independent experiments. Statistical analysis was performed using one-way ANOVA with post-hoc Student Newman-Keuls test (multiple comparison). \* $p < 0.05$ , \*\* $p < 0.01$ , \*\*\* $p < 0.001$  in comparison with LPS control. # $p < 0.05$ , ## $p < 0.01$ , ### $p < 0.001$  in comparison with untreated cells.

#### 4.3 DISCUSSION

Neuroinflammation is a critical component of a broad array of neurodegenerative diseases. Moreover, increasing evidence suggests that chronically hyperactivated microglia cells are mainly responsible for the exacerbation and maintenance of this

condition. To date, the majority of drug treatments are addressed to treat the symptoms of the neurodegenerative disorders rather than preventing the underlying degeneration of neurons. Accordingly, there is a need and desire to develop novel therapies capable of preventing neuronal loss that trigger pathology in these diseases (Spencer *et al.*, 2012). In this project, neuroinflammation inhibitory actions of the dietary isoflavonoid FMN, highly present in red clover and compound **4**, a carbamate ester of FMN, were investigated in LPS-activated BV2 microglia.

Microglia stimulation with bacterial LPS derived from *Salmonella typhimurium* resulted in an increase in the production of pro-inflammatory cytokines like TNF $\alpha$ , IL-1 $\beta$  and IL-6 and other inflammatory modulators such as nitric oxide. Nitric oxide is released by the iNOS and levels of both of them should be interrelated. Activated microglia also produced PGE<sub>2</sub> whose production is controlled by COX-2 enzyme (see chapter 1 and 3).

The present study and other unpublished studies from our group confirm FMN's suppressive capability on BV2 cells inflammatory response. FMN effectively reduces the production of pro-inflammatory modulators NO ( $p < 0.001$ ), TNF $\alpha$  ( $p < 0.001$ ), IL-6 ( $p < 0.05$ ), IL-1 $\beta$  ( $p < 0.05$ ) and PGE<sub>2</sub> ( $p < 0.01$ ) in a dose-dependent manner in LPS-activated BV2 microglia, suggesting that the compound is capable of inhibiting neuroinflammation. These results confirm other reports in which FMN is tested for its anti-inflammatory properties (Wang *et al.*, 2012; Ma *et al.*, 2013).

Compound **4** exhibited the same anti-inflammatory pattern than that of FMN by also decreasing the production of pro-inflammatory modulators NO ( $p < 0.001$ ), TNF $\alpha$  ( $p < 0.01$ ), IL-6 ( $p < 0.05$ ), IL-1 $\beta$  ( $p < 0.01$ ) and PGE<sub>2</sub> ( $p < 0.001$ ) in a dose-dependent manner suggesting that compound **4** is a bioactive derivative. It would be interesting to perform IC<sub>50</sub> assays for this compound for comparison with FMN in order to know whether the addition of a lipophilicity group using the formation of a carbamate ester is a good strategy as a prodrug.

The actions of isoflavones and their metabolites are predominantly mediated by the ERs (ER $\alpha$  and ER $\beta$ ), which differ in tissue distribution. While ER $\alpha$  is mainly found in the adrenals, the kidney, and the testes, typical ER $\beta$ -rich tissues are the brain, the thymus, the prostate, the bladder, the bone, the lungs, and the vasculature. In the breast, the ovaries and the uterus, both ERs are found. In relative binding affinities for

ER $\alpha$  and ER $\beta$  experiments, FMN (along with other isoflavones such as BCA) demonstrated 15,000 times less potency than 17  $\beta$ -estradiol (Wang *et al.*, 1995). The affinity assays performed for FMN have revealed higher affinity towards ER $\beta$  than to ER $\alpha$  just like other isoflavones. Moreover, daidzein, the demethylated metabolite of FMN, increases receptor affinity. In addition, their metabolite equol possess even greater affinity and potency than either of them (Pfitscher *et al.*, 2008).

Despite the promising health benefits mentioned above that FMN might possess, it needs to be taken in consideration the possible carcinogenesis activity of isoflavones like FMN. Contrary to other reports (Wu *et al.*, 2017; Chen *et al.*, 2016) that showed anti-proliferation and lower invasiveness capacity of FMN in carcinogenic bladder cells and arrest of abnormal proliferation and migration of vascular smooth muscle cells respectively, several authors like Wang *et al.* (1995) demonstrated an ability of FMN to support mammary gland proliferation in mice and, Guo *et al.*, (2016) concluded that FMN stimulates CNE2, a nasopharyngeal carcinoma cell line, proliferation and has an inhibitory effect on apoptosis.

On the other hand, it must be beard in mind that FMN is finally metabolized in the organism to equol, which has showed higher receptor transactivation than daidzein and FMN (Pfitscher *et al.*, 2008), concluding that possible beneficial health effects of isoflavone-rich foods and food supplements may be attributed to this secondary metabolite.

Taken together, results on FMN experiments suggest that it may inhibit neuroinflammation in BV2 microglia. On the other hand, the addition of an alkyl chain with a carbamate group resulted in compound **4** having similar anti-inflammatory properties on BV2 cells. Further investigation on molecular studies, ligand binding assays, IC<sub>50</sub> evaluation, transactivation and bioavailability assays could shed some light in determining whether the chemical modification conducted would be beneficial to enhance FMN pharmacological properties.

## CHAPTER 5: DISCUSSION AND CONCLUSIONS

There is no doubt that estrogens have a fundamental role in the development and functioning of various organs and tissues in the body, including, but not limited to, brain, bone, the cardiovascular system, and tissues of the urogenital tract.

Since the discovery of diverse ERs subsets is relatively recent, there is still a long way to go in the understanding of the functioning of the subtypes identified hitherto. Therefore, the concrete study of the existing and newer ER subtype–selective agonists is vital for deciphering their specific roles in health and disease.

Among the ERs subtypes, therapies targeting ER $\beta$  seems to be a safer strategy than targeting ER $\alpha$  because this receptor has been associated with enhanced proliferation features in breast and uterine tissues (Lin *et al.*, 2007; Montanaro *et al.*, 2005). Also, for cancers like prostate cancers and breast cancer ER $\beta$ -selective agonists may become the therapy of choice. Despite this apparent drawback, it is worth highlighting that ER $\alpha$  seems to play a major role in targeting neurodegenerative diseases such as AD and PD. Bearing this in mind, the development of SERMs would be the most logical and rational strategy when it comes to decide on the synthesis strategy used (Elzer *et al.*, 2010). Another strategy would be to use the so-called non-feminizing compounds, which having estrogen-like structures do not bind to or exert a weaker effect on ERs. For example, ZYC-3, an estrogen analogue with no binding affinity for either ER $\alpha$  or ER $\beta$ , was 10-fold more potent than 17 $\beta$ -E<sub>2</sub> against glutamate-induced cytotoxicity (Liu *et al.*, 2002) suggesting a strong capability as a neuroprotective agent.

Numerous *in vitro* and *in vivo* studies suggest that isoflavones have the potential to exert neuroprotective effects by suppressing microglial cells activation, and thus, cytokine release and nitric oxide/superoxide production (Valles *et al.*, 2010; Ong *et al.*, 2017). Such activity may be due to the structural homology between human natural occurring estrogen and isoflavones, which display binding affinity for estrogen receptors, in particular towards ER $\beta$  which is expressed in glial cells (Spencer *et al.*, 2012). Although, the biological activity of phytoestrogens differs and is frequently described as less active than mammalian or synthetic estrogens (Ososki and Kennelly, 2003).

Besides *in vitro* and *in vivo* experiments, molecular docking studies have also confirmed that flavonoids and isoflavonoids identified in red clover (*Trifolium pratense*),

have ER $\alpha$  and ER $\beta$  binding activity showing a binding preference for ER $\beta$  (Powers and Setzer, 2015).

Differences in estrogenic activity of similarly classified chemicals may be due to the structural features or deviations in those structures (Ososki and Kennelly, 2003). To account for the results reported, certain features in terms of ligand-receptor interactions and metabolism are to be taken into consideration.

It is known that ligand binding to ER $\alpha$  and ER $\beta$  depends on a unique combination of structural characteristics starting for two hydroxyl groups (-OH) with a distance between them similar to that of the estradiol's (10.8 Å) (Ososki and Kennelly, 2003; Fokialakis *et al.*, 2004). The planarity ring system and a suitable electron density on the ring A are also factors to take in consideration. Taking as an example the extensively studied isoflavone genistein, their OH in the fourth carbon (4'-OH) and in the seventh (7-OH) are known to mimic those of the estradiol in position 3 and 17. However, both H bond formations may not be possible for BCA and FMN due to the methylation of its 4'-OH (Fokialakis *et al.*, 2012).

As remarked in previous chapters, neurotoxicity related to neuroinflammation contributes to the development of neurodegenerative diseases like AD, PD and ALS. In addition, pro-inflammatory mediators such as TNF $\alpha$ , IL-1 $\beta$  and IL-6 released by activated microglia are shown to induce damage to adjacent neurons. Theoretically, compounds that are able to inhibit the production of pro-inflammatory cytokines would be expected to confer protection against neurotoxicity.

The present work is a preliminary study of novel plant-derived compounds, which aims to pave the way for a further and deeper study on how phytoestrogen inhibit neuroinflammation. Two carbamate ester (compound **1** and **4**), an ester (compound **2**) and a deoxybenzoin intermediate, derivatives from BCA and FMN have been synthesized in this study. Results show that derivatives of the isoflavonoids BCA and FMN may possess anti-inflammatory properties, as well as minor changes in their structure can lead to the opposite effect.

Esterification of hydroxyl group(s) and the use of carbamate esters have been two of the preferred prodrug strategies over the years. Moreover, branched acyl group shows higher lipophilicity and slower chemical or enzymatic hydrolysis. (Férriz *et al.*, 2010). We have followed these approaches in order to make novel derivatives of BCA and

FMN. Logically, these new compounds should display higher pharmacological efficiency.

BCA is an ER- $\beta$  selective isoflavone mostly found in *Trifolium pratense* (family *Fabeaceae*) that has been shown to effectively suppress LPS-stimulated overproduction of cytokines and certain transcriptional factors by inhibiting the activation of the MAPK pathway in BV2 cells (Wang-Yang *et al.*, 2014; Zhang *et al.*, 2015; Wang *et al.*, 2016). The present study confirms that BCA inhibits the production of TNF $\alpha$ , IL-1 $\beta$  and IL-6 in BV2 microglia stimulated with LPS. BCA effectively reduces the production of TNF- $\alpha$  and IL-1 $\beta$  in LPS-activated BV2 microglia, suggesting that the compound is capable of inhibiting neuroinflammation. However, it did not significantly suppress IL-6 release. Such results contrast other previous studies in which IL-6 had been evaluated after treatment with BCA in primary microglial cells. In this latest study, BCA effectively decreases IL-6 along with the other CKs (Wang *et al.*, 2016). After stimulation with LPS, BV2 cells were shown to increase the production of nitric oxide and PGE<sub>2</sub>. Upon treatment with BCA, both inflammatory modulators, NO and PGE<sub>2</sub> decreased.

Compound **1** was synthesized as described by Fokialakis *et al.* (2012) from BCA and we show for the first time its anti-inflammatory effects, however, the mechanism by which it acts has not been elucidated yet. In an attempt to clarify such pharmacological activity, the main pro-inflammatories CKs were evaluated, overall, all CKs were significantly reduced. Compound **1** also inhibited neuroinflammation by blocking iNOS protein expression and nitric oxide production in the microglia. In addition, it reduced the expression of COX-2 and its mediated PGE<sub>2</sub> production in LPS stimulated microglia specially at the dose of 15  $\mu$ M, suggesting that compound **1** possesses neuroinflammation inhibitory activities. Previously, compound **1** was reported to display ten times weaker affinity to ERs than compound BCA (Fokialakis *et al.*, 2012) from which it could be deduced that compound **1** would have lower pharmacological efficacy than BCA. However, conclusions must be carefully taken since, for instance, Pfitscher and co-workers (2008) describe a metabolite (angolensin) that had lower binding affinities to both ERs but comparable transactivation potential to equol, a daidzein metabolite (see Chapter 3) indicating that angolensin would be implicating in other type of molecular mechanisms.

In contrast, compound **2**, also a BCA derivative, has been synthesized from scratch causing, surprisingly, opposite effects by increasing pro-inflammatory CKs and yet

decreasing NO release. From our knowledge, there are no references for compound **2** to be compared with. However, many authors have studied similar compounds and structures on the basis of the ER ligand cavity diversity (Chakrabarti *et al.*, 2014; Powers and Setzer, 2015). Regarding the atypical activity of compound **2**, it might be related not only to the structure itself but also to the concentration used. Some authors have described several isoflavones and their metabolites with a dual activity, acting as an estrogenic agonist or antagonist depending on the estrogen concentration (Ong *et al.*, 2017; Hwang CS *et al.*, 2006). PGE<sub>2</sub> production also augmented significantly ( $p < 0.01$ ). Steroids and non-steroids anti-inflammatory drugs are expected to drop PGE<sub>2</sub> production. However, their effects are reliant on the complex and yet not completely understood regulation of this mediator (Kalinski, 2012). Bearing in mind the importance of the structural characteristics stated above, besides other hydrophobic and hydrophilic interactions, and despite the *in vivo* evidences on phytoestrogen triggering neuroinflammation, it is striking that compound **2** displays the opposite action by increasing the cytokine release in a dose-dependent manner. Even though the mechanism by which this occurs still needs to be elucidated, it is likely that such antagonist action is due to the lack of the possibility of a hydrogen binding between the ester and the ER itself. Unlike compound **1** and **4**, which have a carbamate group and therefore, an –NH capable of forming a hydrogen binding with the ER, compound **2** contains a long carbon chain joined by an ester (-COO-) which does not possess a free hydrogen to interact within the receptor. Such slightly differences between BCA and its derivatives could illustrate the importance of H bond formation between the 7-OH group and the receptor. In fact, Fokialis *et al.* (2012) obtained lower affinities binding to ERs for their novel BCA derivatives rather than for BCA evidencing the inability of this binding.

As for compound **3**, the Biochanin deoxybenzoid, was proved to be cytotoxic for BV2 cells as the dose used increased. Fokialakis *et al.* (2004) also synthesized this compound and observed that its higher affinity was bias the ER $\alpha$  subtype.

FMN is an isoflavone found in red clover plant and widespread in the *Leguminosae* family that has been reported to possess many health benefits. In the present project FMN was synthesized in order to develop a carbamate ester derivate named compound **4**. We demonstrate that both compounds are bioactive in BV2 cells showing possible neuroprotective abilities.

Overall and despite the nature of the compounds studied, the results suggest that only compound **1** and **4** and their scaffold structures exhibited inhibition of neuroinflammation in LPS-activated BV2 microglia.

In the light of the observed effects on pro-inflammatory mediators, there is a need for further investigation of the mechanism(s) of action of these compounds. Further investigation is needed to reveal the structural-activity relationship that is required for a natural product to be active as a phytoestrogen. To do so, we would suggest to synthesize more compounds with the same isoflavone scaffold but modifying the length of the side chain. As for the pharmacology experiments, immunofluorescence along with ligand-binding assays would shed some light on whether all compounds are interacting with ERs or, on the contrary, their effect is due to the interaction with other type of receptors. Moreover,  $IC_{50}$  experiments would determine the effectiveness of the compounds synthesized against the natural compounds. It is evident that BBB represents a major obstacle for the compounds to enter CNS. Therefore, it is crucial to investigate the capability of all these compounds to cross BBB using *in vitro* models such as Human Brain Endothelial Cell Line (HCMEC/D3) cell line.

## REFERENCES

- Abbas AK, Lichtman AHH, Pillai S. Basic. Immunology: Functions and Disorders of the Immune System. 4th ed. Philadelphia, PA: Saunders Elsevier. 2014.
- Akiyama H, Barger S, Barnum S, Bradt B, Bauer J, Cole GM, Cooper NR, *et al.* Inflammation and Alzheimer's disease. *Neurobiol Aging*. 2000; 21(3): 383–421.
- An J, Tzagarakis-Foster C, Scharschmidt TC, Lomri N, Leitman DC. Estrogen receptor beta-selective transcriptional activity and recruitment of coregulators by phytoestrogens. *J Biol Chem*. 2001; 276(21):17808-17814.
- Anderson BD. Prodrugs for improved CNS delivery. *Adv Drug Deliv Rev*. 1996; 19: 171-202.
- Araújo ME, Franco YEM, Messias MCF, Longato GB, Pamphile JA, Carvalho PO. Biocatalytic synthesis of flavonoid esters by lipases and their biological benefits. *Planta Med*. 2017; 83: 7-22.
- Arroyo DS, Soria JA, Gaviglio EA, Rodriguez-Galan MC, Iribarren P. Toll-like receptors are key players in neurodegeneration. *Int Immunopharmacol*. 2011; 11(10): 1415–1421.
- Baker AE, Brautigam VM, Watters JJ. Estrogen modulates microglial inflammatory mediator production via interactions with Estrogen receptor  $\beta$ . *Endocrinology*. 2004; 145(11):5021-5032.
- Baker W, Robinson R. CCLXVI.-Synthetical experiments in the isoflavone group. Part I. *Journal of the Chemical Society, Transactions*. 1925; 127 (0): 1981-1986.
- Balasubramanian S, Nair MG. An efficient —one potll synthesis of isoflavones. *Synthetic Communications*. 2000; 30(3): 469-484.
- Behl C, Skutella T, Lezoualc'h F, Post A, Widmann M, Newton CJ, Holsboer F. Neuroprotection against oxidative stress by estrogens: structure-activity relationship. *Mol Pharmacol*. 1997; 51:535–541.

Biegasiewicz KF, Gordon J S, Rodriguez DA, Priefer R. Development of a general approach to the synthesis of a library of isoflavonoid derivatives. *Tetrahedron Letters*. 2014; 55(37): 5210-5212.

Björnström L, Sjöberg M. Mechanisms of estrogen receptors signalling: convergence of genomic and nongenomic actions on target genes. *Mol Endocrinol*. 2005; 19(4):833842.

Bonizzi G, Karin M. The two NF- $\kappa$ B activation pathways and their role in innate and adaptive immunity. *Trends Immunol*. 2004; 25(6):280-288.

Bradshaw EM, Chibnik LB, Keenan BT, *et al*, and the Alzheimer Disease Neuroimaging Initiative. CD33 Alzheimer's disease locus: altered monocyte function and amyloid biology. *Nat Neurosci* 2013; 16: 848–50.

Brann DW, Dhandapani K, Wakade C, Mahesh VB, Khan MM. Neurotrophic and neuroprotective actions of estrogen: basic mechanisms and clinical implications. *Steroids*. 2007; 72: 381–405.

Bsibsi M, Ravid R, Gveric D, Van Noort JM. Broad expression of Toll-like receptors in the human central nervous system. *J Neuropathol Exp Neurol*. 2002; 61:1013–21.

Butterfield DA, Reed TT, Perluigi M, *et al*. Elevated levels of 3-nitrotyrosine in brain from subjects with amnesic mild cognitive impairment: implications for the role of nitration in the progression of Alzheimer's disease. *Brain Res*. 2007; 1148: 243–48.

Carroll, J.C. & Pike, C.J. Selective estrogen receptor modulators differentially regulate Alzheimer-like changes in female 3xTg-AD mice. *Endocrinology* 149, 2607–2611 (2008).

Chakrabarti M, Haque A, Banik NL, Nagarkatti P, Nagarkatti M, Ray SK. Estrogen receptor agonists for attenuation of neuroinflammation and neurodegeneration. *Brain research bulletin*. 2014; 109:22-31.

Chandrasekharan S, Bhaskar B, Muthiah R, Chandrasekharan AK, Ramamurthy V. Estrogenic effect of three substituted deoxybenzoins. *Steroids*. 2013; 78: 147–155.  
Chattopadhyay M, Goswami S, Rodes DB, Kodela R, Velazquez CA, Boring D,

- Crowell JA, *et al.* NO-releasing NSAIDs suppress NF- $\kappa$ B signaling *in vitro* and *in vivo* through S-nitrosylation. *Cancer letters*. 2010; 298(2): 204–211.
- Chaturvedi D, Zaidi S. Organic Carbamates: An Unique Linkage in Anticancer Drug Design. *J Chem*. 2015; 4(4):92-94.
- Chen FE, Kempiak S, Huang DB, Phelps C, Ghosh G. Construction, expression, purification and functional analysis of recombinant NFkappaB p50/p65 heterodimer. *Protein Eng*. 1999; 12(5):423-428.
- Chen HQ, Wang XJ, Jin ZY, Xu XM, Zhao JW, Xie ZJ. Protective effect of isoflavones from *Trifolium pratense* on dopaminergic neurons. *Neurosci Res*. 2008; 62(2): 123130.
- Cherry JD, Olschowka JA, O'Banion MK. Neuroinflammation and M2 microglia: the good, the bad, and the inflamed. *J Neuroinflammation*. 2014; 11(98).
- Colton CA. Heterogeneity of microglial activation in the innate immune response in the brain. *J Neuroimmune Pharmacol*. 2009; 4(47):399-418.
- Corraliza IM, Soler G, Eichmann K, Modolell M. Arginase induction by suppressors of nitric oxide synthesis (IL-4, IL-10 and PGE2) in murine bone-marrow-derived macrophages. *Biochem Biophys Res Commun*. 1995; 206(2):667–673.
- Dailey ME. The Dailey Lab at the University of Iowa website. <https://dailey.lab.uiowa.edu/>. Accessed September 27, 2016.
- Delves PJ, Martin SJ, Burton DR, Roitt IM. Roitt's Essential Immunology. 12th ed. Hoboken, NJ, USA: Wiley-Blackwell; 2011.
- Dholkawala F, Voshavar C, Dutta AK. Synthesis and characterization of brain penetrant prodrug of neuroprotective D-264: Potential therapeutic application in the treatment of Parkinson's disease. *Europ J Pharmaceutics Biopharm*. 2016; 103: 62–70.
- Erta M, Quintana A, Hidalgo J. Interleukin-6, a Major Cytokine in the Central Nervous System. *Int J Biol Sci*. 2012; 8(9):1254-1266.

Escande A, Pillon A, Servant N, Cravedi JP, Larrea F, Muhn P, Nicolas JC, *et al.* Evaluation of ligand selectivity using reporter cell lines stably expressing estrogen receptor alpha or beta. *Biochem Pharmacol.* 2006; 71(10):1459-1469.

Fokialakis N, Alexi X, Aligiannis N, Siriani D, Meligova AK, Pratsinis H, Mitakou S, *et al.* Ester and carbamate ester derivatives of Biochanin A: synthesis and *in vitro* evaluation of estrogenic and antiproliferative activities. *Bioorg Med Chem.* 2012; 20(9):2962-2970.

Fokialakis N, Lambrinidis G, Mitsiou DJ, Aligiannis N, Mitakou S, Skaltsounis AL, Pratsinis H, *et al.* A new class of phytoestrogens; evaluation of the estrogenic activity of deoxybenzoins. *Chem Biol.* 2004; 11(3):397-406.

Gadani SP, Cronk JC, Norris GT, Kipnis J. IL-4 in the brain: a cytokine to remember. *J Immunol.* 2012; 189(9):4213–4219.

Ghosh AK, Brindisi M. Organic carbamates in drug design and medicinal chemistry. *J Med Chem.* 2015; 58(7):2895-2940.

Gilmore DT. NF- $\kappa$ B Transcription Factors: players, pathways, perspectives. *Oncogene.* 2006; 25(51):6680–6684.

Graeber MB, Streit WJ. Microglia: biology and pathology. *Acta Neuropathol.* 2010; 119(1):89-105.

Green PS, Gordon K, Simpkins JW. Phenolic A ring requirement for the neuroprotective effects of steroids. *J Steroid Biochem & Mol Biol.* 1997; 63:229–235.

Guerreiro R, Wojtas A, Bras J, *et al.* and the Alzheimer Genetic Analysis Group. TREM2 variants in Alzheimer's disease. *N Engl J Med.* 2013; 368: 117–27.

Gulbransen BD. Enteric glia. In: Verkhratsky A, Parpura V, eds. Colloquium series on neuroglia in biology and medicine from physiology to disease. 1<sup>st</sup> ed. Morgan & Claypool publishers. 2014. doi:10.4199/C00102ED1V01Y201401NGL001. Accessed November, 2016.

Hansson GK, Edfeldt K. Toll to be paid at the gateway to the vessel wall. *Arterioscler Thromb Vasc Biol.* 2005; 25(6):1085–1087.

Hassan SM. Soybean, nutrition and health. In: El-Shemy H, ed. *Agricultural and Biological Sciences*. 2013, InTech. doi: 10.5772/54545. Available at: <http://www.intechopen.com/books/soybean-bio-active-compounds/soybean-nutritionand-health>

Heldring N, Pike A, Andersson S, Matthews J, Cheng G, Hartman J, Tujague M, *et al.* Estrogen receptors: how do they signal and what are their targets. *Physiol Rev*. 2007; 87(3):905-931.

Heneka MT, *et al.* *Neuroinflammation in Alzheimer's disease*. *Lancet Neurol*. 2015; 14(4):388-405.

Hsu A, Bray TM, Helferich WG, Doerge DR, Ho E. Differential effects of whole soy extract and soy isoflavones on apoptosis in prostate cancer cells. *Exp Biol Med*. 2010; 235: 90–97.

Hu QF, Zhou B, Ye YQ, Jiang ZY, Huang Z, Li YK, Du G, Yang GY, Gao XM. Cytotoxic Deoxybenzoins and Diphenylethylenes from *Arundina graminifolia*. *J Nat Prod*. 2013; 76: 1854–1859.

Huang P, Chandra V, Rastinejad F. Structural overview of the nuclear receptor superfamily: insights into physiology and therapeutics. *Annu Rev Physiol*. 2010; 72:247-272.

Hwang CS, Kwak HS, Lim HJ, Lee SH, Kang YS, Choe TB, Hur HG *et al.* Isoflavone metabolites and their *in vitro* dual functions: they can act as an estrogenic agonist or antagonist depending on the estrogen concentration. *J Steroid Biochem Mol Biol*. 2006; 101(4-5):246-253.

Kalinski P. Regulation of Immune Responses by Prostaglandin E<sub>2</sub>. *J Immunol*. 2012; 188(1):21–28.

Kim, SH *et al.* The dietary flavonoid Kaempferol mediates anti-inflammatory responses via the Src, Syk, IRAK1, and IRAK4 molecular targets. *Mediators Inflamm*. 2015; 2015:904142. doi: 10.1155/2015/904142.

Kipp M, Hochstrasser T, Schmitz C, Beyer C. Female sex steroids and glia cells: Impact on multiple sclerosis lesion formation and fine tuning of the local neurodegenerative cellular network. *Neurosci Biobehav Rev*. 2016; 67: 125–136.

Kloska A, Narajczyk M, Jakóbkiewicz-Banecka J, *et al.* Synthetic genistein derivatives as modulators of glycosaminoglycan storage. *J Trans Med.* 2012; 10:153.

Krause DL & Muller N. Neuroinflammation, microglia and implications for antiinflammatory treatment in Alzheimer's disease. *International journal of Alzheimer's disease.* 2010; 732806, 1-9.

Kuiper GGJM, Lemmen JG, Carlsson B, Corton JC, Safe SH, van der Saag PT, van der Burg B, *et al.* Interaction of estrogenic chemicals and phytoestrogens with estrogen receptor  $\beta$ . *Endocrinology.* 1998; 139(10):4252–4263.

Kummer MP, Hermes M, Delekarte A, *et al.* Nitration of tyrosine 10 critically enhances amyloid  $\beta$  aggregation and plaque formation. *Neuron.* 2011; 71: 833–44.

Larkin T, Price WE, Astheimer L. The key importance of soy isoflavone bioavailability to understanding health benefits. *Crit Rev Food Sci Nutrition.* 2008; 48: 538–552.

Lawrence T. The Nuclear Factor NF- $\kappa$ B Pathway in Inflammation. *Cold Spring Harb Perspect Biol.* 2009; 1(6):a001651.

Lehnardt S, Massillon L, Follett P, Jensen FE, Ratan R, Rosenberg PA, Volpe JJ, *et al.* Activation of innate immunity in the CNS triggers neurodegeneration through a Tolllike receptor 4-dependent pathway. *Proc Natl Acad Sci.* 2003; 100(14): 8514–8519.

Lei, J. *et al.* Pharmacological Inhibition of TLR4 Reduces Mast Cell Activation, Neuroinflammation and Hyperalgesia in Sickle Mice. *Blood.* 2015; 126(23): 278–278.

Leung YK, Mak P, Hassan S, Ho SM, *et al.* Estrogen receptor (ER)-beta isoforms: a key to understanding ER-beta signaling. *Proc Natl Acad Sci.* 2006; 103(35):13162–13167.

Li T, Zhao X, Mo Z, Huang W, Yan H, Ling Z, Ye Y. Formononetin promotes cell cycle arrest via downregulation of Akt/Cyclin D1/CDK4 in human prostate cancer cells. *Cell Physiol Biochem.* 2014; 34:1351-1358.

Li X, Huang J, Yi P, Bambara RA, Hilf R, Muyan M. Single-chain estrogen receptors (ERs) reveal that the ERalpha/beta heterodimer emulates functions of the ERalpha

- dimer in genomic estrogen signaling pathways. *Mol Cell Biol.* 2004; 24(17):7681–7694.
- Li Y, Yang F, Wang L, Cao Z, Han T, Duan Z, Li Z, *et al.* Phosphoramidate protides of five flavones and their antiproliferative activity against HepG2 and L-O2 lines. *Eur J Med Chem.* 2016; 112: 196-208.
- Li Z, Dong X, Zhang J, Zeng G, Zhao H, Liu Y, Qiu R, *et al.* Formononetin protects TBI rats against neurological lesions and the underlying mechanism. *J Neurol Sci.* 2014; 338(1-2): 112-117.
- Lin CC, Tsai YL, Ho CT, Teng SC. Determination of the differential estrogenicity of isoflavonoids by E2-ER-ERE-dependent gene expression in recombinant yeast and MCF-7 human breast cancer cells. *Food Chem.* 2007; 108(2):719-726.
- Liu MM, Albanese C, Anderson CM, Hilty K, Webb P, Uht RM, Price RH Jr, *et al.* Opposing Action Of Estrogen Receptors And On Cyclin D1 Gene Expression. *J Biol Chem.* 2002; 277(27):24353-24360.
- Liu S, Liu Y, Hao W, Wolf L, Kiliaan AJ, Penke B, *et al.* TLR2 is a primary receptor for Alzheimer's amyloid  $\beta$  peptide to trigger neuroinflammatory activation. *J Immunol.* 2012; 188:1098–1107
- Lu YC, Yeh WC, Ohashi PS. LPS/TLR4 signal transduction pathway. *Cytokine.* 2008; 42(2):145-151.
- Ma Z, Ji W, Fu Q, Ma S. Formononetin inhibited the inflammation of LPS-induced acute lung injury in mice associated with induction of PPAR gamma expression. *Inflammation.* 2013; 36(6):1560-1566.
- Mantovani A, Sica A, Sozzani S, Allavena P, Vecchi A, Locati M. The chemokine system in diverse forms of macrophage activation and polarization. *Trends Immunol.* 2004; 25(12):677–686.
- Martínez-Gómez A. Comunicación entre células gliales y neuronas I. Astrocitos, células de Schwann que no forman mielina y células de Schwann perisinápticas. *Medicina e investigación.* 2014; 2(2):75-84.

- Minghetti L. Cyclooxygenase-2 (COX-2) in inflammatory and degenerative brain diseases. *J Neuropathol Exp Neurol.* 2004; 63(9): 901–910.
- Montanaro D, Maggiolini M, Recchia AG, Sirianni R, Aquila S, Barzon L, Fallo F, *et al.* Antiestrogens upregulate estrogen receptor beta expression and inhibit adrenocortical H295R cell proliferation. *J Mol Endocrinol.* 2005; 35(2):245–256.
- Moon YJ, Sagawa K, Frederick K, Zhang S, Morris ME. Pharmacokinetics and Bioavailability of the isoflavone Biochanin A in rats. *AAPS J.* 2006; 8(3):433-442.
- Morales I, *et al.* Neuroinflammation in the pathogenesis of Alzheimer's disease. A rational framework for the search of novel therapeutic approaches. *Front Cell Neurosci.* 2014; 8: 112.
- Mu H, Bai YH, Wang ST, Zhu ZM, Zhang YW. Research on antioxidant effects and estrogenic effect of formononetin from *Trifolium pratense* (red clover). *Phytomed.* 2009; 16:314-319.
- Nagano T, Nishiyama R, Sanada A, Mutaguchi Y, Ioku A, Umeki H, Kishimoto S, *et al.* Prostaglandin E2 potentiates interferon- $\gamma$ -induced nitric oxide production in cultured rat microglia. *J Neurochem.* 2016. doi: 10.1111/jnc.13926. Accessed December, 2016.
- Nilsson S, Mäkelä S, Treuter E, Tujague M, Thomsen J, Andersson G, Enmark E, *et al.* Mechanisms of estrogen action. *Physiol Rev.* 2001; 81(4):1535–1565.
- Nilsson S, Gustafsson JÅ. Estrogen Receptors: Therapies Targeted to Receptor Subtypes State of the art. *Nature publishing group.* 2011; 89(1).
- Olajide OA, Kumar A, Velagapudi R, Okorji UP, Fiebich BL. Punicalagin inhibits neuroinflammation in LPS-activated rat primary microglia. *Mol Nutr Food Res.* 2014. 58(9):1843-1851.
- Ong W, Farooqui T, Ho CF, Ng Y, Farooqui AA. Neuroprotective Effects of Phytochemicals in Neurological Disorders. In: Farooqui T, Farooqui AA (Ed). *Use of Phytochemicals against Neuroinflammation.* 2017. The Ohio State University, Columbus, OH, USA.
- Ososki AL, Kennelly EJ. Phytoestrogens: a review of the present state of research. *Phytother. Res.* 2003; 17(8):845–869.

Papoutsia Z, Kassia E, Fokialakisb N, Mitakoub S, Lambrinidisc G, Mikrosoc E, Moutsatsou P. Deoxybenzoins are novel potent selective estrogen receptor modulators. *Steroids*. 2007; 72: 693–704.

Pavese JM, Farmer RL, Bergan RC. Inhibition of cancer cell invasion and metastasis by genistein. *Cancer and Metastasis Reviews*. 2010; 29:

Petrone AB, Gatson JW, Simpkins JW, Miranda N. Non-Feminizing Estrogens: A Novel Neuroprotective Therapy. *Reed Mol Cell Endocrinol*. 2014; 389(0): 40–47.

Phelps CB, Sengchanthalangsy LL, Malek S, Ghosh G. Mechanism of kappa B DNA binding by Rel/NF-kappa B dimers. *J Biol Chem*. 2000; 275(32):24392-24399.

Pietras RJ, Szego CM. Specific binding sites for oestrogen at the outer surfaces of isolated endometrial cells. *Nature*. 1977; 265(5589):69-72.

Popovich PG, Longbrake EE. Can the immune system be harnessed to repair the CNS? *Nat Rev Neurosci*. 2008; 9:481–93.

Powers CN, Setzer WN. A molecular docking study of phytochemical estrogen mimics from dietary herbal supplements. *In Silico Pharmacol*. 2015; 3:4. doi: 10.1186/s40203015-0008-z

Pugazhendhi D, Watson KA, Mills S, Botting N, Pope GS, Darbre PD. Effect of sulphation on the oestrogen agonist activity of the phytoestrogens genistein and daidzein in MCF-7 human breast cancer cells. *J Endocrinol*. 2008; 197(3):503-515.

Purves D, Augustine GJ, Fitzpatrick D, Katz LC, LaMantia AS, McNamara JO, Williams SM eds. *Neuroscience*. 2nd edition. Sunderland (MA): Sinauer Associates; 2001.

Ren J, Xu HJ, Cheng H, Xin WQ, Chen X, Hu K. Synthesis and antitumor activity of formononetin nitrogen mustard derivatives. *Eur J Med Chem*. 2012; 54: 175-187.

Rietjens IM, Sotoca AM, Vervoort J, Louisse J. Mechanisms underlying the dualistic mode of action of major soy isoflavones in relation to cell proliferation and cancer risks. *Mol Nutr Food Res*. 2013. 57: 100–113.

Sachdeva C, Mishra N, Sharma S. Development and characterization of enteric-coated microparticles of biochanin A for their beneficial pharmacological potential in estrogen deficient-hypertension. *Drug Deliv.* 2016; 23(6): 2044–2057.

Simpkins JW, Singh M. More than a decade of estrogen neuroprotection. *Alzheimers Dement.* 2008; 4:(1 Suppl 1):S131-136.

Sirotkin AV, Harrath AH. Phytoestrogens and their effects. *Eur J Pharmacol.* 2014; 741:230-236. doi: 10.1016/j.ejphar.2014.07.057

Somjen D *et al.* Membranal effects of phytoestrogens and carboxy derivatives of phytoestrogens on human vascular and bone cells: new insights based on studies with carboxy-biochanin A. *J Steroid Biochem & Mol Biol.* 2005; 93:293-303.

Spencer JP, Vafeiadou K, Williams RJ, Vauzour D. Neuroinflammation: modulation by flavonoids and mechanisms of action. *Mol Aspects Med.* 2012; 33(1):83-97.

Srivastava K, Tyagi AM, Khan K, Dixit M, Lahiri S, Kumar A, Changkija B, *et al.* Isoformononetin, a methoxydaidzein present in medicinal plants, reverses bone loss in osteopenic rats and exerts bone anabolic action by preventing osteoblast apoptosis. *Phytomed.* 2013; 20: 470-480.

Stansley B, Post J, Hensley K. A comparative review of cell culture systems for the study of microglial biology in Alzheimer's disease. *J Neuroinflammation.* 2012; 9:115122.

Sun J, Zhang X, Broderick M, Fein H. Measurement of nitric oxide production in cbiological systems by using Griess Reaction Assay. *Sensors.* 2003; 3(8):276-284.

Sun T, Liu R, Cao Y. Vasorelaxant and antihypertensive effects of for-mononetin through endothelium-dependent and independent mechanisms. *Acta Pharmacol Sin.* 2011; 32:1009-1018.

Suzumura A, Ikenaka K eds. Neuron-Glia Interaction in Neuroinflammatio, advances in neurobiology. 7th ed. New York NY:Springer. 2013.

Tan JW & Kim MK. Neuroprotective Effects of Biochanin A against  $\beta$ -Amyloid-Induced Neurotoxicity in PC12 Cells via a Mitochondrial-Dependent Apoptosis Pathway. *Molecules.* 2016 ; 25 : 21(5).

Tolleson WH, Doerge DR, Churchwell MI, Marques M, Roberts DW. Metabolism of Biochanin A and Formononetin by Human Liver Microsomes *in vitro*. *J Agric Food Chem*. 2002; 50(17):4783-4790.

Valles SL, Dolz-Gaiton P, Gambini J, Borrás C, Lloret A, Pallardo FV, Viña J. Estradiol or genistein prevent Alzheimer's disease-associated inflammation correlating with an increase PPAR gamma expression in cultured astrocytes. *Brain Res*. 2010; 1312:138–144.

Verkhatsky A, Butt A. Microglia. In: Verkhatsky A, Butt A, eds. *Glial Physiology and Pathophysiology*. Chichester, UK: John Wiley & Sons, Ltd; 2013. doi: 10.1002/9781118402061.ch3. Accessed October, 2015: 343-380.

Verkhatsky A, Butt A. Neuroglia: Definition, Classification, Evolution, Numbers, Development. In: Verkhatsky A, Butt A, eds. *Glial Physiology and Pathophysiology*. Chichester, UK: John Wiley & Sons, Ltd; 2013. doi: 10.1002/9781118402061.ch3. Accessed October, 2015: 73-104.

Vernieri E, Gomez-Monterrey I, Milite C, Grieco P, Musella S, Bertamino A, Scognamiglio I *et al*. Design, Synthesis, and Evaluation of New Tripeptides as COX-2 Inhibitors. *J Amino Acids*. 2013; (2013):606282.

Wähälä K, Hase TA. Expedient synthesis of polyhydroxyisoflavones. *Journal of the Chemical Society, Perkin Transactions*. 1991; 1(12): 3005-3008.

Wang J, Wu WY, Huang H, Li WZ, Chen HQ, Yin YY. Biochanin A protects against lipopolysaccharide-induced damage of dopaminergic neurons both *in vivo* and *in vitro* via inhibition of microglial activation. *Neurotox Res*. 2016; 30(3):486-498.

Wang Y, Zhu Y, Gao L, Yin H, Xie Z, Wang D, Zhu Z, *et al*. Formononetin attenuates IL-1 $\beta$ -induced apoptosis and NF- $\kappa$ B activation in INS-1 cells. *Molecules*. 2012; 17(9): 10052-10064.

Woodroffe N, Amor S. *Neuroinflammation and CNS Disorders*. 1st ed. Somerset, NJ, USA: Wiley Blackwell; 2014: 1-36.

Wu W, Wu Y, Huang H, He C, Li W, Wang H, Chen H, Yin Y. Biochanin A attenuates LPS-induced pro-inflammatory responses and inhibits the activation of the MAPK pathway in BV2 microglial cells. 2014; 391-398.

Wu WF, *et al.* Targeting estrogen receptor beta in microglia and T cells to treat experimental autoimmune encephalomyelitis. *Proc Natl Acad Sci U.S.A.* 2013; 110(9): 3543–3548.

Wu XY, Xu H, Wu ZF, Chen C, Liu JY, Wu GN, Yao XQ, *et al.* Formononetin, a novel FGFR2 inhibitor, potently inhibits angiogenesis and tumor growth in preclinical models. *Oncotarget.* 2015; 6: 44563-44578.

Wuttke W, Jarry H, Becker T, Schultens A, Christoffel V, Gorkow C, Seidlová-Wuttke D. Phytoestrogens: endocrine disrupters or replacement for hormone replacement therapy? *Maturitas.* 2008; 61(1-2):159-170.

Yang Chuyan, Qianrong Li, Yong Li. Targeting Nuclear Receptors With Marine Natural Products. *Marine Drugs.* 2014; 12(2):601-635.

Yao L, Enci Mary Kan, Jia Lu, Aijun Hao, S Thameem Dheen, Charanjit Kaur, EngAng Ling. Toll-like receptor 4 mediates microglial activation and production of inflammatory mediators in neonatal rat brain following hypoxia: role of TLR4 in hypoxic microglia. *J Neuroinflammation.* 2013; 10(23).

Yu J, Bi X, Yu B, Chen D. Isoflavones: anti-inflammatory benefit and possible caveats. *Nutrients.* 2016; 8: 361-376.

Zarubin T, Han J. Activation and signaling of the p38 MAP kinase pathway. *Cell Research.* 2005. 15(1): 11-18.

Zhang Y, Chen WA. Biochanin A inhibits lipopolysaccharide-induced inflammatory cytokines and mediators production in BV2 microglia. *Neurochem Res.* 2015; 40(1): 165-71

Zhu P, Genc A, Zhang X, Zhang J, Bazan NG, Chen C. Heterogeneous expression and regulation of hippocampal prostaglandin E2 receptors. *J Neurosci Res.* 2005; 81(6): 817–826.

# ANNEX I: ADDITIONAL MATERIAL

## Mass Spectrometry Report



<b>Sample Details:</b> IPOS Sample I.D.: MSS2015/07/49      User Sample I.D.: BCA Undecyl Isocyanate S Enquiry Form Submitted: 21/07/15      Samples Received: 23/07/15 Sample Injection volume: 5 µl      Sample Inj conc.: 100 ppm		<b>Service User Details:</b> Name: Mireia Boluda      Supervisor: K. Hemming	
<b>Mass Spectrometry Details:</b> Instrument: Agilent6210 TOF MS      Mass Spectrometry: HRMS Ionisation Mode: Positive      Acquisition Rate: 2.07 spectra/s		<b>Ionisation Source Details:</b> Source: Dual ESI      Nebuliser Pressure: 40 psig Gas Temp: 350 °C      Drying Gas Flow Rate: 10 l/min Fragmentor Voltage: 150 V      Skimmer Voltage: 65 V Octopole OCT 1 RF Vpp: 250 V      VCap Voltage: 3000 V	

### Mass Spectrometry Data Summary:

Observed m/z	Most likely adduct	Observed neutral mass	Theoretical neutral mass	Certainty score / 100	Mass diff. / ppm
482.2523	[M+H] <sup>+</sup>	481.2450	481.2464	94.07	3.02
985.4821	[2M+Na] <sup>+</sup>	-	-	-	-

### Expected Mass for [C<sub>28</sub>H<sub>35</sub>NO<sub>6</sub>+?]<sup>+</sup>:

Species	Calc m/z
M	481.2464
(M+H) <sup>+</sup>	482.2537
(M+NH <sub>4</sub> ) <sup>+</sup>	499.2803
(M+Na) <sup>+</sup>	504.2357
(M+K) <sup>+</sup>	520.2096

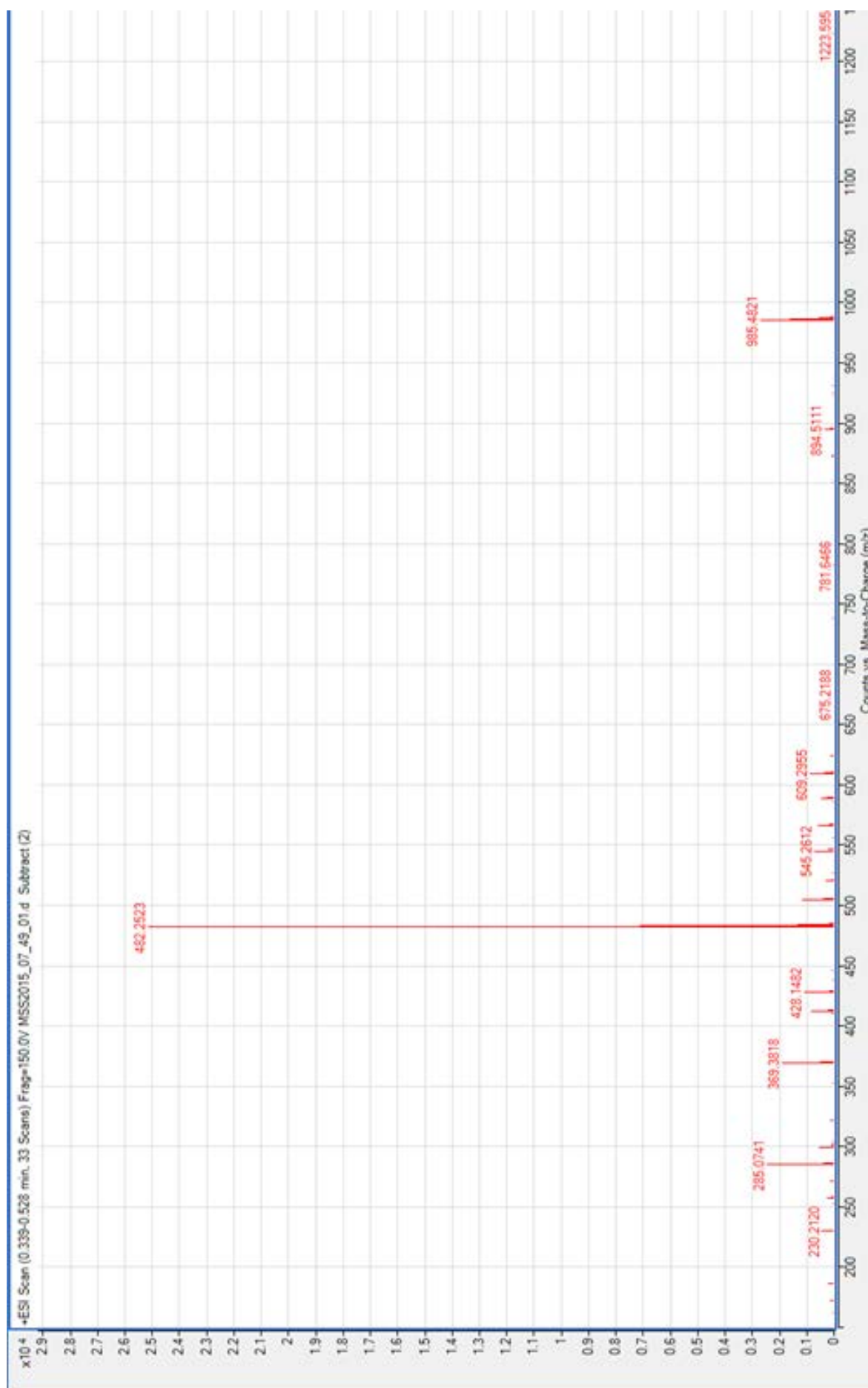
### Spectrum I.D results (optimised) 482.2523m/z:

Best	Formula	Species	m/z	Mass	Mass (MFG)	Score	Diff (ppm)
	C <sub>25</sub> H <sub>37</sub> O <sub>9</sub>	(M+H) <sup>+</sup>	482.2523	481.245	481.2438	96.35	-2.53
▶	C <sub>28</sub> H <sub>35</sub> N O <sub>6</sub>	(M+H) <sup>+</sup>	482.2523	481.245	481.2464	94.07	3.02
	C <sub>35</sub> H <sub>31</sub> N O	(M+H) <sup>+</sup>	482.2523	481.245	481.2406	60.73	-9.15
	C <sub>36</sub> H <sub>49</sub>	(M+H) <sup>+</sup>	482.3928	481.3855	481.3834	38.97	-4.37

### Conclusion:

BCA Undecyl Isocyanate S observed as the [M+H]<sup>+</sup> & [2M+Na]<sup>+</sup> adducts corresponding to the desired compound (94%) with a relative mass difference of 3.02 ppm.

Mass spectrum:



# Mass Spectrometry Report



<b>Sample Details:</b> IPOS Sample I.D.: MSS2015/07/48    User Sample I.D.: Compound 2 Enquiry Form Submitted: 21/07/15    Samples Received: 23/07/15 Sample Injection volume: 5 µl    Sample Inj conc.: 100 ppm		<b>Service User Details:</b> Name: Mireia Boluda    Supervisor: K. Hemming	
<b>Mass Spectrometry Details:</b> Instrument: Agilent 6210 TOF MS    Mass Spectrometry: HRMS Ionisation Mode: Positive    Acquisition Rate: 2.07 spectra/s		<b>Ionisation Source Details:</b> Source: Dual ESI    Nebuliser Pressure: 40 psig Gas Temp: 350 °C    Drying Gas Flow Rate: 10 l/min Fragmentor Voltage: 150 V    Skimmer Voltage: 65 V Octopole OCT 1 RF Vpp: 250 V    VCap Voltage: 3000 V	

## Mass Spectrometry Data Summary:

Observed m/z	Most likely adduct	Observed neutral mass	Theoretical neutral mass	Certainty score / 100	Mass diff. / ppm
467.2414	[M+H] <sup>+</sup>	466.2342	466.2355	92.74	2.95
594.2833	[M+Na] <sup>+</sup>	-	-	-	-
955.4597	[2M+Na] <sup>+</sup>	-	-	-	-

## Expected Mass for [C<sub>28</sub>H<sub>35</sub>NO<sub>6</sub>+?]<sup>+</sup>:

Species	Calc m/z
M	466.2355
(M+H) <sup>+</sup>	467.2428
(M+NH <sub>4</sub> ) <sup>+</sup>	484.2694
(M+Na) <sup>+</sup>	489.2248
(M+K) <sup>+</sup>	505.1987

## Spectrum I.D results (optimised) 467.2414m/z:

Best	Formula	Species	m/z	Mass	Mass (MFG)	Score	Diff (ppm)
●	C <sub>28</sub> H <sub>34</sub> O <sub>6</sub>	(M+H) <sup>+</sup>	467.2414	466.2342	466.2355	92.74	2.95
○	C <sub>35</sub> H <sub>30</sub> O	(M+H) <sup>+</sup>	467.2414	466.2342	466.2297	56.67	-9.62

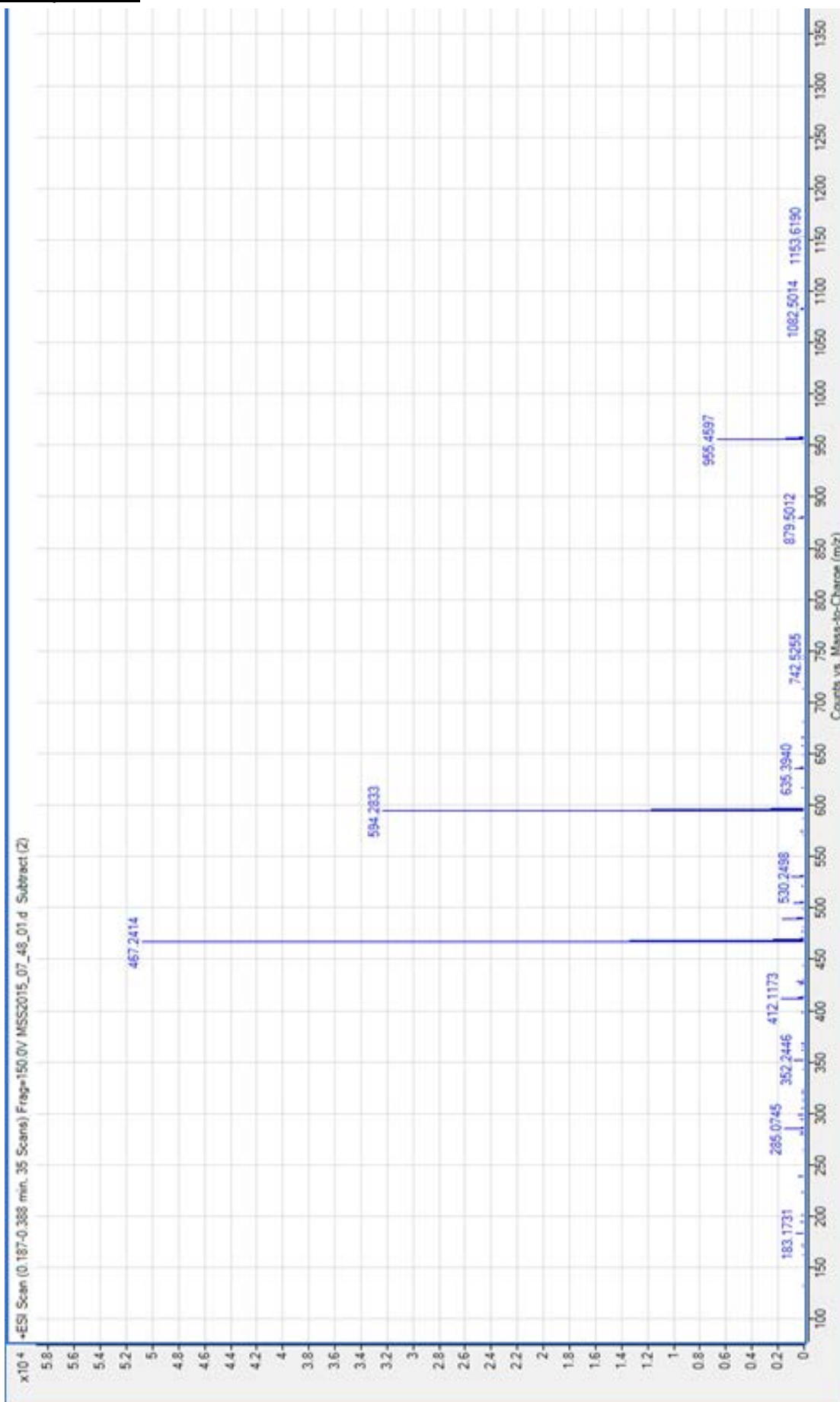
## 594.2833m/z:

Best	Formula	Species	m/z	Mass	Mass (MFG)	Score	Diff (ppm)
○	C <sub>34</sub> H <sub>41</sub> O <sub>9</sub>	(M+H) <sup>+</sup>	594.2833	593.2762	593.2751	97.53	-1.9
○	C <sub>27</sub> H <sub>45</sub> O <sub>14</sub>	(M+H) <sup>+</sup>	594.2833	593.2762	593.2809	69.12	7.96

## Conclusion:

BCA Dodecanoic Ester observed as the [M+H]<sup>+</sup> & [2M+Na]<sup>+</sup> adducts corresponding to the desired compound (93%) with a relative mass difference of 2.95 ppm. One significant impurity observed, with MS data strongly suggesting a formula of C<sub>34</sub>H<sub>41</sub>O<sub>9</sub>.

Mass spectrum:



# Mass Spectrometry Report



<b>Sample Details:</b> IPOS Sample I.D.: MSS2016/05/60      User Sample I.D.: FMN Enquiry Form Submitted: 16/05/16      Samples Received: 18/05/16 Sample Injection volume: 5 µl      Sample Inj conc.: 100 ppm		<b>Service User Details:</b> Name: Mireia Boluda      Supervisor: K. Hemming	
<b>Mass Spectrometry Details:</b> Instrument: Agilent6210 TOF MS      Mass Spectrometry: HRMS Ionisation Mode: Positive      Acquisition Rate: 2.07 spectra/s		<b>Ionisation Source Details:</b> Source: Dual ESI      Nebuliser Pressure: 40 psig Gas Temp: 350 °C      Drying Gas Flow Rate: 10 l/min Fragmentor Voltage: 150 V      Skimmer Voltage: 65 V Octopole OCT 1 RF Vpp: 250 V      VCap Voltage: 3000 V	

## Mass Spectrometry Data Summary:

Observed m/z	Most likely adduct	Observed neutral mass	Theoretical neutral mass	Certainty score / 100	Mass diff. / ppm
269.0808	[M+H] <sup>+</sup>	268.0735	268.0736	97.14	0.33
291.0626	[M+Na] <sup>+</sup>	268.0734	268.0736	96.71	0.68
559.1349	[2M+Na] <sup>+</sup>	-	-	-	-

## Expected Mass for [C<sub>16</sub>H<sub>12</sub>O<sub>4</sub>+?]<sup>+</sup>:

Species	Calc m/z
M	268.0736
(M+H) <sup>+</sup>	269.0808
(M+NH <sub>4</sub> ) <sup>+</sup>	286.1074
(M+Na) <sup>+</sup>	291.0628
(M+K) <sup>+</sup>	307.0367

## Spectrum I.D results 269.0808m/z:

Best	Formula	Species	m/z	Mass	Mass (MFG)	Score	Diff (ppm)
●	C16 H12 O4	(M+H) <sup>+</sup>	269.0808	268.0735	268.0736	97.14	0.33
○	C14 H14 O4	(M+Na) <sup>+</sup>	269.0808	246.0915	246.0892	82.67	-9.42
○	C19 H7 O	(M+NH <sub>4</sub> ) <sup>+</sup>	269.0808	251.0469	251.0497	68.6	10.99
○	C11 H18 O5	(M+K) <sup>+</sup>	269.0808	230.1177	230.1154	68.21	-9.75

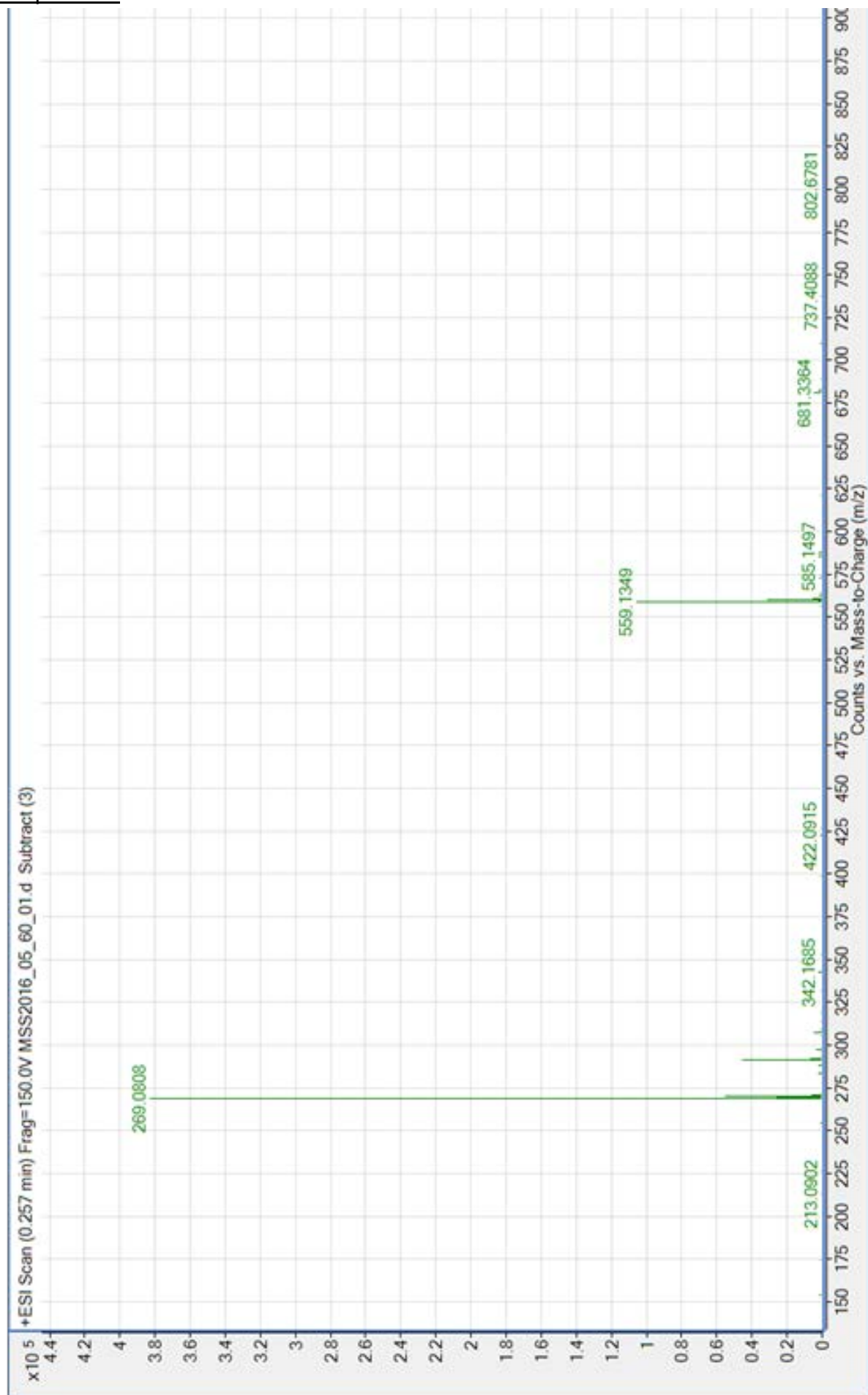
## 291.0626m/z:

Best	Formula	Species	m/z	Mass	Mass (MFG)	Score	Diff (ppm)
●	C16 H12 O4	(M+Na) <sup>+</sup>	291.0626	268.0734	268.0736	96.71	0.68
○	C13 H16 O5	(M+K) <sup>+</sup>	291.0626	252.0996	252.0998	86.98	0.88
○	C18 H10 O4	(M+H) <sup>+</sup>	291.0626	290.0553	290.0579	73.89	8.92

## Conclusion:

FMN was observed as the [M+H]<sup>+</sup> & [M+Na]<sup>+</sup> adducts corresponding to the desired compound (97%) with a relative mass difference of 0.33 ppm.

Mass spectrum:



## ANNEX II: BUFFERS PREPARATION

### 1. GELS COMPOSITION FOR WESTERN BLOT

#### Stacking gel (5% of acrylamide)

Acrylamide solution/bis-acrylamide 30% w/v	330 $\mu$ l
1M Tris HCl pH 6.8	250 $\mu$ l
SDS 10%	20 $\mu$ l
Amonium persulphate to 10%	20 $\mu$ l
TEMED	2 $\mu$ l
Water miliquore (q.s.)	2 ml

#### Running gel (10% of acrylamide)

Acrylamide solution/bis-acrylamide 30% w/v	3.3 ml
1M Tris Base pH 8.3	2.5 ml
SDS 10%	100 $\mu$ l
Amonium persulphate to 10%	100 $\mu$ l
TEMED	4 $\mu$ l
Water miliquore (q.s.)	10 ml

### 2. BUFFERS PREPARATION FOR WESTERN BLOT

#### Running Buffer 10X

Tris Base	30.3 g
Glycine	144.0 g
SDS	10.0 g
Distilled water (q.s.)	1 L

#### Transfer Buffer 10X

Tris Base	30.3 g
Glycine	144.0 g
Distilled water (q.s.)	1 L
<b>Add 20% of methanol to prepare Transfer Buffer 1X</b>	

